Study on Precise Tidal Data Processing(Dissertation_全文)

AUTHOR(S):

Tamura, Yoshiaki

主論文

Study on Precise Tidal Data Processing

潮汐の精密解析に関する研究

田　村　良　明

Index

Abstract

The purpose of the earth tide studies is to investigate the response of the earth to the external tidal forces derived from the moon and the sun. The earth's tidal response is studied from global scale to regional or local scale problems in a frequency band of much longer than seismic one. In order to examine the response of the earth to the tidal force, it is required to know the theoretical tidal force with adequate precision at first. It is also required to develop tidal analysis procedure to extract information on earth's behaviors from observation data. The procedure should resolve the tidal signals from observed data which is usually contaminated by environmental changes around observation sites and instrumental noises.

The tide generating force was developed by Tamura (1987, 1995) by employing numerical expansion method in which numerical ephemerides of the moon and the sun given by JPL were used. The developed harmonic tables contain direct and indirect terms derived from planets Venus and Jupiter. Since the development of the 4th degree potential from the moon was not completed in Tamura (1995), it is revised in this thesis. The aimed harmonic expansion threshold level (i.e. the aimed accuracy in frequency domain) of Tamura (1987) is 1 nano Gal ($10^{-11}ms^{-2}$). The aimed harmonic expansion threshold levels of Tamura (1995) and the present revision are 0.2 and 0.1 nano Gal, respectively. The accuracy of the harmonic tables is examined in several ways in this thesis. The mean error of Tamura (1987) is less than 10 nano Gal in time domain, but the maximum error reaches 30 nano Gal in worst case. Meanwhile, if we adopt the harmonic tables of Tamura (1995) and present revision, the maximum error can be prevented within 0.2 nano Gal in frequency domain, the mean error will be less than 1 nano Gal in time domain, and the maximum error can be prevented within 5 nano Gal. This accuracy is well high for the precise analysis of tidal data which is obtained with such as a superconducting gravimeter.

A computer algorithm for tidal analysis is developed by Tamura *et al.* (1991), which is based on a Bayesian method proposed by Ishiguro (1981). This procedure has a characteristic in modeling of the drift. The basic assumption of the model is the smoothness of the drift. The smoothness of the drift is controlled by a hyper-parameter, whose best value is selected by ABIC (Akaike's Bayesian Information Criterion, Akaike 1980). The tidal parameters are determined by harmonic method, while meteorological influences are modeled by non-harmonic method. The tidal analysis program is named BAYTAP-G, which can treat tidal data such as gravity, tilts, strains, ocean tides and so on.

The necessity of the high precision harmonic tables and the applicability of the tidal analysis program are demonstrated using real strain and gravity tidal data, and synthetic ones. The procedure is widely applicable even for studies to search for core undertones, earth rotation, and other geophysical signals.

1. Introduction

The observations and analyses of earth tides are intended to investigate the earth's behaviors against the external force of the tidal-generating forces derived from the moon and the sun. The phenomena of earth tides are global ones, but the objects of earth tide studies are not only to resolve global problems but also to resolve regional and local problems. As for global problems, the fluid core resonance phenomenon (FCR: Sasao *et al.*, 1980; Wahr, 1981) is studied through analysis of earth tidal data. Also, improvement of an earth model in the tidal frequency bands is carried out. The nonlinear response of the solid earth (mantle) becomes larger if the period of external force becomes longer. The dissipation (or the quality factor Q) in the mantle is discussed using the seismic data, but the object period is limited in shorter than the earth's free oscillation period of one hour for this case. The periods of tidal phenomena are quite longer compared with that of seismic wave or earth's free oscillation. It is considered that the nonlinear effect of the mantle will appear in the period longer or equal to tidal band. As for regional and local problems, locality of the tidal parameters, which are reflected by the difference of the elastic constants of the crust or the upper mantle, are investigated. Furthermore, in places such as volcanic or tectonic active regions, estimation of the time variations of the internal physical properties is intended by analyzing the time variations of the tidal parameters. In the analyses of ocean tides, not only the exploration of the oceanic physical phenomena themselves but also satisfying the daily requirements such as ocean tide forecasts at harbors or tidal current forecasts in channels and gulfs are the major purposes. In the analyses of crustal strain or tilt changes with the purpose of monitoring crustal movements, the interpretation of the drift components obtained by removing tidal changes from the observation data is sometimes more essential than the precise determination of tidal factors and phases.

In order to advance the earth tide studies mentioned above, the author developed fundamental facilities for earth tidal analysis. They are the precise developments of the tide-generating force, and the development of a tidal analysis method. The harmonic tables of tide-generating potential are developed by Tamura (1987, 1995). Furthermore, the tidal analysis procedure named BAYTAP-G is developed by Tamura *et al.* (1991). In this thesis, the developments of tide-generating potential is discussed at first. Next the development of the tidal analysis procedure BAYTAP-G is explained, and its analysis model is investigated. Next the harmonic tables and the analysis program are applied to several kinds of real earth tide data and the synthesized ones. Their usefulness is discussed with the gravity, strain and other tide data. At last, the contributions of those studies to the field of earth tides are summarized, and the future prospect on tidal studies is mentioned.

In the section of tide-generating potential, the differences of ephemeris tide and

harmonic tide, astronomical arguments used in the harmonic developments, comments on Tamura (1987) development, additional terms in Tamura (1995) and present revision, and the accuracy of the harmonic developments are investigated. In order to study the response of the earth to the tidal force, it is necessary to estimate the theoretical tidal force with adequate precision in the beginning. Doodson (1921, 1954) developed tidal potential and obtained detailed harmonic tables in early years. Later, Cartwright and Tayler (1971) and Cartwright and Edden (1973) developed more detailed harmonic tables which contains 505 tidal waves in total. Their harmonic tables are used as standard harmonic ones for a long time in the study of earth tides. However, the precision of their tables becomes insufficient for the present high precision tidal observations such gravity tide observations with a super-conducting gravimeter. Tamura (1987) developed new harmonic tables using numerical ephemerides by Jet Propulsion Laboratory (JPL). The harmonic tables were revised later with considering more minor terms and the planetary direct terms (Tamura, 1995). The latter results were not perfect in some parts still, then the harmonic development is refined again and the results are investigated in this thesis.

The recent computer technology has allowed important progress in the tidal data processing. The application of sophisticated analysis models on huge data set became available today. In the section of tidal analysis procedure, the analysis program named BAYTAP-G (Tamura *et al.*, 1991) is interpreted and the analysis model adopted in it is investigated. The program BAYTAP-G is based on a Bayesian method proposed by Ishiguro (1981). In the BAYTAP-G, the best analysis model is selected automatically from the variation of them by using an information criterion ABIC (Akaike's Bayesian Information Criterion, Akaike 1980). In the section, harmonic and non-harmonic analysis methods developed until now, drift models in tidal analysis, the treatments associated observation data such as atmospheric pressure data, grouping of the tidal constituents, observation model adopted in BAYTAP-G, how to calculate ABIC, and the implementation techniques are explained and examined.

In the section of application to practical tidal data, the harmonic tables and the analysis program are applied to the actual strain and gravity tide data. The usage for other geophysical data analysis is also mentioned in this section. The tidal observation data such as strain data often has a strong correlation with the atmospheric pressure changes. To make the matters worse, there often appear large drift, steps and interruptions of the record due to instrumental instability, earthquakes, and so on in the actual record. The program BAYTAP-G can be applied to the tidal data which includes such irregularities in drift, occasional steps and disturbances caused by meteorological influences. The applicability of the program to such data is discussed in the section.

2. Tide-Generating Potential

2.1. Ephemeris Tide and Harmonic Tide

There are two kinds of method to calculate tide-generating potential. One is to calculate tide-generating potential directly from the position of the moon and the sun. The other is to develop the tidal potential in the frequency domain and calculate the potential by summing up sinusoid constituents. The former method is called direct method or ephemeris tide (hereafter we use the terminology "ephemeris tide"). The latter method is called harmonic method or harmonic tide.

The ephemeris tide can be calculated by using suitable ephemerides of the moon and the sun. (Most ephemerides give the motion of the sun based on geocentric coordinates traditionally, though the earth is revolving around the sun.) The motion of the sun can be expressed by ellipsoidal orbit (Kepler's motion) with the accuracy of 1'. Only a few perturbation terms are required for the sun's ephemeris to obtain the accuracy of 0.'1, which accuracy is enough to calculate the solar tidal potential. Meanwhile, several tens perturbation terms are required for the moon's ephemeris to obtain the same accuracy of 0.'1. The algorithm of ehpemeris tide is rather simple compared with that of harmonic one, and the computation time is usually shorter than it. There are several programs for ephemeris tide. For example, Tamura (1982) released a FORTRAN program by using the ephemerides by Kubo(1980). Tamura (1982) considered the degree 3 potential by the sun and the degree 4 potential by the moon using analytical ephemerides. By using numerical high precision ephmerides (for example, Standish and Williams, 1981, 1982), we can easily obtain high precision theoretical data which can be used as a standard reference data set. We can give tidal factors and phase differences for each degree potential and each tidal specie in the computation of ephemeris tide, but can not give fine frequency structure within a tidal specie. This is the most weak point of ephemeris tide.

One purpose of tidal study is to investigate frequency response of the earth to external forces. Moreover, ocean tide factors and phases usually show strong frequency dependency against tidal potential. Thus the theoretical tidal developments in the frequency domain is required in the both cases for the analysis and prediction. Doodson (1921, 1954) developed tidal potential and obtained detailed harmonic tables in early years. His development dedicated ocean tide analysis and its prediction at that time. Later, Cartwright and Tayler (1971) and Cartwright and Edden (1973) developed more detailed harmonic tables which contain 505 tidal waves including Doodson's prior development (we call them CTE tables hereafter). The CTE tables developed by a numerical method considering degree 3 potential for the moon and degree 2 potential for the sun. Each constituent is treated as a sinusoid wave. The constituents whose amplitudes are relatively large are considered the secular changes of their amplitudes. Their amplitude changes are mainly caused by the secular

change of the obliquity of the ecliptic. The CTE tables were used as standard harmonic developments for the studies in both earth tides and ocean tide for a several years.

Recent earth tide observations, such as gravity tide ones with a superconductivity gravimeter or a null method LaCoste Romberg gravimeter have high quality (i.e. high resolution, precision and stability). These observations give us variable information of earth's interior. In order to obtain much more knowledge of the earth, not only precise and intense observations but precise analysis methods are required. It is needless to say that the accurate theoretical tide calculations are required in tidal analysis and prediction. If the theoretical tide computations in analysis have some systematic errors or large errors compared with observation accuracy, the analysis results shall be distorted artificially. To avoid such situation, the theoretical tide calculations (the precision of harmonic tables) must have enough precision compared with the precision of recent earth tide observations. A few times or ten times margin in the accuracy is desirable in the theoretical tide calculations.

The CTE tables are used as a standard in 1970s and early in 1980s, but their precision is not enough for recent requirements. The CTE developments are not so perfect nowadays and the harmonic coefficients are given only five digits validity. Moreover, after the development of CTE tables, the astronomical constants were revised. If we use CTE tables at present, there will be a slight inconsistency. Several authors have developed the tide-generating potential till now to improve its accuracy (Büllesfeld, 1985; Xi, 1987; Tamura, 1987, 1995; Hartmann and Wenzel, 1994, 1995; Roosbeek, 1996). Büllesfeld (1985), Tamura (1987, 1995), and Hartmann and Wenzel (1994, 1995) developed the potential by using numerical methods, while Xi (1987) and Roosbeek (1996) used analytical methods. All authors developed the potential at least up to degree 4 potential for the moon and degree 3 for the sun. Tamura (1995), Hartmann and Wenzel (1994), and Roosbeek (1996) were taking account of the tidal potential derived form planets. The direct effect from Venus or other outer planets comes up to a few nano Gal level in the gravity tide, and it is not so small to be neglected at present. Hartmann and Wenzel (1995), and Roosbeek (1996) developed degree 5 or 6 potential for the moon. Their amplitudes are in the order of 0.1 nano Gal or less, thus the degree 5 and the higher degree potentials may be neglected.

The author (Tamura 1987, 1995) developed the harmonic tables of the tide-generating potential numerically by using the MERIT (a programme of international collaboration to Monitor Earth Rotation and Intercompare the Techniques of observation and analysis) standards (1983) and the JPL numerical ephemerides (Standish and Williams, 1981, 1982). In this thesis, the author revised the previous developments and examined the accuracy of the current development results. In the following sections, details of the developments and investigation results are explained.

2.2. Astronomical Arguments in the Harmonic Developments

Doodson and several authors who developed tidal potential used below traditional six astronomical arguments to express phase and angular velocity for each constituent.

1	τ	:	time angle in lunar days
2	s	:	moon's mean longitude
3	h	:	sun's mean longitude
4	p	:	longitude of moon's mean perigee
5	N'	:	negative longitude of moon's mean node
6	p_1	:	longitude of sun's mean perigee

The orbits of the moon and the sun are illustrated in Figure 1. The term "mean" means the motion in circular orbit (not ellipsoidal one) of the moon or the sun, only taking account of precession and long period perturbations. In above arguments, τ can be expressed with s and h ignoring the aberration and the difference between the dynamical time (TD) and the universal time (UT) like as

$$\tau = 15^\circ \times t + h - s + \lambda \qquad (1)$$

where t is the universal time in hour, and λ is the east longitude of a site. Those variables are related to the fundamental arguments of nutation series used in the MERIT standards by

$$\left.\begin{aligned} s &= F + \Omega, \\ h &= F + \Omega - D, \\ p &= F + \Omega - l, \\ N' &= -\Omega, \\ p_1 &= F + \Omega - D - l' \end{aligned}\right\} \qquad (2)$$

where

F	:	moon's mean elongation from node,
D	:	moon's mean elongation from sun,
Ω	:	longitude of moon's node,
l	:	moon's mean anomaly,
l'	:	sun's mean anomaly.

The moon's node Ω is illustrated in Figure 1. In Tamura (1987), Ω was explained as the perigee in mistake. Ω is the longitude of moon's node in correct. F, l and l' are

described by the "mean" motions of the moon and the sun like as $F = l_2$, $l = l_1 + l_2$, and l' = sun's longitude − P shown in Figure 1. D is the difference of ecliptic longitude between the moon and the sun in other words.

In order to develop the tidal potential up to 10×10^{-6} amplitude constituents for the second degree, following eight arguments are necessary. They are defined by the author as

$$\left.\begin{aligned} f_1 &= 15^\circ \times t + \alpha_m - s + \lambda, \\ f_2 &= s + \Delta s, \\ f_3 &= h + \Delta h, \\ f_4 &= p, \\ f_5 &= N', \\ f_6 &= p_1, \\ f_7 &: \text{period of Jupiter's opposition}, \\ f_8 &: \text{period of Venus's conjunction} \end{aligned}\right\} \qquad (3)$$

where α_m is the right ascension of a supposed object to define the universal time. Δs and Δh denote the long period perturbations in the longitude of the moon and the sun, respectively. These corrections of Δs and Δh are added to reduce the phase shift for the principal constituents such as O_1, K_1, M_2, S_2 and K_2. The existence of the arguments f_7 and f_8 does not mean the direct tidal effect by Jupiter and Venus, but the indirect effect of Sun generating potential by perturbing the earth's orbit.

Concerning to the argument f_1, we should use α_m instead of h. There are differences between α_m and h in two points. For the first one, the time argument for α_m is UT, but h is TD. For the second one, there is a permanent difference of the aberration (about 20."5) between their constant terms. If we uses h in place of α_m like as Doodson's definition, tidal potential becomes to be calculated based on "apparent" places of the moon and the sun. On the other hand, if we uses α_m, tidal potential is calculated based on "true" places. In other words, when we compute the angle hour of an object whose right ascension is α, we calculate $h - \alpha$ in former case, and $\alpha_m - \alpha$ in latter case. Though this difference between apparent and true places is only 20."5, this gives systematic phase shift for all constituents. For example, all components of semidiurnal species are caused 0.°01 phase shift by this difference.

Since the gravitation operates as an "action at a distance" (note that the gravity field is not energy propagation nor particle movement!), true place should be used in dynamics computations. (In addition, the aberration is a phenomenon proportional to v/c, where v is the velocity of the earth's revolution, and c is the light velocity. Some forces proportional to $(v/c)^2$ exist if we consider the theory of relativity.)

The eight arguments used in the harmonic developments (equation (3)) are actually defined as follows (Aoki *et al.*,1982), (Kubo,1980).

$$
\left.
\begin{aligned}
\alpha_m &= 280.^\circ4606184 + 36000.^\circ7700536\, t_u + 0.^\circ00038793\, t_u^2 \\
&\quad - 0.^\circ0000000258\, t_u^3, \\
s &= 218.^\circ316656 + 481267.^\circ881342\, t_d - 0.^\circ001330\, t_d^2, \\
h &= 280.^\circ466449 + 36000.^\circ769822\, t_d + 0.^\circ0003036\, t_d^2, \\
\Delta s &= 0.^\circ0040 \cos(29^\circ + 133^\circ t_d), \\
\Delta h &= 0.^\circ0018 \cos(159^\circ + 19^\circ t_d), \\
f_4 &= 83.^\circ353243 + 4069.^\circ013711\, t_d - 0.^\circ010324\, t_d^2, \\
f_5 &= 234.^\circ955444 + 1934.^\circ136185\, t_d - 0.^\circ002076\, t_d^2, \\
f_6 &= 282.^\circ937348 + 1.^\circ719533\, t_d + 0.^\circ0004597\, t_d^2, \\
f_7 &= 248.^\circ1 + 32964.^\circ47\, t_d, \\
f_8 &= 281.^\circ5 + 22518.^\circ44\, t_d
\end{aligned}
\right\} \quad (4)
$$

where t_u is the universal time measured from 2000 Jan. 1 12^h UT1 (JD 2451545.0) in 36525 days unit, and t_d is the dynamical time measured from 2000 Jan. 1 12^h TD in 36525 days unit. The arguments s, h, p, N' and p_1 are slightly differ from those of the MERIT standards. However those differences are small enough to calculate the tidal potential.

2.3. Comments on Tamura (1987) Development

The harmonic development of Tamura (1987) is numerically made based on the MERIT standards and the JPL ephemerides. The expansion is made up to the 4th degree potential for the moon and the 3rd degree for the sun, and the secular variation of harmonic amplitude was taken into account. All tidal constituents, whose amplitudes are larger than 10×10^{-6} for the 2nd degree potential, 7×10^{-6} for the 3rd one and 5×10^{-6} for the 4th one in Doodson's scale, are picked up. These amplitude thresholds are correspond to 0.8 nano Gal for each constituent.

Traditional astronomical arguments are adopted in the developments. In order to express indirect planetary terms (i.e. to express perturbations by Venus and Jupiter to the revolution orbit of the earth), two arguments (f_7 and f_8 explained in section 2.2) are used in the developments. There are 2 indirect planetary terms in long period tide, 2 indirect terms in diurnal tide and 4 terms in semidiurnal tides.

The harmonic developments are adjusted for the period between 1950 and 2030. The secular changes of the amplitudes for major constituents are estimated from the amplitudes of four different epochs.

The motion of the sun's perigee is very slow compared with the above period of 80 years. Its period is about 21000 years. It is impossible to resolve two tidal waves whose periods are differs only 1/21000 years by numerical development. We named

such waves "paired terms". There are several paired terms whose angular velocities differs only by $2f_6$ in actual. For example, ϕ_1 wave is formed with two terms of whose angular velocities are defined by $f_1 + f_2 + 2f_3 - 2f_6$ and $f_1 + f_2 + 2f_3$. The numerical development can determine the amplitudes of such paired terms if the angular velocities of them are given, but the exact coefficients for f_6 term cannot be determined by numerical method. Therefore, the angular velocities are given a priori for the known paired terms such as ϕ_1 wave in the numerical developments. If the one of a pair's amplitude is smaller than 12×10^{-6}, those terms can be represented by one term, whose angular velocity is the same as that of the bigger one, and whose amplitude is defined by "bigger one"−"smaller one". This simplification is possible because the phase difference of $2f_6$ is 205° which is close to 180°. This simplification cannot be applied to ϕ_1 wave, because it has rather large amplitudes of 104×10^{-6} and 7545×10^{-6} in pair. A systematic phase bias will be yielded if the terms are united into one term forcibly.

The constants used in the development is listed in Table 1. The MERIT standards slightly differs from present constants. For example, the earth's equatorial radius of 6378137m is adopted in MERIT standards, while it is 6378136m in IAG1980 system. There is no inconsistency if the same value of 6378137m is used in the calculation of theoretical tides. Because the earth's equatorial radius is used only as a normalization factor in the developments, its value is not necessarily equal to real earth's radius.

The aimed accuracy of the development is 1 nano Gal in frequency domain. The accuracy of time domain becomes worse than that of frequency domain, because there are 1200 components in total and all of them must be added to obtain the theoretical value for each epoch. There are also minor constituents which are neglected in the harmonic tide calculation. For those reasons, the maximum error in time domain reaches 30～40 nano Gal in worst case, though the mean error is less than 10 nano Gal.

In the second degree potential, there are a few terms whose amplitudes are slightly larger than the expansion threshold level of 10×10^{-6}, and whose frequencies and phases cannot be denoted by the combination of the eight arguments. They have angular velocities of about 0.4671°/h , 12.8496°/h, 13.3918°/h and 27.8910°/h. This result shows that more precise harmonic development is difficult if we use only the traditional arguments which are defined by Doodson or by the author.

2.4. Additional Terms

In order to improve the accuracy of the theoretical tide calculation, Tamura (1995) revised by the harmonic tables by applying numerical expansion method. The error level in the theoretical tide calculation for solid earth can be reduced to about half by applying extra 500 harmonic terms to the Tamura (1987) tables. By taking additional 860 terms (in total 2060 terms), it can be reduced to about one third level

compared with Tamura (1987). The direct planetary terms by Venus and Jupiter were also developed in Tamura (1995). In Tamura (1987), eight indirect planetary terms whose amplitudes were larger than 1 nano Gal were taken into account. The direct term by Venus reaches about 4 nano Gal in time domain at the inferior conjunction, though the amplitude of each component is smaller than 0.4 nano Gal. The direct term by Jupiter is smaller than 1 nano Gal in time domain even at the opposition.

In Tamura (1995), the degree 2 and 3 potentials of the moon and the sun were revised, but the 4th degree potential was not revised at that time. In this thesis, complete development is carried out up to the degree 4 potential. For the results, the mean error and the maximum error can be reduced to about one fifth level by applying additional 1800 terms to the Tamura (1987) tables.

a) for the moon and the sun

Tamura (1995) revised by the harmonic tables for degree 2 and 3 potentials by applying numerical expansion method. The expansion threshold level is 0.2 nano Gal for each constituent in that development. That of Tamura (1987) was 0.8 nano Gal. A least squares fitting method is applied for the year from 1940 to 2040 in that development. For the reference of ephemeris tide, the numerical ephemerides DE200/LE200 (Standish and Williams, 1982) are used.

In the development of additional terms for the moon and the sun, traditional astronomical arguments (equation 4) are not used. Instead of them, the angular velocity and the initial phase for each constituent at the epoch J2000 (12^h UT, January 1, 2000) are given. This is because the periods of some harmonic terms cannot be expressed by the traditional arguments of mean longitudes of the moon and the sun, mean perigees of them and mean node of the moon. Moreover, we can get higher precision with fewer terms by applying best fitting for the restricted fitting period for the year from 1940 to 2040.

The numerical least squares fitting process was applied in the development. It is explained simply as follows. At first, time series of ephemeris tide for the period from 1940 to 2040 was generated respectively for each potential degree and for tidal species. Second, the known harmonic tide (Tamura, 1987) was subtracted from the time series. Next , a rough frequency of an additional term was searched by applying first Fourier transform to the time series of 100 years data. Next, fine frequency of that term was searched around the frequency of spectrum peak. Last, the amplitude of its constituent was determined by the procedure which made residuals minimum. In Tamura (1995), the search for fine angular velocity (search for fine frequency) was done with a finite step of about 0.00002°/h.

b) planetary direct terms

The direct terms by Venus and Jupiter must be considered in the developments to obtain 1 nano Gal accuracy. Those direct planetary terms were developed in Tamura

(1995) by numerical method. For the Venus terms, they converge extremely slowly because of large range ratio between inferior and superior conjunction, though their total effect is only a few nano Gal level. Contrary, the Jupiter terms converge rather faster. Only a few terms are necessary for consideration. The required accuracy of planetary ephemerides is not so high, thus the more convenient ephemerides by Kubo (1980) and Fukushima (1981) instead of DE200/LE200 are used in the developments.

The results of development for Venus are listed in Table 1 of Tamura (1995). The amplitude of each component is shown in Doodson's scale. The amplitude of 12×10^{-6} is equivalent to 1 nano Gal for degree two potential. The argument V used in Tamura (1995) is defined as the difference between mean heliocentric longitude of Venus and that of the earth (i.e. negative longitude of the sun). It is expressed as $V = 81.^{\circ}5 + 22518.^{\circ}44\ t_d$, where t_d is the dynamical time same as used in equation (4). All terms should be multiplied by the latitude functions which are same as for the moon and the sun in the theoretical tide calculation. The amplitude of each component developed here is smaller than 0.4 nano Gal. Nevertheless, the Venus direct terms will have same phases at the inferior conjunction (i.e. when $V = 0$) and the each term cannot be resolved. At that time, the total effect from Venus becomes about 4 nano Gal.

The results of development for Jupiter are listed in Table 2 of Tamura (1995). The definition of amplitude and arguments are similar to those of the Venus terms. The argument J is the difference between mean heliocentric longitude of the earth and Jupiter. It is expressed as $J = 248.^{\circ}1 + 32964.^{\circ}47\ t_d$. The maximum amplitude for Jupiter each term is less than 0.3 nano Gal, and the total amplitude is smaller than 1 nano Gal even at the opposition.

The direct terms derived from other planets are negligible small considering the mass of planets and their distance from the earth. Mars gives the largest effect among remaining planes, but its effect is less than 0.1 nano Gal even at the opposition.

c) present revision

In this thesis, the 4th degree potential of the moon is revised to complete the additional harmonic terms. The adopted expansion threshold level is 0.1 nano Gal. The harmonic tables for degree 2 and 3 are revised again adopting same expansion threshold level is 0.1 nano Gal. For the results, the mean error and the maximum error are reduced to about one fifth compared with Tamura (1987) tables.

The numerical expansion method with least squares fitting is almost same as that of Tamura (1995). The numerical ephemerides DE200/LE200 (Standish and Williams, 1982) are also used in this revision. The period for numerical fitting is from the year 1951 to 2048 in this time. The central epoch is adjusted to J2000. In Tamura (1995), the angular velocity of each constituent was searched with a finite step of about 0.00002°/h. In this revision, the angular velocities of additional terms are determined more rigorous way. Therefore, the angular velocity of each

constituent revised in this time may differ about 0.00002°/h from that in Tamura (1995).

The numbers of constituents for each development are listed in Table 2. The columns of degree 4 for Tamura (1995) are shown with parenthesis. In the Tamura (1995), the degree 4 potential was not expanded, but the table is filled for the convenience of comparison. The numbers are given by assuming the expansion threshold level of 0.2 nano Gal which is compatible with Tamura (1995).

In appendix, total additional harmonic terms of the moon and the sun are listed.

2.5. Examination of Accuracy

a) frequency domain

In the harmonic development by Tamura (1987), the expansion threshold level of 1 nano Gal is adopted. Also 0.2 nano Gal threshold level is adopted in Tamura (1995). Much low threshold level is adopted in the current revision. To check the accuracy of the harmonic tables, the harmonic tides are compared with the ephemeris tides for each species. The ephemeris tides are based on the numerical ephemerides of DE200/LE200, they are considered as reference standards. The comparisons are carried out at the latitudes in which the maximum tidal amplitude can be obtained for each species.

In Figure 2-20, the black line shows the spectrum of theoretical gravity tide (ephemeris tide) of degree 2, long period, and at latitude 90°. Eighteen years data is used in the spectrum calculation. The blue line in Figure 2-20 shows the spectrum of "ephemeris tide − harmonic tide by Tamura (1987) (with 211 waves)" of degree 2, long period tide. This result shows that the maximum error of the harmonic tide is less than 1 nano Gal in frequency domain and the intended accuracy is obtained. The red line in Figure 2-20 shows the spectrum of "ephemeris tide − harmonic tide with the additional terms (in total 493 waves)" of degree 2, long period. This result shows that the maximum error of the harmonic tide with additional terms is less than 0.1 nano Gal, and the intended accuracy is obtained.

In Figure 2-21, the black line shows the spectrum of theoretical gravity tide (ephemeris tide) of degree 2, diurnal and at latitude 45°. Two years data is used in the spectrum calculation. The blue line in Figure 2-21 shows the spectrum of "ephemeris tide − harmonic tide by Tamura 1987 (with 345 waves)" of degree 2, diurnal. The red line in Figure 2-21 shows the spectrum of "ephemeris tide − harmonic tide with the additional terms (in total 757 waves)" of degree 2, diurnal. This result shows that the maximum error of the harmonic tide with additional terms is less than 0.2 nano Gal in frequency domain. It is somewhat higher than the intended accuracy of 0.1 nano Gal in the development. It may be caused by the insufficient frequency resolution in the spectrum calculation.

Figure 2-22 shows the case of degree 2, semidiurnal tide at latitude 0°. The black

line is the spectrum of theoretical gravity tide. The blue line in Figure 2-22 is the residual spectrum when 281 terms are taken into account in the harmonic tide calculation which is based on Tamura (1987). The red line in Figure 2-22 is the residual spectrum when 633 terms are taken into account in the harmonic tide calculation. The maximum error in frequency domain is estimated about 0.2 nano Gal. It is somewhat higher than the intended accuracy of 0.1 nano Gal like as diurnal band. The cause may be similar to that of diurnal band.

Figure 2-33 shows the case of degree 3, terdiurnal tide at latitude 0°. The black line is the spectrum of theoretical gravity tide. The blue line in Figure 2-33 is the residual spectrum when 68 terms of Tamura (1987) are taken into account The red line in Figure 2-33 is the residual spectrum when 194 terms are taken into account in the harmonic tide calculation. In both cases, intended accuracy of 1.0 and 0.2 nano Gal is obtained.

Figure 2-44 shows the case of degree 4, 1/4 day period tide at latitude 0°. The black line is the spectrum of theoretical gravity tide. The blue line in Figure 2-44 is the residual spectrum when 10 terms of Tamura (1987) are taken into account. The red line in Figure 2-44 is the residual spectrum when 39 terms are taken into account in the harmonic tide calculation. In both cases, intended accuracy of 1.0 and 0.15 nano Gal is obtained.

2) time domain

Figure 3 group shows the variations of time domain maximum and mean errors of harmonic gravity tide given by changing the maximum number of adopted harmonic terms. The reference theoretical gravity tides are calculated directly from the lunar and solar ephemerides. The error of each degree and species is estimated at the latitude which gives maximum tidal amplitude. For degree 2, geographical coefficients at latitude 90°, 45° and 0° give maximum amplitude for long period, diurnal and semidiurnal tide, respectively. For degree 3, geographical coefficients at latitude 90°, 58.9°, 35.3° and 0° give maximum amplitude for long period, diurnal, semidiurnal and terdiurnal tide, respectively. For degree 4, geographical coefficients at latitude 90°, 66.1°, 49.1°, 30° and 0° give maximum amplitude for long period, diurnal, semidiurnal, terdiurnal and 1/4 day period tide, respectively.

Those Figures show that the maximum error of Tamura (1987) development is about 20～30 nano Gal in time domain while the mean error is a few nano Gal level. To obtain 10 nano Gal accuracy in time domain, almost all harmonics (about 3000 terms) developed by current revision must be used in theoretical tide calculations.

3) planetary direct term

Figure 4a shows long period gravity tide generated by Venus. Figures 4b and 4c show that of diurnal and semidiurnal tides, respectively. The amplitudes by Venus direct terms reach about 4 nano Gal at the inferior conjunctions, while they will be negligible small at the superior ones. The distance of Venus from Earth is 1.7 a.u. at

the superior conjunction, while it is 0.3 a.u. at the inferior conjunction. The ratio of tide-generating potential by Venus at the superior and inferior conjunction is about 1/180 (= $(0.3/1.7)^3$), thus the amplitude at superior conjunction becomes negligible small. The maximum amplitudes of long period tide and diurnal tide at the inferior conjunction depend strongly on the declination of Venus at that time.

Figures 5a, 5b and 5c show the long period gravity tide, diurnal one and semidiurnal one generated by Jupiter, respectively. The direct term by Jupiter was smaller than 1 nano Gal in time domain even at the opposition. For semidiurnal the maximum amplitude is about 0.5 nano Gal at the Jupiter's opposition. The distance of Jupiter from Earth is 4.2 a.u. at the opposition, while it is 6.2 a.u. at the superior conjunction. The ratio of tide generating potential by Jupiter at the superior conjunction and opposition is about 0.3 (= $(4.2/6.2)^3$). Therefor, there is no drastic amplitude change like as Venus.

4) gravity tide residuals

The harmonic tables by Tamura (1987) and CTE (Cartwright and Tayler, 1971; Cartwright and Edden, 1973) are compared in the analysis of actual gravity tide records. The gravity tide data obtained by a superconducting gravimeter at Esashi Earth Tides Station (39.°1 N, 141.°3 E) is used in the comparison. The data length is 6 months. Mean residuals of 0.0687 μ Gal is obtained in tidal analysis by using the former tables. While that of 0.0697 μ Gal is obtained by using the latter tables. (The tidal analysis method will be discussed in the section 3.) The improvement might be not so clear at a glance, but it becomes clear if we compare the residuals in frequency domain. The Figure 6a is a spectrum of residuals around terdiurnal band which residuals are obtained by applying Tamura (1987) tables. Figure 6b is that obtained by applying CTE tables. In Figure 6b, several tidal components whose periods are 8.1772, 8.3863 and 8.4940 hours are remaining. Those tidal components derived from degree 4 potential which is not taken into account in CTE tables. On the other hand, those residual spectrum peaks disappear in Figure 6a. This comparison result shows that the CTE harmonic table has not enough precision for the precise tidal analysis at present. Moreover, we can say that a superconducting gravimeter has a potential sensitivity to detect a few nano Gal gravity changes if the signals are coherent and continues for a few months or longer.

2.6. Remarks

The degree 3 tidal potential of long period tide is developed up to the 4×10^{-6} amplitude terms in Tamura (1987) , though the expansion threshold of other species of third degree is adopted to 7×10^{-6}. This is because Doodson (1921) made a mistake in geographical normalization factor 2 for $2/\sqrt{5}$. The same normalization factor which was adapted by Doodson is used in Tamura (1987, 1995) and current revision for the convenience in comparison with his results.

The constants used in the harmonic developments series are listed in Table 1. The sine parallax of the moon is not included in the MERIT standards, but it is used conveniently. There is no trouble with its precision in the theoretical tide calculations, as long as we use the same value of the moon's sine parallax used in the harmonic development. This constant is used only a normalization factor in harmonic developments and harmonic tide calculations. This situation is same as the constant of earth's equatorial radius.

The numerical developments can obtain same accuracy of analytical developments with smaller number of harmonic terms. For example, Xi (1987) developed harmonic tables which contain about 3000 terms by analytical method. The same precision as Xi (1987) can be obtained by using about 1500 terms developed by numerical methods. The numerical expansion method can achieve this precision since the amplitude and phase of each tidal constituent is determined to fit for only the limited epoch period. For example, Tamura (1987) developed for the period between 1950 to 2030. Also, the additional terms were adjusted to the period between 1951 to 2048. Within the applied period, harmonic tables developed by numerical methods usually give higher precision with smaller number of terms. However, if we try to calculate harmonic tide at the epoch of the outside of the applied expansion period, the precision may become worse rapidly. The applicable period must be checked in the use of any developments.

3. Tidal Analysis Procedure

3.1. Harmonic and Non-Harmonic Methods

There are currently two different approaches to the tidal analysis: harmonic analysis and non-harmonic one. The harmonic analysis, which attempts to express the tide record as the sum of harmonic functions of time, has been used for a long time both in the ocean tide and earth tide studies. The harmonic methods are available for tidal data analyses, because we know beforehand the theoretical amplitudes, phases and periods of particular tidal constituents from knowledge of the orbital motions of the moon and the sun, which are discussed in the section 2. Various harmonic methods have been developed by several authors (Venedikov, 1966; Melchor and Venedikov, 1968; Tamura *et al.*, 1991; Wenzel, 1998). The latter two methods adopt hybrid models. They used harmonic models for the determination of tidal parameters, while non-harmonic models were used for the environmental data such as atmospheric pressure data.

On the other hand, as a non-harmonic method for analysis and prediction of the oceanic tide, Munk and Cartwright (1966) developed the "response method" which takes the form of a multiple linear regression analysis. This method has the advantage over the harmonic method that we can separate the admittances of different tidal species of spherical harmonics and can represent effects of regional or local disturbances caused by meteorological variations. Lambert (1974) applied this method to earth tide data and discussed the confidence limits of the response weights and admittances considering the effect of extraneous noise.

The response method, however, has two shortcomings compared with the harmonic analysis method. The first is that the frequency resolution is not so high, and the second is that the drift and step changes are not allowed for in the record. Later, Ooe and Sato (1983) developed the "extended response method" to remove these shortcomings. They extended the response method to include drift and steps by adding an autoregressive (AR) process in a form which keeps high resolution. This method was applied to actual strain tide data (Sato *et al.*, 1980).

A new method for tidal analysis was proposed by Ishiguro (1981) which is based on the concept of the Bayesian statistical modeling (ABIC: Akaike's Bayesian Information criterion, Akaike 1980). This method is one particular example of Bayesian modeling for linear problems. In all the methods mentioned above, the drift is assumed to be represented by a low order polynomial, but this assumption may be too simple and not flexible for actual earth tide records. In contrast with the previous methods, only the smoothness of the drift is assumed in this procedure. This tidal analysis procedure is realized by Ishiguro and Tamura (1985) and Tamura *et al.* (1991). The computer program developed by them is named "BAYTAP-G" (BAYesian Tidal Analysis Program, Grouping model). The analysis model used for the present version of BAYTAP-G is

a hybrid model including in both harmonic and non-harmonic terms. In following sections, the analysis model used in the BAYTAP-G is examined and the directions for the practical use are explained.

3.2. Drift Models

In the construction of a tidal analysis mode, one of the most difficult problem is how to treat the drift contained in observational data. In the cases of crustal movement analyses, the estimation of drift component itself is often very important rather than the estimation of tidal parameters. In the case of ocean tide data analysis, the drift components are relatively small compared with the amplitudes of tidal changes. In other words, the mean sea level change is usually not so large and it can be expressed in a polynomial of the time t or a constant for a certain period. It is a very rare case that the drift of earth tide records can be expressed as such a way.

In order to express the drift components, we may use methods to obtain continuos drift by dividing the analysis interval successively every few days and applying simple polynomials or spline functions or Chebyshev polynomials to the individual intervals. The drift also can be estimated by digital filtering methods. General low pass filters or special designed low pass filters to diminish tidal components are also used to determine the drift of the observation data. Actually, the tidal analysis has been made conventionally in such manners mentioned above. However in applying such polynomials for successive period or such filters, it is difficult to separate the necessary information from the drift component perfectly.

In the proposed method (Ishiguro and Tamura, 1985; Tamura *et al.*, 1991), it is assumed that the drift only changes smoothly in time without assuming a specific function on the pattern of the drift. We assumed here that the drift component is represented by the integrated random walk model,

$$d_i = 2\,d_{i-1} - d_{i-2} + u_i, \tag{5}$$

where d_i is a drift term at each observation epoch and u_i denotes the white noise sequence with zero mean and variance σ^2. The tidal parameters and the drift part of the each observation epoch d_i are estimated by assuming the conditions of

$$d_i - 2\,d_{i-1} + d_{i-2} \fallingdotseq 0. \tag{6}$$

This binding conditions are added to the observation equations in the least squares methods. In case of the tidal parameter estimation, it is an important problem that how strong (or how weak) binding conditions must be given in the parameter estimations by least squares method. The estimation problem of this drift d_i is equivalent to the smoothing problem of the one-dimensional series data. By

introducing a suitable type of prior distribution under the expectation that $d_I - 2\,d_{i-1} + d_{i-2}$ distributes around zero. The problem can be solved by applying the Bayes statistical model proposed by Akaike (1974, 1980).

3.3. Associated Data

In order to remove the influence of atmospheric pressure change or temperature change affecting on the tidal observations, the response model is applied in the analysis model. We call such observational environmental data an associated data. Denoting the associated data such as atmospheric pressure data x_i, the perturbation R_i is expressed as

$$R_i = \sum_{k=0}^{K} b_k \; x_{i-k} . \tag{7}$$

The coefficient b_k is a response coefficient (response weight) and K is the maximum number of the lag. Only a simple proportional relation is assumed when the maximum lag of K=0 is given. Equation (7) represents convolution integral in finite element. There is a well know relation between convolutional integral and Fourier transformation. If we apply Fourier transformation to the both side of equation (7), we get the result of

$$\mathrm{F}(R_i) = \mathrm{F}(b_k)\;\mathrm{F}(x_i) . \tag{8}$$

Where F(A) represents Fourier transform of A. Equation (7) expresses the relation of R_i, b_k and x_i in time domain, while equation (8) expresses their relation in frequency domain. Therefore, considering the time lag in the response is equivalent to considering the frequency structure in the response.

If we have plural number of associated data sets, we can apply the response model for each data respectively. In that case, we should pay attention to the interpretation of the obtained response coefficients if a strong correlation exists between two kinds of associated data sets. For example, there is a correlation between atmospheric pressure change and the rain fall. There is a clear relation that it rains much when the pressure is low, and it is fine when the pressure is high. For more example, in the observation of crustal strains in a tunnel, adiabatic expansion and compression are caused by the change of the atmospheric pressure. For the result, a considerable strong correlation is often seen between pressure change an the temperature change. There is a tendency that the correlation is higher in the short period variation, and less correlation in the long period (experimentally longer than several hours) change. Thought the interpretation of response mechanism becomes complicated when the

correlated associated data sets are used in the analysis, such date sets may be used in the analysis in order to remove disturbances from both noise sources. In this case, the total amount R_i obtained by summing up both response parts has a meaning.

3.4. Grouping of Tidal Constituents

There are a lot of minor tidal constituents around major constituents. Those minor constituents cannot be resolved from major ones within a restricted observation period. Around M_2 tide, for example, there are 55 minor constituents which cannot be resolved from one month observations (Tamura 1987). There are still 18 minor constituents which cannot be resolved from M_2 tide even if the observation period is longer than one year. We call such minor constituents side band of M_2 tide, or M_2 tidal group including principal M_2 tide. The situation around other principal tides is similar to that of M_2 tide. The tidal constituents form tidal groups around principal tides. This situation can be seen in a spectrum of theoretical tide (for example, see Figure 2-21). The minor constituents in a tidal group cannot be resolved from each other, and it is considered that the earth's frequency response to the tide-generating potential does not differ so much within a tidal group in which the angular velocities of each constituent is close to that of principal tide. When we call M_2 tide hereafter, there are two cases in the meanings. One is a pure single cosine wave of M_2 tide and the other is the M_2 group.

Assuming that the amplitude factor and phase difference are constant within a group, we obtain a model for observed tide T_i,

$$T_i = \sum_{m=1}^{M} a_m \sum_{j=1}^{J_m} a^*_{mj} \cos(\omega^*_{mj} i + \phi^*_{mj} + \phi_m), \qquad (9)$$

where i is the time index, m denotes the tidal group, M is the number of total groups, j is the tidal constituent index in the group, and J_m is the total number of tidal constituents in the group j. ω^*_{mj} is the angular velocity, a^*_{mj} and ϕ^*_{mj} are the amplitude and the initial phase of the jth constituent in the mth group which are given from tidal harmonic tables, respectively. a_m and ϕ_m are the observed amplitude factor and phase lead of the mth group, respectively. With the concept of the tidal groups, we can represent the tidal model with a few tens of parameters. We need not estimate thousands of parameters for each tidal constituent.

3.5. Observation Model in BAYTAP-G

The observation model adopted in BAYTAP-G is expressed by

$$y_i = \sum_{m=1}^{M} (\alpha_m C_{mn} + \beta_m S_{mn}) + \sum_{k=0}^{K} b_k x_{i-k} + d_i + \varepsilon_i , \qquad (10)$$

in consideration of the response to associated data x_i and drift d_i of observation data, where y_i is the observed time series, m represents the number of the tidal component group, M is the total number of the group, α_m, β_m are unknown tidal parameters to be estimated, C_{mn}, S_{mn} are the theoretical values of the tidal group number m. They express the theoretical value of in-phase and 90° out-phase components, respectively. The tidal parameters C_{mn}, S_{mn} and response weight b_k are estimated by minimizing following equation $J(d)$ by applying least squares methods.

$$J(d) = \sum_{n=1}^{N} \left\{ y_i - \sum_{m=1}^{M} (\alpha_m C_{mn} + \beta_m S_{mn}) - \sum_{k=0}^{K} b_k x_{i-k} - d_i \right\}^2$$

$$+ v^2 \sum_{n=1}^{N} \left\{ d_i - 2 d_{i-1} + d_{i-2} \right\}^2 . \qquad (11)$$

where v^2 is a coefficient to control the smoothness of the drift. It must be noted that the all d_i at the each observation epoch are treated as unknowns in the analysis model. This is a most typical characteristic adopted in BAYTAP-G. The treatment of missing data which is occasionally occurred in observation is easily handled. It can be carried out by only removing one observation equation which corresponds to the epoch of missing observation from the observation equations. Even in this case, the drift d_i at that epoch is estimated by BAYTAP-G. The offset (step) estimation in drift is also easy if the position of offset is specified manually. It is estimated by a response coefficient of a step function which value is zero until the occurrence time of the step and one after that time. Equation (11) can be expressed schematically like as,

$$J(d) = \sum_{n=1}^{N} \{ \text{ irregular part (residual) } \}^2 + v^2 \sum_{n=1}^{N} \{ \text{ second difference of drift } \}^2 . \qquad (12)$$

The first half of the equation is same as the scheme of general least squares method, which allows the square sum of the errors to be minimize. The second half part express binding condition imposed on the drift model. This term can be said "penalty term" in the construction on observation equations.

To determine tidal parameters α_m, β_m by minimizing $J(d)$, the value of v^2 must

be given before applying least squares method. If the value is taken as exceedingly large, the freedom of the drift becomes smaller, then the close straight line drift will be estimated. Contrary, if the smaller value of v^2 is taken in the analysis, the freedom of the drift become lager, then the winding drift will be obtained. The parameter v^2 is named *hyperparameter* which determines the prior distribution of the parameters (the value d_i at each epoch) and controls the feature of the drift.

3.6. ABIC

The hyperparamter v^2 must be selected suitably to determine tidal parameters and drift by least squares method. The value of v^2 can be chosen by introducing an adequate Bayes model. The use of Bayesian information criterion proposed by Akaike (ABIC, Akaike's Bayesian Information Criterion, Akaike, 1974, 1980) is to select such hyperparameters.

BAYTAP-G selects suitable v^2 automatically by searching various v^2 which gives minimum ABIC. The ABIC* can be calculated actually by following equation. ABIC is slightly modified by the number of parameters (by the number of freedom).

$$\mathrm{ABIC} = N\log 2\pi + N\log\sigma^2 + N + \log\det(I + v^2 D^t D) - N\log v^2$$

$$\mathrm{ABIC}^* = \mathrm{ABIC} + 2\,(\text{number of parameters}) \qquad (13)$$

Where $\sigma^2 = J(d)/N$, I is a unit matrix and D is the $N\times N$ matrix defined as

$$D = \begin{pmatrix} 1 & & & & 0 \\ -2 & 1 & & & \\ 1 & -2 & 1 & & \\ & \cdot & \cdot & \cdot & \\ 0 & & 1 & -2 & 1 \end{pmatrix} . \qquad (14)$$

In the calculation of ABIC, initial values d_0 and d_{-1} of the drift is required. In BAYTAP-G, they are estimated by considering as unknowns. If the initial values are known in case such the analysis period is shifted successively, the drift determined in the previous analysis period will be used.

3.7. Implementation

In the programming of the procedure, we first take general precautions to keep a precision in numerical processing. Our model has many unknowns because we are going to evaluate the drift d_i at each observation epoch. The number of unknowns N often comes up to the order of 10^4 when we analyze a tidal data of several years duration. Therefore we must select the numerical implementation of least squares

analysis carefully to avoid numerical errors.

In the first step, the observation equations are build up including a "penalty term" of drift terms (the second term on the right hand side of equation (11)). We do not solve the normal equations to obtain the unknown parameters but adopt the QR decomposition of Givens' method. The use of normal equations is not appropriate for solving a large scale least squares problem from the viewpoint of numerical errors and stability.

In the calculation of σ^2, it is not necessary to use equation (12) directly. If we use QR decomposition of observation equations in the computation of least squares method, σ^2 is automatically obtained at the last process of QR decomposition. On the other hand, if we use normal equations in the least squares method, σ^2 must be calculated from equation (12). The $\det(I + v^2 D\,{}^tD)$ is also calculated in the process of QR decomposition. The determinant is obtained by the multiple of diagonal elements in the process of QR decomposition. The $\det(I + v^2 D\,{}^tD)$ becomes quite a large number which can not be expressed by the digital computer's floating decimals. In the actual case, $\log \det(I + v^2 D\,{}^tD)$ is not calculated directly but the summation of log(diagonal element) is calculated.

In search for the minimum ABIC, it is done in a finite step in v. The step of $\sqrt{2}$ or $1/\sqrt{2}$ in v is considered moderate step experimentally. The search range of lower limit can be given by the user of the program. The upper limit is fixed in 1024 in the program. There is no case to obtain such a large value for the parameter v, if illegal data are suitably removed in the analysis. Usually we get the minimum ABIC in the range of from 0.5 to 8.0 for actual tidal data.

The matrix of observation equations has the special feature of structural sparseness. The matrix is very sparse because of the use of 2nd order difference in the drift model. This simple structure of the matrix helps us to reduce memory size and also to reduce computation time when we are solving a large scale ($10^3 \sim 10^4$ order) least squares problems.

In the theoretical tide calculation, a lot of calculations of cos and sin functions are required. A simple minded least squares method often wastes computation time in the calculation of cos and sin. Fortunately, observation epoch of tidal data is usually equal interval (for example, one hour interval). In that case, the calculation of cos and sin can be optimized by applying a recurrence formula (Tamura, 1982). The adopted recurrence formula is a stable one, and helps to reduce computation time.

The features of the program are summarized as:

- The grouping model is adopted for the tidal component.
- The responses to the associated phenomena can be estimated.
- The drift at each data point is estimated.
- Occasional steps and missing observations are allowable if their positions are specified.

- Resolution in the frequency domain is dependent on the data length used for analysis. The default number of the principal tidal waves are listed in Table 3.

For given data set, the ABIC is used to select the optimal value of the combination of adjustable parameters in the model. The adjustable parameters are the number of groups of tidal components, the degree of smoothness of the variation in tidal factors, the maximum lag number of the response terms.

The minimum required memory size for BAYTAP-G is about 2MB. About 20 MB memory is required to estimate the drift of a few yeas data. If we need only the tidal parameters and need not to obtain drift part, we need only a few MB memory size. In many cases, the required memory size is not so large in the present computer of a workstation or a PC.

3.8. Usage and Examinations

a) Tidal analysis and residuals

The tidal analysis procedure BAYTAP-G is applied to the real gravity tide data which is obtained with a superconducting gravimeter at Esashi Earth Tides Station. Figure 7a shows the spectrum of gravity tide record of a suitable one year period. The response part by the atmospheric pressure change is subtracted before the spectrum calculation. The response coefficient of pressure change against gravity change is about -0.34 μ Gal/hPa. There are few time delay in the atmospheric response experimentally, thus a maximum lag K is taken to be 0 in the analysis.

Figure 7b shows the spectrum of residual time series data of one year. The original gravity data is same as Figure 7a. The tidal components and atmospheric pressure change effect are subtracted from original data in the analysis. This residual spectrum is a rather good sample experimentally though several peaks remains in the tidal bands.

Figure 7c shows the spectrum of gravity tide residuals around semidiurnal band. The data is same as that of Figure 7c. In Figures 7b and 7c, 15 tidal components are assumed in the analysis for one year records. This is a default number of tidal component adopted in BAYTAP-G. Figure 7d shows the spectrum of gravity tide residuals around semidiurnal band which is obtained by assuming 31 tidal components for one year records. Several peaks ($2N_2$, μ_2, T_2) which are seen in Figure 7c diminish in Figure 7d. The amplitudes and phases of minor tidal components (ex. $2N_2$, μ_2, ν_2, T_2) are usually assumed that they are same as those of major components whose angular velocities are close to them. This assumption works well when the frequency response structure of tidal signal is rather flat and usually this assumption is acceptable. The sample shown here suggests that it may be better to assume a fine frequency structure for precise tidal data processing.

In Figures 7a, 7b, 7c and 7d, spectrums for rather good quality data are referred. Figure 8a shows a gravity tide residual spectrum for the different observation period

in which rather large spectrum peaks remain in tidal bans contrary. Though 31 tidal components are assumed for one year records like as Figure 7d, large spectrum peaks remain. Figure 8b shows the residual spectrum for the same data used in Figure 8a. In this case, the tidal factors and phases are determined at every one month assuming 12 components successively for the same data used in Figure 8a. The spectrum peaks in semidiurnal band become lower and those of diurnal and terdiurnal disappear which are seen in Figure 8a. This result suggests that there may be a sensitivity change in gravity records or the existence of poor data period in the one year records. Figure 8c shows the residual spectrum for the same data set used in Figures 8a and 8b. The tidal factors and phases are determined at every 24 days assuming 12 components successively in this case. Each analysis period of 24 days is shorter than the recommended period of one month which is necessary to resolve principal tidal components. As a result of "over resolution" of tidal components, the power density around tidal bands shrinks abnormally.

Figure 9 shows the relative sensitivity change of a superconducting gravimeter at Esashi Earth Tides Station for the period including that of used in Figures 8a, 8b and 8c. There is unusual low sensitivity period in March 1997 (around 50580 modified Julian date) . The quality of tidal data around this period is considered not good. (The reason of bad observation condition is not certain.) In Figure 8a, one year gravity data which contains this poor observation period is used to demonstrate large residual peaks in tidal bands.

b) minimum ABIC search

The significant feature of BAYTAP-G is that the drift d_i at the all observation epoch are treated as unknowns, and the form of the drift is conditioned by the hyperparameter which is selected by the search for the minimum ABIC (or ABIC*). Therefore, we must investigate in what conditions the ABIC works well or not.

First of all, the minimum ABIC search for the synthesized drift data is tested (Figure 10). Hereafter, the notation of D is used instead of v for the hyperparameter. (In the BAYTAP-G user's manual, same notation D is used for the hyperparameter. Hereafter, D is not the matrix defined in equation (14)). The minimum ABIC is obtained at D=4.0 in this simulation. The estimated drift becomes more straight and the residuals become larger if a larger hyperparameter D is given. In opposite, the estimated drift becomes winding and the residuals becomes smaller if a smaller hyperparameter D is given in the drift estimation.

Next, the test for minimum ABIC search is carried out for the maximum lag number selection for associated data. Figure 11 shows the result of minimum ABIC search for varying maximum lag number for associated data set. The gravity tide record is used as a tidal data set and the atmospheric pressure records is used as a associated data set in this test. The upper part of Figure 11 shows the variation of

ABIC against the maximum lag number of response model in atmospheric pressure data. Lower Figure shows the decrease of mean residual against maximum lag number. The minimum ABIC is obtained at the 0 lag in this case. This result means that the assuming simple minded a linear coefficient without time delay (i.e. proportional) model is the best model for atmospheric pressure effect. There is a local minimum ABIC at the 4 lags. This means that there is a very weak frequency response structure in atmospheric response, but the decrease of mean residual is not so clear even considering the frequency response structure.

Next, a peculiar case of minimum ABIC search is investigated. A synthesized tidal data set is prepared which contains systematic errors. Figure 12 shows the result of minimum ABIC search for varying hyperparameter D. The global minimum ABIC is obtained at D=16.0 and a local minimum ABIC is obtained at D=1.0 in this test. Normally, local minimums never come if the analysis model is suitable and there is no outlying data in the input data set. The sample used here is obtained by giving systematic sinusoid residuals in the synthesized tidal data. Figure 13 shows the determined drift for the different D. The synthesized input data has systematic error of sinusoid wave of about 7 hour period. The mark × shows the given synthetic drift data. The black line is a drift model determined with a hyperparameter D=1.0 (in the case of local minimum ABIC). The red one is a drift model determined with D=16.0 (in the case of global minimum ABIC). More smooth drift model is obtained in the latter case.

At last, the relations among ABIC, parameter estimation errors and mean residual are investigated. In Table 4, the variations of amplitude factor estimation errors of major tidal components, ABIC and mean residuals (S.D.) are listed by changing the hyperparameter D. The sampling interval of tidal data is one hour. Gravity tide data set is used in this test. It is noted that the minimum ABIC is obtained at D=1.414, but minimum estimation errors of the tidal factors are obtained at different D. The minimum estimation errors of the diurnal components are obtained in the case of larger D is given compared with semidiurnal ones. The resolution between drift and tidal components becomes relatively worse if the periods of tidal components become longer (i.e. the estimation errors of diurnal components become larger compared with semidiurnal ones). In Table 5, the similar results are listed when the tidal data is resampled in two hour interval. The same gravity tide data set for Table 4 is used in this test. The minimum ABIC is obtained at D=2.828. The minimum estimation errors of the tidal factors of semidiurnal band are obtained at D=2.0～2.828, while the minimum estimation errors of diurnal components are obtained at D=8.0.

From those results, we might say that the interval of drift model might be allowed to set two hours or longer when the drift change of observation data is quite low like observations with a superconductiong gravimeter. In the present version of

BAYTAP-G, the sampling interval of input observation data and that of drift model are handled in same time interval. There is no necessity to treat the sampling intervals to be the same. The same sampling interval of the observation and the drift model is adopted for the convenience of the procedure implementation.

c) long period tide

The BAYTAP-G estimates the tidal parameters for diurnal, semidiurnal and terdiurnal bands ignoring the existence of long period tides. The components of long period tides will be remained in the estimated drift. In middle latitude (around 35°), the amplitudes of long period tides become small, because the observation site is close to the node of zonal tide. On the other hand, tidal observations at high latitude, such as at Syowa Station, Antarctica (69°S) or at Ny-Alesund, Norway (79°N) where gravity tide is observed with a superconducting gravimeter, the amplitudes of long period tides become larger than 10 μ Gal.

To estimate the influence of the existence of long period component in the estimation of diurnal, semidiurnal and terdiurnal components, analyses of synthesized gravity tide data at latitude 80°N is carried out. In this test, five different data sets are prepared to check the systematic biases which might be derived from long period tides in the estimation of diurnal, semidiurnal and terdiurnal tidal parameters. The five data sets are contain long period tides with the a priori factor of 0.0, 1.0, 2.0, 5.0 and 10.0, respectively. The artificial drifts are given to the data by random walk model and about 0.1 micro Gal random noise are given to the synthesized data sets. The results are shown in Table 6. No significant biases are derived from long period tides in the estimation of tidal parameters. However, if we want to study the long term drift change (for example, annual change of gravity, pole tide, secular change, etc.) the long period tide must be remove from estimated drift. It can be removed by the long period version of BAYTAP-G, or by theoretical tide calculation with a priori tidal parameters.

It is difficult to determine the tidal parameters of long period tides and short period ones at the same time. The binding condition for the drift adopted in BAYTAP-G becomes relatively weaker as the period becomes longer. The drift might become too flexible to determine long period tidal factors though the drift modeling works well for diurnal and semidiurnal tides. The sampling interval of 24 hours is recommended for the analysis of long period tides. At that time, short period tides must be removed before the analysis of long period tides.

3.9. Remarks

BAYTAP-G does not treat the leap second rigorously though the difference of dynamical time TD and universal time UT are taking into account. There is uncertainty of time system within 0.5 seconds in the present version. The time

difference of 1 second derives systematic phase shift of 0.°008 for semidiurnal tide. If we want to discuss tidal phase in the order of 0.°001, we must treat the time system rigorously at the three steps in the observations, in data preprocessing of digital filtering, and in tidal analysis.

The statistical criterion ABIC is introduced to determine the goodness or poorness of the analysis model. It is used to determine which variation of an analysis model is the best one. The selection of a model must be done for the same data sets. It can not be used to judge the data quality. The ABIC varies with the data length N, or the existence of missing data. The ABIC has a meaning of the relative difference between two analysis models. The ratio of two cases nor the sign of ABIC value has no meanings.

There are special uses of BAYTAP-G. It can be used for the smoothing of the input data set employing a Bayes model without estimating tidal parameters. It can be used as a response analysis program without estimating tidal parameters. Three kinds of response sources can be treated in this case. The maximum number of data sets can be changed by modifying the PARAMETER statements in the program.

4. Applications to Practical Tidal Data

The tidal analysis procedure BAYTAP-G can be applied to several kinds of tidal data. It can analyze gravity tide, tilt tide, strain tide, ocean tide and so on. The long period version of BAYTAP-G can analyze UT1 or LOD (length of day) of earth rotation data beside them. Here we show several applications of tidal data processing with BAYTAP-G and the harmonic tables of Tamura (1987).

1) strain data

Figure 14 gives an example of tidal analysis of the crustal strain data with BAYTAP-G. The sample strain data is north-south component of strain data of one month period in June 1998. It is obtained at the Esashi Earth Tides Station (39.°1 N, 141.°3 E, 393mH), National Astronomical Observatory. BAYTAP-G resolves input data into four parts, tidal part, response part, drift part and irregular part. The left side in the upper part is the raw observation data including missing observation period. The observation unit is 10^{-9} strain and expansion of the ground is taken to be positive. In the left side of the middle, the estimated tidal part is shown. In the left side of the bottom, the response part of atmospheric pressure is shown. In the right side of the upper row, the drift part is shown. Even in the period of missing observations, the drift part is continuously estimated under the binding condition of equation (6). Since the tidal components of the diurnal and the shorter bands are removed, and the response components to the atmospheric pressure are removed from original data, it becomes clear how the drift is in detail to the extent of the of 10^{-9} strain. In the right side of the middle, the irregular part (residuals) is shown. There are slightly large residual parts to show hereby as an example. In the case of analysis whose purpose is the precise determination of tidal parameters, re-analysis should be carried out after removing such outliers, if exist. In the right side of the bottom, the drift part in the case of not considering the atmospheric pressure is shown.

It is obvious that almost all of the irregular drift fluctuation comes from the change of the atmospheric pressure in the last case. It is exceedingly difficult to express such drift pattern seen in right side bottom of Figure 14 in a polynomial of the time t or sinusoidal waves. In the study of earthquake prediction by watching the detailed precursory phenomena, it might be understood that it is very effective to estimate the drift at every observation epoch by removing tidal variation and disturbances such as atmospheric pressure change. It is quite difficult to estimate strain accumulation or a precursory phenomenon directly from such raw observation data shown in the left side top.

2) gravity tide

The gravity tide data at Syowa Station, Antarctica was analyzed by BAYTAP-G. Detail of the observations and analysis results are discussed in Sato *et al.* (1995) and Tamura *et al.* (1997). Here we introduce the outline of the observations and analyses

results. Also the effect of free core resonance (FCR: Sasao *et al.*, 1980; Wahr, 1981) will be mentioned.

The gravity tide observations with a superconducting gravimeter at Syowa Station, Antarctica (39.°6 E, 69.°0 S 24m H) started in January 1993. The first three-year data was analyzed by Tamura *et al.* (1997). The observations is still continued at present (1999). The original data is sampled at every 2 second (at present, 1 second interval). A digital low-pass filter was applied to the original data at first step in the analysis, then one hour sampling data set was prepared for the tidal analysis. Next pre-processing of the data was carried out with BAYTAP-G in the purposes to reject abnormal data from the data set and to point out the existence of steps by dividing the whole observation period into a few months period. After removing outliers, the three-year data was processed at once.

The tidal factors and phases can be obtained rather business like way by BAYTAP-G, if a data set of one hour sampling with a suitable format is prepared. To extract geophysical meanings from obtained tidal factors and phases, several corrections are necessary for the results.

The required corrections are, (1) the characteristic of the analogue low-pass filter which is build in the electronic circuit of the SG, (2) inertial change, and (3) ocean tide loading effects. The tidal gravity signal from the gravimeter is low-pass filtered with a cutoff period of about 50s, and the associated linear phase delay of 0.1558 degree/cpd must be corrected for. The gain of the filter can be accepted as flat in the tidal frequency bands. The inertia correction is to be corrected. It is a correction for the additional gravity acceleration change caused by the dynamic vertical motion of the observation site due to the sinusoidal tidal displacement. The magnitude of this correction is roughly $-0.°001$ and $-0.°004$ for diurnal and semidiurnal factors, respectively.

The ocean tide loading effects have just the same frequencies as those of the solid earth tides. Consequently, these effects cannot be distinguished in tidal observations or statistical methods. To estimate these effects, the global convolutional integral method is required using both global ocean tide models and loading Green function models. For our analysis, recent global ocean tide models of Matsumoto *et al.* (1995) were used. The convolutional integration method GOTIC developed by Sato and Hanada (1984) was applied to estimate ocean tide loading effects. The effects for diurnal tides reach almost 10% of solid tides, while those of semidiurnal tides attain 20% of solid tides. The ocean tide models by Schwiderski (1980, 1983) are also available by optionally in GOTIC.

Those three corrections are not necessary in the prediction of tidal variation. The predicted (or synthetic) tidal data are used to extract tidal change from the observed gravity records to discuss non-tidal gravity changes.

Figure 15 shows the results of gravity tide analysis at the Syowa Station,

Antarctica. The marks ■ show tidal factors on diurnal band of raw analysis result. The marks ◆ show the result of after three corrections including ocean tide effects. At that time, only four principal components in diurnal band (Q_1, O_1, P_1 and K_1) were available as the global ocean model, thus the corrected results of only four components are illustrated in Figure 15. The solid line gives theoretical admittance curve considering fluid core resonance effect (Wahr, 1981). Without ocean tide correction, the obtained tidal factors differ in large way from the theoretical values based on solid earth model. After correcting the ocean tide effects, it becomes clear that the factor of K_1 is smaller than that of Q_1, O_1 and P_1, which is one of the evidence of the fluid core resonance effect.

3) core undertones

Core undertones are oscillation of fluid outer core whose restoring forces are gravity and the Coriolis force. They are internal gravity waves of fluid core in other words. Their existence and their oscillation frequencies are especially sensitive to the stability profile of the outer core. If the core undertones are detected and the frequencies are identified, they give the restrictions for the density profile, turbulence aspect, viscosity of the fluid core. Those parameters are not constrained enough from seismic data. Those oscillations are considered very small signal even if they exist. There periods are considered in the order of a day and it becomes complicated to determine the theoretical periods by the existence of strong coupling of Coriolis force. There are other core modes oscillation named Slichter mode (Slichter, 1961; Slichter *et al.*, 1979). They are translational oscillation of earth's solid inner core. Attempts to search for core undertones are made by several groups by using gravity acceleration data. There are some reports of the detection of core undertones or the Slihiter mode, but it can be said that there are no obvious evidences and the detection is not confirmed yet (Melchior and Ducarme, 1986, Zürn *et al.* 1987, Cummins *et al*, 1991, Smylie, 1999).

The negative result of core undertone search was reported by Cummins *et al.* (1991). They used gravity data of global IDA network. In the gravity acceleration data, the tidal variation has the most large spectrum power and it must be removed from the original records. The expected signals of core undertones may have the amplitude of only a few nano Gal level, while the tidal signals have the amplitude about 100 μ Gal. Moreover, the periods of core undertones are close to the tidal bands and the leakage from this band will seriously give biases to the gravity spectrum in the frequency of interest. Thus the tidal signals must be reduced carefully from the observed gravity data. They subtracted tidal signals from the data at each station by estimating tidal components by BAYTAP-G. After removing tidal parts, typical 100 μ Gal amplitude in tidal peaks are reduced to roughly 0.05 μ Gal. The noise level is rather higher compared with the bad case of a superconducting gravimeter shown in Figure 8a. They used the IDA network data whose gravity

sensors are spring type gravimeters of LaCoste and Romberg. The noise level of a superconducting gravimeter is lower than such gravimeters in the period of tidal band or longer.

4) long period tides

The tidal deformation of the solid earth follows the periodical change of moment of inertia around earth's rotational axis. The zonal change of tidal deformation caused by long period tide yields the periodical change of earth's moment of inertia. The deformation of tesseral function pattern by diurnal tide and the sectorial function pattern by semidiurnal tide do not yield the periodical changes of moment of inertia around earth's rotational axis. The total angular momentum of the earth should be conserved even if the earth deforms. For the result, the earth's axial rotation speed must vary according to the long period tidal deformation. Therefore, the harmonic table of long period tide can be converted to the tables of Δ UT1 or Δ LOD series by some roles (Yoder *et al.*, 1981; Tamura, 1993). The fortnightly change (Mf) of UT1 has a amplitude of about 0.9 milli second, and that of monthly change (Mm) is about 0.8 milli second. Their amplitudes are related to the global mass distribution change by the tidal deformation, the Love's number k_2 can be discussed from the analysis of Δ UT1 or Δ LOD. The real earth has a fluid core inside, and it can rotate differentially form the solid part (mantle) of the earth. Considering several effects including existence of fluid core, Merriam (1980) introduced a coefficient κ which represents earth's zonal response. The earth's nonlinear response to outer force is expected in the phenomena whose periods are longer than diurnal tidal band. A larger κ is expected for Mm tide compared with that of Mf tide if the solid earth (mantle) has somewhat nonlinearity in those frequencies.

Chao *et al.* (1995) analyzed the LOD data which were obtained by the IERS (International Earth Rotation Service). They analyzed 13 years of LOD data (1980-1992) and revealed strong signals for 9 long period tides ranging from 5 to 35 days period. Major tides of 27 components were analyzed and obtained the coefficients κ for 11 components with the sufficient signal to noise ratio. The obtained κ is close to the theoretical value of 0.315, but somewhat small than it. The theoretical value is based on the model for an elastic mantle completely decoupled from the fluid core and equilibrium long period ocean tides. A small amount of dispersion was also detected, where longer period tides tend to have larger κ magnitude and shorter phase lag, with correction of recent non-equilibrium ocean tide models. However, an equilibrium long period ocean tide model and a pure elastic mantle model is not disallowed from the analysis of LOD data.

5) others

The BAYTAP-G is applicable to other kind of tidal data such as tilt tide and ocean one. There are several tidal phenomena which are hard to develop theoretical model in quantity. For examples, ground water level or pressure, chemical changes in deep

wells, ground electric potential or current, and so on often show tidal variations but they don't have theoretical values. Such kind of data can be analyzed by referring the local phase of tidal potential. The theoretical time series of non-dimensional "potential / gravity / earth's radius" can be used as a reference theoretical tide in the analyses of such kind of data. This reference value can be also applicable in the analysis of a strain data, an areal or a volumetric strain data if we don't want to use Love's number h and Shida's number l in the concept that the h and l are the unknowns and to be estimated from the tidal observations and analyses.

5. Concluding Remarks

5.1. Supplemental Comments

a) Necessary harmonic terms

The harmonic tables are developed aiming to process high precision tidal data such as that obtained from a superconducting gravimeter. In case of that we don't require so high accuracy in the theoretical tide calculation, of course we need not uses current additional tables listed in Appendix. If we want to obtain only 0.1 μ Gal precision in the gravity tide calculation, Tamura (1987) tables are enough. Moreover, only a half of terms in the tables may be enough to obtain 0.1 μ Gal precision as shown in Figure 3. However, the author recommend to use all terms (1200 terms) in any case to avoid unexpected troubles. Recent computers even PCs are powerful enough to compute theoretical tides. It may not necessary to reduce only a slight computation time except in the case of some kind of real time control system.

The treatment of permanent tide M_0S_0 is recommended to use the tidal factor of 1.0 (not 1.16 or 0.0) in the correction of gravity survey. The difference of the factor 1.16 and 1.0 might be small if the gravity observation is carried out in the middle latitude like in Japan. It must be carefully corrected in the observation in high latitude or around the equator where the amplitudes of long period tides become larger. If we use a tidal correction program based on "ephemeris tide", it will be complicated to give the factor 1.0 only to M_0S_0 and give 1.16 (or other) to other time varying components. The computation with harmonic tables can simply give different tidal factor and phases to individual tidal component.

b) Atmospheric pressure response

BAYTAP-G models the effect of atmospheric pressure change by a response method. In the gravity tide data analysis, about 80% or 90% of that effect can be removed using the atmospheric pressure data on site. Nevertheless, somewhat atmospheric pressure effect still remains in estimated drift part. The one point atmospheric pressure data has a limit to represent the spatial structure of the atmosphere. The atmosphere has two different spatial structures, one is a regional pressure distribution following weather changes, the other is the global phenomenon of atmospheric tide. The response coefficients for two kinds of phenomena are different from each other considering the difference of atmospheric mass distributions of two phenomena. The BAYTAP-G models the atmospheric pressure effect by a statistical model, not considers the physical processes. Therefore, both effects cannot be removed at the same time by the analysis program. Usually, atmospheric tide of S_1, S_2, S_3, S_4 and S_5 signals remain in the drift parts in the case of gravity data analysis.

c) ABIC

We introduced a statistical criterion ABIC in BAYTAP-G, and the essential part of the parameter estimation algorithm is same as that of least squares method. Thus

the ABIC is not an almighty criterion which can be applied in *any* case. It works well under the conditions that the least squares method requires. The conditions are,

- There is no modeling error itself.
- The observations are carried out impartially.
- The observation error distributes in normal distribution.

The actual data often contain illegal data in it, and the assumption of error distribution can not be realized. Thus the illegal data should be removed in the final result by using a suitable pre-processing method. Usually, tidal analysis is repeated several times to the same data set to remove such illegal data iterative. This pre-processing can be performed by BAYTAP-G itself. Considering the existence of outlying data in the input data set, BAYTAP-G assumes the upper and lower limits for the hyperparameter D in search for the minimum ABIC.

The use of ABIC must be paid attention to. ABIC is a criterion to compare the goodness of the different analysis models for the same data set. The use of ABIC is utterly nonsense for the judgment as to which quality of the observation data is better in January or February. For such comparison, how large the hyperparameter D, which determines the straightness of the drift, can be used a quality index.

d) Sampling interval

The sampling interval of tidal data to be analyzed is expected one hour interval. The main tidal bands are diurnal and semidiurnal, thus the one hour sampling data is considered adequate to represent the variation of tidal frequency. If we can use dense data in time space, a low-pass filter should be applied to construct one hour sampling data. In BAYTAP-G, assumption that the second difference of the drift becomes close to zero is adopted as the restriction condition in the drift form. For the sake of giving effective constraints to the drift model, an adequate sampling interval is required for the phenomenon to be analyzed. For example, one hour sampling is not proper to analyze long period tide. In that case, 24 hour sampling data should be compiled after removing diurnal and shorter period tides. When the response of rather slowly changing atmospheric pressure variation with several-day cycle is to be determined, it is occasionally advisable for the sampling interval to be taken 2 or 3 hour interval instead regular one hour sampling.

e) Program and sample data sets

The tidal analysis program BAYTAP-G was distributed in a part of time series analyses program package TIMSAC-84 from the Institute of Statistical Mathematics at first. The program BAYTAP-G was revise several times after that, and now it is distributed with suitable sample analysis data set from the author. It is written by the standard FORTRAN77 language regulation carefully, and thus it has very high portability. It is available in several kinds of workstations or personal computers.

5.2. Contributions and Prospect

The development of various tidal harmonic tables and that of tidal analysis method are carried out for the purpose of high precision tidal data processing. The harmonic tables developed by Tamura (1987) are integrated into the analysis program BAYTAP-G. The CTE tables are optionally available in BAYTAP-G for the comparison of both developments. The tables given by Tamura (1995) and the revised ones discussed in this thesis are not integrated into the program yet. For most cases, the accuracy of the harmonic tables which are integrated into the present version of the program is enough to analyze tidal data. It is considered that more high accuracy in the theoretical tide calculation will be required in the analysis of extremely high quality tidal data. If the noise level of gravity tide observations with a superconducting gravimeter is improved to half level in some way compared with present status, the accuracy of the harmonic tables by Tamura (1987) will be insufficient. At that time, we will need to integrate the harmonic tables by Tamura (1995) and the revised ones into the tidal analysis model.

The Working Group on "High Precision Tidal Data Processing", under the Commission V (Earth Tide Commission) of International Association of Geodesy (IAG), reported in 1990 that "For high precision data we recommend the use of potentials which include the 4th order term. We realize that at present it is not possible to decide which of the new potentials (Tamura, 1987; Xi, 1987) is better. According to the comparison to high precision data they look equivalent, although they apply different constants and different approaches of the problem." Although the precision of both developments are almost equivalent, the former development looks like to be used widely not only in Japan but in the world. It is because that the author (Tamura) distributed not only the harmonic tables of own development but sample program to use the harmonic tables, actively. In the early time, they were distributed with suitable magnetic media. At present, they are distributed by computer networks freely.

The tidal analysis program BAYTAP-G is also distributed widely. The number of domestic users that the author grasps is more than 70. The program is also distributed to more than 20 overseas institutes and universities. The number of overseas users is not grasped correctly since the program is allowed to re-distribute to the third party, and it can be copied freely from the Internet home page of the Earth Tide Commission at present. The tidal analysis program BAYTAP is developed aiming to handle tidal data whose drift is fluctuating irregularly, and aiming to obtain high precision tidal parameters from observations. The author developed the program and maintains it for having interest in the determination of tidal parameters, but not all of BAYTA-G users don't have interest in tidal signals themselves. A part of users have interest in the determination of drift features instead of tidal variations. They use the program as a handy tool to remove tidal variation or to remove

environmental disturbances from some kind of observation data. In the analyses of crustal strains and tilt changes for the purpose of monitoring crustal movements, the interpretation of the drift components is sometimes more essential than the determination of tidal parameters. The program BAYTAP-G is now used widely for the analyses of various geophysical data by many users.

In the early stage of the development of BAYTAP-G, it was not considered to analysis data sets whose drift rates are quite low such as obtained by superconducting gravimeters. It was designed to be used for multipurpose at that time. In practice, it is used for the analyses of strain, tilt, gravity, ocean, underground water level, ground electric potential data, etc., and their quality or noise levels differ in wide range. As mentioned in section 3.8, the drift model adopted in BAYTAP-G might be too flexible to treat tidal data of a superconducting gravimeter. It is desired to construct a special designed analysis model to handle the data whose drift is quite low and quality is very fine. The recent computer, even for a personal one, has enough ability to construct a new sophisticated analysis model on huge data set.

The long period tides and pole tide are notable to study non-elastic response of the earth. It is estimated that the non-elasticity of the mantle will appear in the period longer than fortnightly Mf or monthly Mm tides. The long period tides are observed by gravity change in high latitudes or close at the equator. It is also observed in the periodical UT1 variations. It is consider that the difference of the earth model and the actual one becomes larger when the period of subjected phenomenon becomes longer. We have much scopes in the study of long period phenomena since the observations analyses of long period tides and pole tide are not so much done still at present.

This thesis is based on following three papers.

1. A harmonic development of the tide generating force,
   Marées Terrestres Bulitin d'Informations, **99**, 6813-6855, 1987,
   Tamura, Y.

2. A procedure for tidal Analysis with a Bayesian information criterion,
   Geophys. J. Int., **104**, 507-516, 1991,
   Tamura, Y., Sato, T., Ooe, M., and Ishiguro, M.

3. Additional terms to the tidal harmonic tables,
   Proc. 12th Int. Sympos. Earth Tides, ed. H.-T. Hsu., Beijing, China, 345-350, 1995,
   Tamura, Y.

Acknowledgments

The author is indebted to the following collegues for providing necessary data used in this study: T. Tsubokawa and S. Tsuruta of National Astronomical Observatory, Mizusawa (NAOM) for strain tide data at the Esashi Earth Tides Station; T. Sato and K. Asari of NAOM for gravity tide data by the superconducting gravimeter at Esashi; K. Nawa of Geological Survey Institute, Y. Aoyama of the Graduate University for Advanced Studies, the members of the 34th Japanese Antarctic Research Expedition (JARE-34), JARE-35, JARE-36 for the gravity tide data at Syowa Station, Antarctica; R. S. Gross of Jet Propulsion Laboratory for earth rotation data Space92; S. Manabe for the numerical ephemerides by JPL. The author would like to thank M. Ooe of NAOM and M. Ishiguro of the Institute of Statistical Mathematics for discussing on the statistical models. The author also would like to thank S. Takemoto of Kyoto University for his kind advice on tidal studies.

Early phases of this study were partially supported by a Grant in Aid for Scientific Research of the Ministry of Education, Science and Culture (58740178, 0474022), a grant of the Institute of Statistical Mathematics Cooperative Research Program (88-ISM.CRP-61), a grant for Joint Research of the National Institute of Polar Research (form 1994 to 1996) and a grant for Joint Research Program of the Graduate University for Advanced Studies (from 1995 to 1999).

References

Akaike, H., 1974, A new look at the statistical model information, *IEEE Trans. Automat. Control*, **AC-9**, 716-723.

Akaike, H., 1980, Likelihood and Bayes procedure, *Bayesian Statistics*, Valencia, eds. J. M. Bernado, M. H. De Groot, D. U. Lindley and A. F. M. Smith, University Press, 143-166.

Aoki, S., Guinot, B., Kaplan, G. H., Kinoshita, H, McCarthy, D. D., and Seidelman, P. K., 1982, The new definition of universal time, *Astron. Astrophys.*, **105**, 359-361.

Büllesfeld, F.-J., 1985, Ein Beitrag zur harmonischen Darstellung des gezeitenrzeugenden Potentials, Deutsche Geodätische Kommission, Reihe C, Heft Nr. 314, Munchen.

Cartwright, D. E., and Tayler, R. J., 1971, New computation of the tide- generating potential, *Geophys. J. Roy. Astron. Soc.*, **23**, 45-74.

Cartwright, D. E., and Edden, A. C., 1973, Corrected table of tidal harmonics, *Geophys. J. Roy. Astron. Soc.*, **33**, 253-264.

Chao, B. F., Merriam, J. B., and Tamura, Y., 1995, Geophysical analysis of zonal tidal signals in length of day, *Geophys. J. Int.*, **122**, 765-775.

Cummins, P., Wahr, J. M., Agnew, D. C., and Tamura, Y., 1991, Constraining core undertones using stacked IDA gravity records, *Geophy. J. Int.*, **106**, 189-198.

Doodson, A. T., 1921, The harmonic development of the tide-generating potential, *Proc. Roy. Soc. London*, **A**, **100**, 305-329.

Doodson, A. T., 1954, Re-print of above with minor corrections, same title, *Int. Hydrog. Rev.*, **31**, 11-35.

Fukushima, T., 1981, Trigonometric series for the coordinates of the objects in the solar system II the outer planets, *Rept. Hydrog. Res.*, **16**, 149-166.

Hartmann, T., and Wenzel, H.-G., 1994, The harmonic development of the earth tide generating potential due to the direct effect of the planets, *Geophys. Res. Lett.*, **21**, 1991-1993.

Hartmann, T., and Wenzel, H.-G., 1995, The HW95 tidal potential catalogue, *Geophys. Res. Lett.*, **22**, 3553-3556.

Ishiguro, M., 1981, A Bayesian approach to the analysis of the data of crustal movements, *J. Geodetic Soc. Japan*, **27**, 256-262.

Ishiguro, M., and Tamura, Y., 1985, BAYTAP-G in TIMSAC-84, *Computer Science Monographs*, **22**, 56-117.

Kubo, Y., 1980, Trigonometric series for the coordinates of the objects in the solar system, *Rept. Hydrog. Res.*, **15**, 171-184.

Lambert, A., 1974, Earth tide analysis and prediction by the response method, *J. Geophys. Res.*, **79**, 4952-4960.

Matsumoto, K, Ooe, M., Sato, T., and Segawa, J., 1995, Ocean tide model obtained

from TOPEX/POSEIDON altimeter data. *J. Geophys. Res.*, **100**, 25319-25330.

Melchior, P., and Ducarme. M., 1986, "Detection of inertia gravity oscillations in the earth's core with a superconducting gravimeter at Brussels", *Phys. Earth Planet. Inter.*, **36**, 1-16.

Melchior, P., and Venedikov, A. P., 1968, Derivation of the wave M_3 (8.^{h}279) from the periodic tidal deformation of the earth, *Phys. Earth Planet. Inter.*, **1**, 363-372.

MERIT Standards, 1983, United States Naval Observatory Circular No.167.

Merriam, J. B., 1980, Zonal tides and changes in the length of day, *Geopyhs J. Roy. Astron. Soc.*, **62**, 551-561.

Munk, W. H., and Cartwright, D. E., 1966, Tidal spectroscopy and prediction, *Phil. Trans. Roy. Soc. London*, **A259**, 531-581.

Ooe, M., and Sato, T., 1983, An extended response method for analysis of disturbed earth tides data, *Proc. 9th Int. Sympos. Earth Tides*, ed. J.T. Kuo, New York, E. Schweizerbart'sche Verlangsbuchhandlung, Stuttgart, 299-310.

Roosbeek, F., 1996, RATGP95: a harmonic development of the tide-generating potential using an analytical method, *Geophys. J. Int.*, **126**, 197-204.

Sasao, T., Okubo, S., Saito, M., 1980, A simple theory on the dynamical effects of a stratified fluid core upon nutational motion of the Earth, *Proc. IAU Sympos. 78, "Nutation and the Earth's Rotation"*, eds. E. P. Fedrov, M. L. Smith and P. L. Bender, 165-183.

Sato, T., Ooe, M., and Sato, N., 1980, Observations of the tidal strain at the Esashi Earth Tides Station, *J. Geod. Soc. Japan*, **26**, 35-49. (in Japanese with English abstract)

Sato, T., and Hanada, H., 1984, Computer program 'GOTIC' for the computations of oceanic tidal loading effects, *Publ. Int. Latit. Obs. Mizusawa*, **18**, 29-47.

Sato, T., Shibuya, K., Tamura, Y., Kanao, M., Ooe, M., Fukuda, Y., Seama, N., Nawa, K., Kaminuma, K., Ida, Y., Kumazawa, M., and Yukutake, T., 1995, One year observations with a superconducting gravimeter at Syowa Station, Antarctica, *J. Geod. Soc. Japan*, **41**, 75-89.

Schwiderski, E. W., 1980, On charting global ocean tides, *Rev. Geophys. Space Phys.*, **18**, 243-268.

Schwiderski, E. W., 1983, NSWC ocean tide data tape, GOTD 1983, U.S. Naval Surface Weapons Center, Virginia.

Slichter, L. B., 1961, The fundamental free oscillation of the earth's inner core, *Proc., Nat., Acad. Sci. U.S.A.*, **47**, 186-190.

Slichter, L. B., Zürn, W., Syrstad, E., Knopoff, L., Smythe, W. D., and Uffelman, H., 1979, Long-period gravity tides at the South Pole, *J. Geophys. Res.*, **84**, 6207-6212.

Smylie, D. E., 1999, Viscosity near earth's solid inner core, *Science*, **284**, 461-463.

Standish, E. M. Jr. and Williams, J. G., 1981, The lunar and planetary ephemerides, DE118/LE62.

Standish, E. M. Jr. and Williams, J. G., 1982, The lunar and planetary ephemerides, DE200/LE200.

Tamura, Y., 1982, A computer program for calculating the tide-generating force, *Publ. Int. Latit. Obs. Mizusawa*, **16**, 1-20.

Tamura, Y., 1987, A harmonic development of the tide generating force, *Marées Terrestres Bulitin d'Informations*, **99**, 6813-6855.

Tamura, Y., Sato, T., Ooe, M., and Ishiguro, M., 1991, A procedure for tidal Analysis with a Bayesian information criterion, *Geophys. J. Int.*, **104**, 507-516.

Tamura, Y., 1993, Periodic series of Δ UT1, *IAG Sympos. 112, Geodesy and Physics of the Earth*, Springer Verlag, 435-438.

Tamura, Y., 1995, Additional terms to the tidal harmonic tables, *Proc. 12th Int. Sympos. Earth Tides*, ed. H.-T. Hsu, Beijing, China, 345-350.

Tamura, Y., Aoyama, Y., and Nawa, K.: 1997, Gravimetric tidal factors at Syowa Station obtained from three-year observations with a superconducting Gravimeter, *Proc. NIPR Symp. Antarct. Geosci.*, **10**, 1-10.

Tamura, Y., 1999, Analysis of earth tides data, *The Practice of Time Series Analysis*, eds. H. Akaike and G. Kitagawa, Springer, 327-339.

Venedikov, A. P., 1966, Une méthode pour l'analyse des marées terrestres à partir d'enregistrements de longueur arbitraire, *Communications de l'Observatoire Royal de Belgique*, No.250, Serie Geophysique, No.71.

Wahr, J. M., 1981, Body tides of an elliptical, rotating, elastic and oceanless earth, *Geophys. J. Roy. Astron. Soc.*, **64**, 677-703.

Wenzel, H.-G., 1998, Earth tide data processing package ETERNA 3.30: the nanogal software, *Proc. 13th Int. Sympos. Earth Tides*, Brussels, 487-494.

Xi, Q.-W., 1987, A new complete development of the tide-generating potential for the epoch J2000.0, *Marées Terrestres Bulitin d'Informations*, **99**, 6766-6812.

Yoder, C. F., Williams, J. G., and Parke, M. E., 1981, Tidal variation of earth rotation, *J. Geohys. Res.*, **86**, 881-889.

Zürn, W., Richter, B., Rydelek., P. A., and Neuberg, J., 1987, Comments on "Detection of inertia gravity oscillations in the earth's core with a superconducting gravimeter at Brussels", *Phys. Earth Planet. Inter.*, **49**, 176-178.

Tables

Table 1. Constants used in the harmonic developments by Tamura (1987) and the later ones by the author.

Geocentric Constant of Gravitation	$GE = 3.98600448 \times 10^{14}$ m3s^{-2}
Heliocentric Constant of Gravitation	$GS = 1.3271244 \times 10^{20}$ m^{3}s^{-2}
Earth-Moon Mass Ratio	$\mu = 0.012300034$
Equatorial Radius of the Earth	Re = 6378137 m
Astronomical Unit	$1au = 1.4959787066 \times 10^{11}$ m
Moon's Sine Parallax	$\sin \Pi = 3422."448$

Table 2. Number of harmonic terms for each potential degree and species. The additional terms for degree 4 potential are developed at this time.

Potential	Tamura (1987)	Tamura(1995)	Present Revision (1999)
20	211	180	282
21	345	256	412
22	281	207	352
30	60	67	132
31	91	118	189
32	84	94	145
33	68	67	126
40	10	(19)	26
41	14	(26)	40
42	12	(23)	41
43	14	(18)	29
44	10	(16)	29
Total	1200	1091	1803

Table 3. Number of tidal components assumed in tidal analysis program BAYTAP-G according to the observation data period.

Observation data period (days)	Number of tidal components assumed in BAYTAP-G automatically
$P < 8$	3
$8 \leqq P < 16$	5
$16 \leqq P < 180$	12
$180 \leqq P < 364$	14
$364 \leqq P < 2000$	15
$2000 \leqq P$	20
optionally	22 or 31

Table 4.

Relations among hyperparameter D and amplitude factor estimation errors of major tidal components, ABIC and mean residuals (S.D.). The sampling interval of tidal data is *one* hour. Gravity tide data set is used in this test. It is noted that the minimum ABIC is obtained at D=1.4142, but minimum estimation errors of the tidal factors are obtained at different D. Minimum estimation errors of the diurnal components are obtained in the case of larger D is given compared with semidiurnal ones. Resolution between drift and tidal components becomes relatively worse if the periods of tidal components become longer (i.e. the estimation error of diurnal components becomes larger compared with semidiurnal ones).

	Amplitude Factor Estimation Error						
D	O_1	K_1	M_2	S_2	M_3	ABIC	S.D.
0.1250	0.00162	0.00091	0.00020	0.00042	0.00579	−17790.02	0.0139
0.1768	0.00153	0.00086	0.00019	0.00040	0.00547	−17955.81	0.0185
0.2500	0.00140	0.00078	0.00018	0.00036	0.00501	−18196.46	0.0238
0.3536	0.00123	0.00069	0.00015	0.00032	0.00443	−18495.47	0.0295
0.5000	0.00104	0.00058	0.00013	0.00027	0.00381	−18800.87	0.0352
0.7071	0.00085	0.00048	0.00011	0.00023	0.00324	−19050.56	0.0409
1.0000	0.00069	0.00038	0.00009	0.00018	0.00277	−19203.20	0.0465
1.4142	0.00055	0.00031	0.00007	0.00015	0.00245	−19251.97	0.0522
2.0000	0.00043	0.00024	0.00006	0.00013	0.00225	−19216.99	0.0579
2.8284	0.00034	0.00019	0.00005	0.00011	0.00218	−19126.62	0.0636
4.0000	0.00026	0.00015	0.00005	0.00010	0.00218	−19005.79	0.0690
5.6569	0.00021	0.00012	0.00004	0.00009	0.00224	−18870.03	0.0743
8.0000	0.00016	0.00009	0.00004	0.00009	0.00234	−18715.32	0.0793
11.3137	0.00013	0.00008	0.00004	0.00009	0.00246	−18520.35	0.0845
16.0000	0.00012	0.00007	0.00004	0.00010	0.00260	−18265.11	0.0900
22.6274	0.00011	0.00007	0.00005	0.00010	0.00277	−17940.88	0.0962
32.0000	0.00010	0.00007	0.00005	0.00011	0.00297	−17543.26	0.1033
45.2548	0.00011	0.00007	0.00005	0.00012	0.00321	−17065.27	0.1116
64.0000	0.00011	0.00007	0.00006	0.00013	0.00349	−16498.41	0.1213
90.5097	0.00012	0.00008	0.00006	0.00014	0.00382	−15836.19	0.1331
128.000	0.00013	0.00008	0.00007	0.00015	0.00423	−15074.38	0.1475

underline indicates minimum values

Table 5.

Relations among hyperparameter D and amplitude factor estimation errors of major tidal components, ABIC and mean residuals (S.D.). The sampling interval of tidal data is *two* hour. Gravity tide data set is used in this test. The minimum ABIC is obtained at D=2.8284. The minimum estimation errors of the tidal factors of semidiurnal bans are obtained at D=2.0～2.8284, while the minimum estimation errors of diurnal components are obtained at D=8.0.

	Amplitude Factor Estimation Error						
D	O_1	K_1	M_2	S_2	M_3	ABIC	S.D.
0.5000	0.00052	0.00029	0.00008	0.00016	0.00289	−7790.85	0.0487
0.7071	0.00043	0.00024	0.00007	0.00014	<u>0.00288</u>	−7919.61	0.0564
1.0000	0.00035	0.00020	0.00006	0.00013	0.00293	−8034.96	0.0636
1.4142	0.00028	0.00016	0.00006	0.00013	0.00305	−8130.96	0.0701
2.0000	0.00022	0.00013	<u>0.00006</u>	<u>0.00013</u>	0.00321	−8199.64	0.0761
2.8284	0.00019	0.00011	<u>0.00006</u>	0.00013	0.00340	<u>−8229.12</u>	0.0821
4.0000	0.00016	0.00010	0.00006	0.00013	0.00363	−8210.72	0.0883
5.6569	0.00015	0.00009	0.00006	0.00014	0.00389	−8142.60	0.0951
8.0000	<u>0.00015</u>	<u>0.00009</u>	0.00007	0.00015	0.00418	−8025.21	0.1026
11.3137	0.00015	0.00009	0.00007	0.00016	0.00453	−7857.17	0.1111
16.0000	0.00016	0.00010	0.00008	0.00018	0.00493	−7635.67	0.1212
22.6274	0.00017	0.00011	0.00009	0.00019	0.00542	−7358.27	0.1332
32.0000	0.00019	0.00012	0.00010	0.00022	0.00601	−7023.46	0.1477

<u>underline</u> indicates minimum values

Table 6.

Analyses of synthesized gravity tide data at latitude 80N. Five different data sets are prepared to check the systematic biases which might be derived from long period tides in the estimation of diurnal, semidiurnal and terdiurnal tidal parameters. The five data sets are contains long period tides with the a priori factor of 0.0, 1.0, 2.0, 5.0 and 10.0, respectively. Artificial drifts are given to the data by random walk model and about 0.1 micro Gal random noise are given to the synthesized data sets. The results shows that no significant biases except L_2 wave are derived from long period tides in the estimation of tidal parameters.

Comparison of Factors

Wave	Given factor	Estimated factor 0.0	1.0	2.0	5.0	10.0
Q_1	1.15820	1.15586	1.15586	1.15585	1.15584	1.15580
O_1	1.15800	1.15788	1.15789	1.15789	1.15790	1.15791
M_1	1.15740	1.16256	1.16232	1.16228	1.16182	1.16111
P_1	1.15290	1.15329	1.15328	1.15328	1.15326	1.15323
K_1	1.13860	1.13856	1.13856	1.13855	1.13855	1.13855
J_1	1.15990	1.15866	1.15863	1.15864	1.15857	1.15840
OO_1	1.15920	1.15886	1.15891	1.15900	1.15914	1.15936
$2N_2$	1.16000	1.15584	1.15616	1.15614	1.15630	1.15652
N_2	1.16000	1.15860	1.15863	1.15861	1.15864	1.15871
M_2	1.16000	1.16071	1.16072	1.16072	1.16072	1.16072
L_2	1.16000	1.19505	1.18957	1.18963	1.18268	1.17561
S_2	1.16000	1.16033	1.16034	1.16034	1.16036	1.16039
K_2	1.16000	1.16823	1.16827	1.16826	1.16823	1.16805
M_3	1.07000	1.33212	1.33138	1.33153	1.32954	1.32647
Hyperparam. D for min. ABIC		4.000	2.828	2.828	2.000	1.414

Table 6. (continued.)

Comparison of Phases

Wave	Given phase	Estimated phase 0.0	1.0	2.0	5.0	10.0
Q_1	0.000	−0.063	−0.060	−0.059	−0.052	−0.042
O_1 0.000	−0.050	−0.050	−0.049	−0.049	−0.047	
M_1	0.000	0.260	0.253	0.253	0.240	0.219
P_1	0.000	−0.032	−0.031	−0.031	−0.029	−0.027
K_1	0.060	0.063	0.064	0.064	0.064	0.065
J_1	0.000	0.016	0.016	0.018	0.023	0.030
OO_1	0.000	−0.272	−0.269	−0.270	−0.264	−0.244
$2N_2$	0.000	−1.681	−1.643	−1.646	−1.568	−1.430
N_2	0.000	0.229	0.226	0.226	0.219	0.209
M_2	0.000	−0.150	−0.150	−0.151	−0.151	−0.152
L_2	0.000	5.697	4.927	4.929	3.870	2.708
S_2	0.000	0.092	0.091	0.091	0.089	0.087
K_2	0.000	0.477	0.484	0.485	0.491	0.499
M_3	0.000	−11.639	−11.599	−11.574	−11.441	−11.262
Hyperparam. D for min. ABIC		4.000	2.828	2.828	2.000	1.414

Figures and Figure Captions

Figure 1.

Orbit of the sun (upper) and the moon (lower). The motion of the sun is conventionally expressed by geocentric system. Eccentricity of the sun's orbit is exaggerated to show the perigee in upper Figure. Ecliptic longitudes of the sun and the moon (L in lower Figure) are measured from vernal equinox γ. Ecliptic latitude of the sun is less than 1" since the ecliptic plane is defined by the mean orbital plane of the sun. Ecliptic latitude of the moon is shown as β. The inclination of the moon's orbit against ecliptic plane is about 5.°1 , thus the maximum value of β becomes 5.°1. The obliquity of the ecliptic (the angle between ecliptic and equatorial planes) is about 23.°4. The node of the moon retrogrades with the period of 18.6 years. Therefore, the inclination of the moon's orbit against earth's equator varies in the range of 23.°4 $\pm$5.°1 with period of 18.6 years.

Fig.1

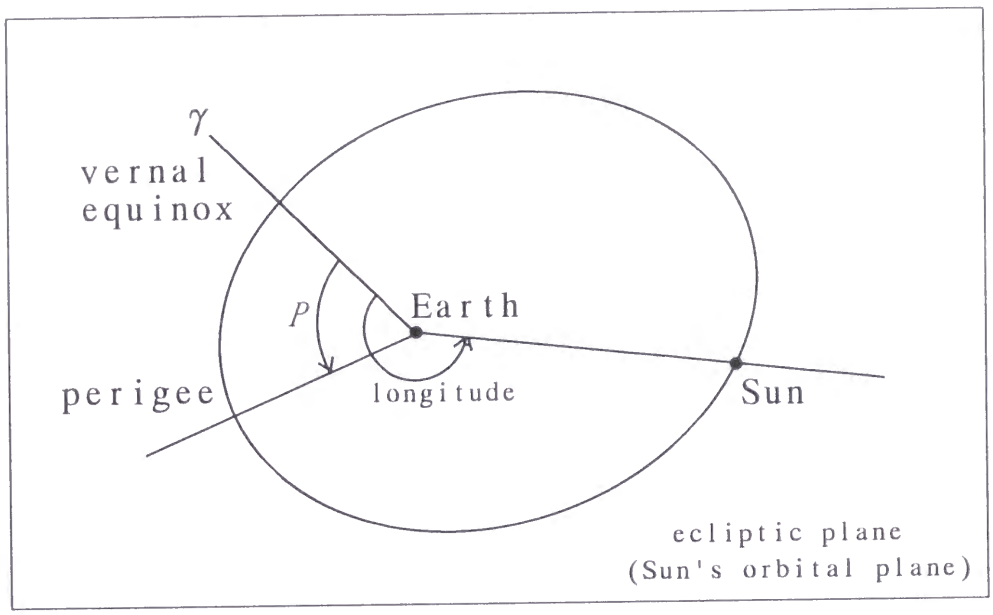

celestial sphere

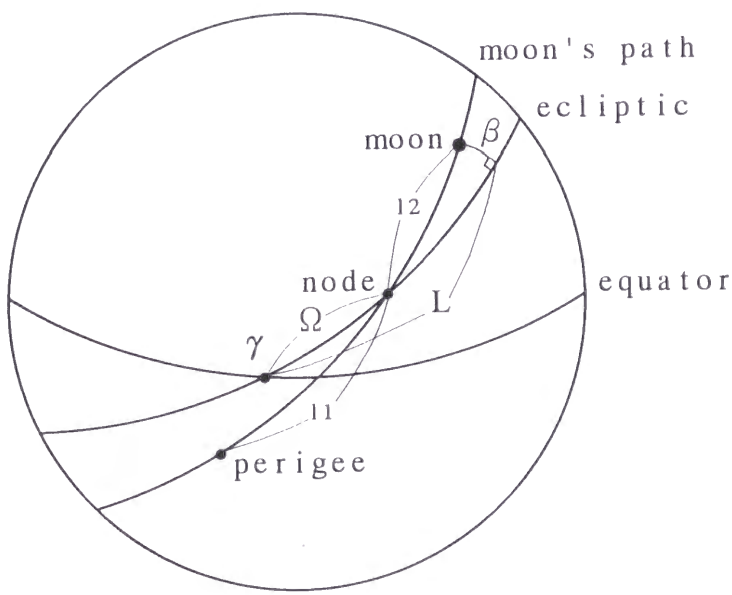

Figures 2-nm.

Accuracy of harmonic tides is investigated in frequency domain. The accuracy is checked for each potential degree and tidal species for gravity tide. The Figure sub-number n denotes potential degree (2～4) and sub-number m denotes tidal species (0 : long period; 1 : diurnal; 2 : semidiurnal; 3 : terdiurnal; 4 : 1/4 day period). In each figure, black line shows the spectrum of the theoretical gravity tide calculated from ephemerides, blue one shows residual spectrum for harmonic tide by Tamura (1987) , and red one shows residual spectrum for present revised development. For the degree 3 and 4 potentials, the results of terdiurnal and 1/4 day period tides are described for the samples, respectively.

Figure 2-20.

The case for gravity tide of degree 2, long period and at latitude 90°.

Black line shows the spectrum of theoretical tide (ephemeris tide).

Blue line shows the spectrum of "ephemeris tide - harmonic tide by Tamura (1987) (with 211 waves)". This shows that the maximum error of harmonic tide by Tamura (1987) is less than 1 nano Gal ($10^{-11}ms^{-2}$) in frequency domain.

Red line shows the spectrum of "ephemeris tide - harmonic tide with the additional terms (in total 493 waves)". This shows that the maximum error of the harmonic tide with additional terms is less than 0.1 nano Gal in frequency domain.

Fig.2–

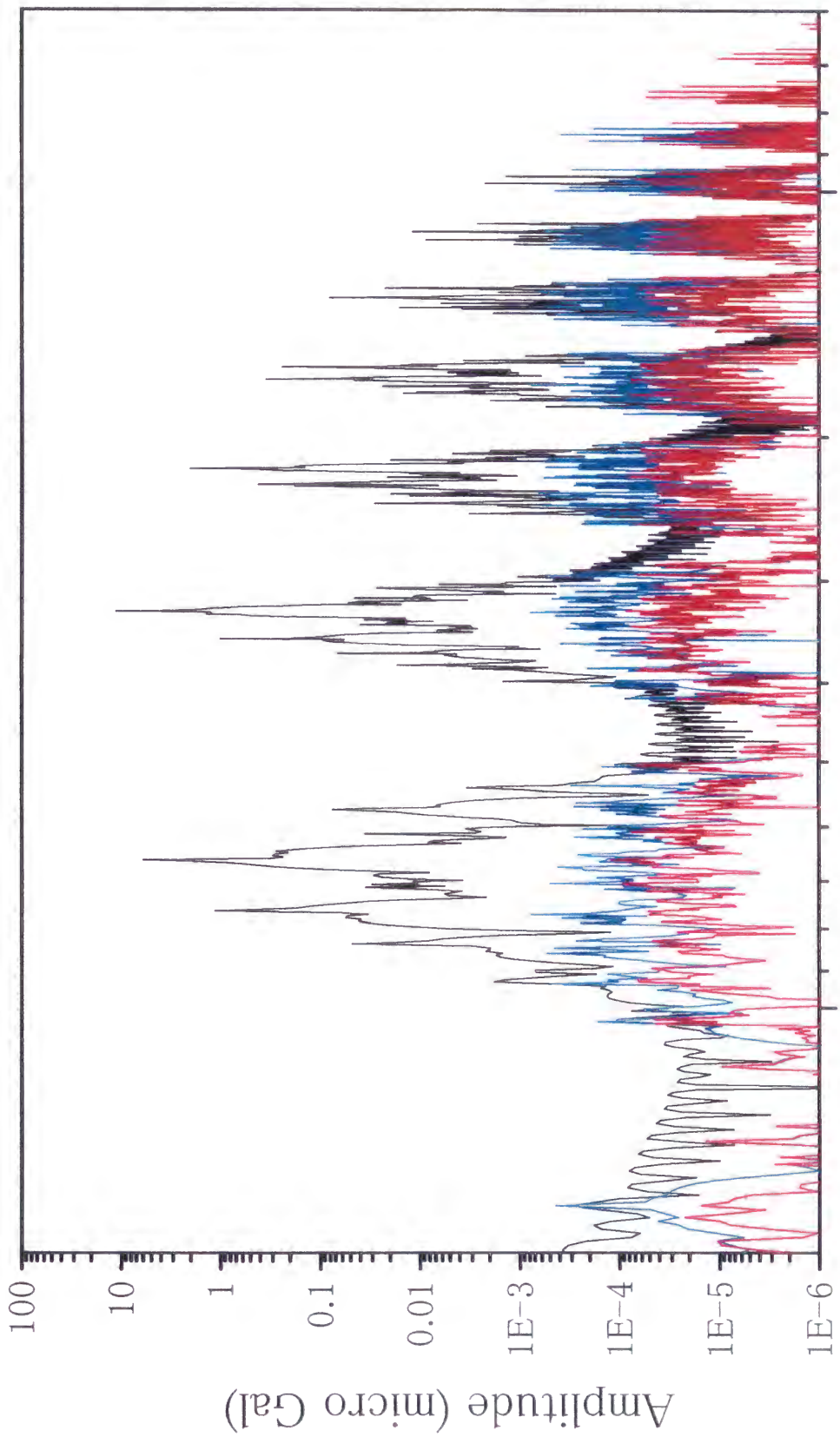
Amplitude (micro Gal)
100
10
1
0.1
0.01
1E−3
1E−4
1E−5
1E−6
1000
100
Period (Hour)

Figure 2-21.

The case for gravity tide of degree 2, diurnal tide at latitude 45°.

Black line shows the spectrum of theoretical gravity tide (ephemeris tide). Leakage of the spectrum whose relative power is less than −120dB is visible around the period from 16 to 18 hours. It is a false and there is no power at that period in the real tide.

Blue line shows the spectrum of "ephemeris tide − harmonic tide by Tamura (1987) (with 345 waves)". This shows that the maximum error of harmonic tide by Tamura (1987) is almost less than 1 nano Gal ($10^{-11}ms^{-2}$) in frequency domain.

Red line shows the spectrum of "ephemeris tide − harmonic tide with the additional terms (in total 757 waves)". This shows that the maximum error of the harmonic tide with additional terms is less than 0.2 nano Gal in frequency domain.

Fig. 2–

Amplitude (micro Gal)
100
10
1
0.1
0.01
1E−3
1E−4
1E−5
1E−6
16
18
20
22
24
26
28
30
32
34
36
Period (Hour)

Figure 2-22.

The case for gravity tide of degree 2, semidiurnal tide and at latitude 0°.

Black line shows the spectrum of theoretical gravity tide (ephemeris tide). Leakage of the spectrum whose relative power is less than −120dB is visible around the period from 10 to 10.8 hours. It is a false and there is no power at that period in the real tide.

Blue line shows the spectrum of "ephemeris tide − harmonic tide by Tamura (1987) (with 281 waves)". This shows that the maximum error of harmonic tide by Tamura (1987) is almost less than 1 nano Gal ($10^{-11}ms^{-2}$) in frequency domain.

Red line shows the spectrum of "ephemeris tide − harmonic tide with the additional terms (in total 633 waves)". This shows that the maximum error of the harmonic tide with additional terms is less than 0.2 nano Gal in frequency domain.

Fig.2-2

Amplitude (micro Gal)
100
10
1
0.1
0.01
1E-3
1E-4
1E-5
1E-6
10
11
12
13
14
15
Period (Hour)

Figure 2-33.

The case for gravity tide of degree 3, terdiurnal tide and at latitude 0°.

Black line shows the spectrum of theoretical gravity tide (ephemeris tide).

Blue line shows the spectrum of "ephemeris tide – harmonic tide by Tamura (1987) (with 68 waves)". This shows that the maximum error of harmonic tide by Tamura (1987) is less than 1 nano Gal ($10^{-11}ms^{-2}$) in frequency domain.

Red line shows the spectrum of "ephemeris tide – harmonic tide with the additional terms (in total 194 waves)". This shows that the maximum error of the harmonic tide with additional terms is less than 0.2 nano Gal in frequency domain.

Fig.2-3

Amplitude (micro Gal)
100
10
1
0.1
0.01
1E-3
1E-4
1E-5
1E-6
7.0
7.5
8.0
8.5
9.0
9.5
Period (Hour)

Figure 2-44.

The case for gravity tide of degree 4, 1/4 day period tide and at latitude 0°.

Black line shows the spectrum of theoretical gravity tide (ephemeris tide).

Blue line shows the spectrum of "ephemeris tide – harmonic tide by Tamura (1987) (with 10 waves)". This Figure shows that the maximum error of harmonic tide by Tamura (1987) is less than 1 nano Gal ($10^{-11}ms^{-2}$) in frequency domain.

Red line shows the spectrum of "ephemeris tide – harmonic tide with the additional terms (in total 39 waves)". This Figure shows that the maximum error of the harmonic tide with additional terms is less than 0.15 nano Gal in frequency domain.

Fig.2-4

Amplitude (micro Gal)
10
1
0.1
0.01
1E-3
1E-4
1E-5
1E-6
1E-7
7.0
6.8
6.6
6.4
6.2
6.0
5.8
5.6
5.4
Period (Hour)

Figures 3-nm.

The variations of time domain maximum and mean errors of harmonic gravity tide are examined by changing the maximum number of adopted harmonic terms. The reference theoretical gravity tides are calculated directly from the lunar and solar ephemerides. The error of each degree and species is estimated at the latitude which gives maximum tidal amplitude.

Figure sub-number n and m denote the potential degree (2～4) and tidal species, respectively. They are,

Figure 3-20 : degree 2, long period gravity tide, at latitude 90°,

Figure 3-21 : degree 2, diurnal gravity tide, at latitude 45°,

Figure 3-22 : degree 2, semidiurnal gravity tide, at latitude 0°,

Figure 3-30 : degree 3, long period gravity tide, at latitude 90°,

Figure 3-31 : degree 3, diurnal gravity tide, at latitude 58.9°,

Figure 3-32 : degree 3, semidiurnal gravity tide, at latitude 35.3°,

Figure 3-33 : degree 3, terdiurnal gravity tide, at latitude 0°,

Figure 3-40 : degree 4, long period gravity tide, at latitude 90°,

Figure 3-41 : degree 4, diurnal gravity tide, at latitude 66.1°,

Figure 3-42 : degree 4, semidiurnal gravity tide, at latitude 49.1°,

Figure 3-43 : degree 4, terdiurnal gravity tide, at latitude 30°,

Figure 3-44 : degree 4, 1/4 day period gravity tide, at latitude 0°.

Fig. 3-20

Degree 2, Long Period
Difference (nano Gal)
$10^{-11}ms^{-2}$
10000
1000
100
10
1
0.1
0
100
200
300
400
500
600
700
800
Number of Terms
maximum
r.m.s.
← Tamura (1995)
← Tamura (1987)

Fig. 3-21

Degree 2, Diurnal
Difference (nano Gal)
$10^{-11}ms^{-2}$
10000
1000
100
10
1
0.1
0
100
200
300
400
500
600
700
800
Number of Terms
maximum
r.m.s.
←Tamura
(1995)
← Tamura
(1987)

Fig. 3-22

Degree 2, Semidiurnal
$10^{-11}ms^{-2}$
10000
1000
100
10
1
0.1
Difference (nano Gal)
0
100
200
300
400
500
600
700
800
Number of Terms
maximum
r.m.s.
←Tamura
(1995)
← Tamura
(1987)

Fig. 3-30

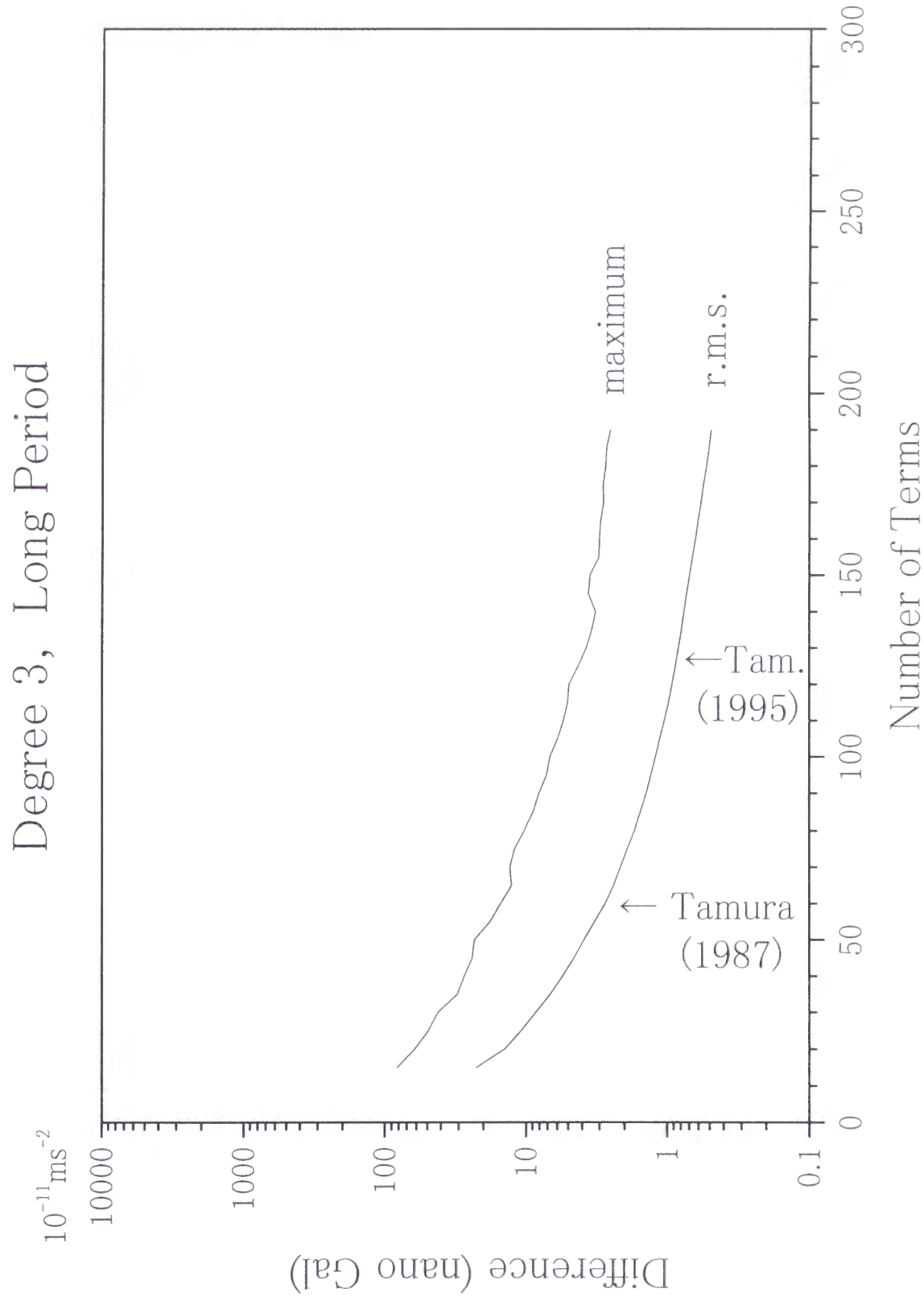
Degree 3, Long Period
Difference (nano Gal)
$10^{-11}ms^{-2}$
10000
1000
100
10
1
0.1
0
50
100
150
200
250
300
Number of Terms
maximum
r.m.s.
←Tam.
(1995)
← Tamura
(1987)

Fig. 3-31

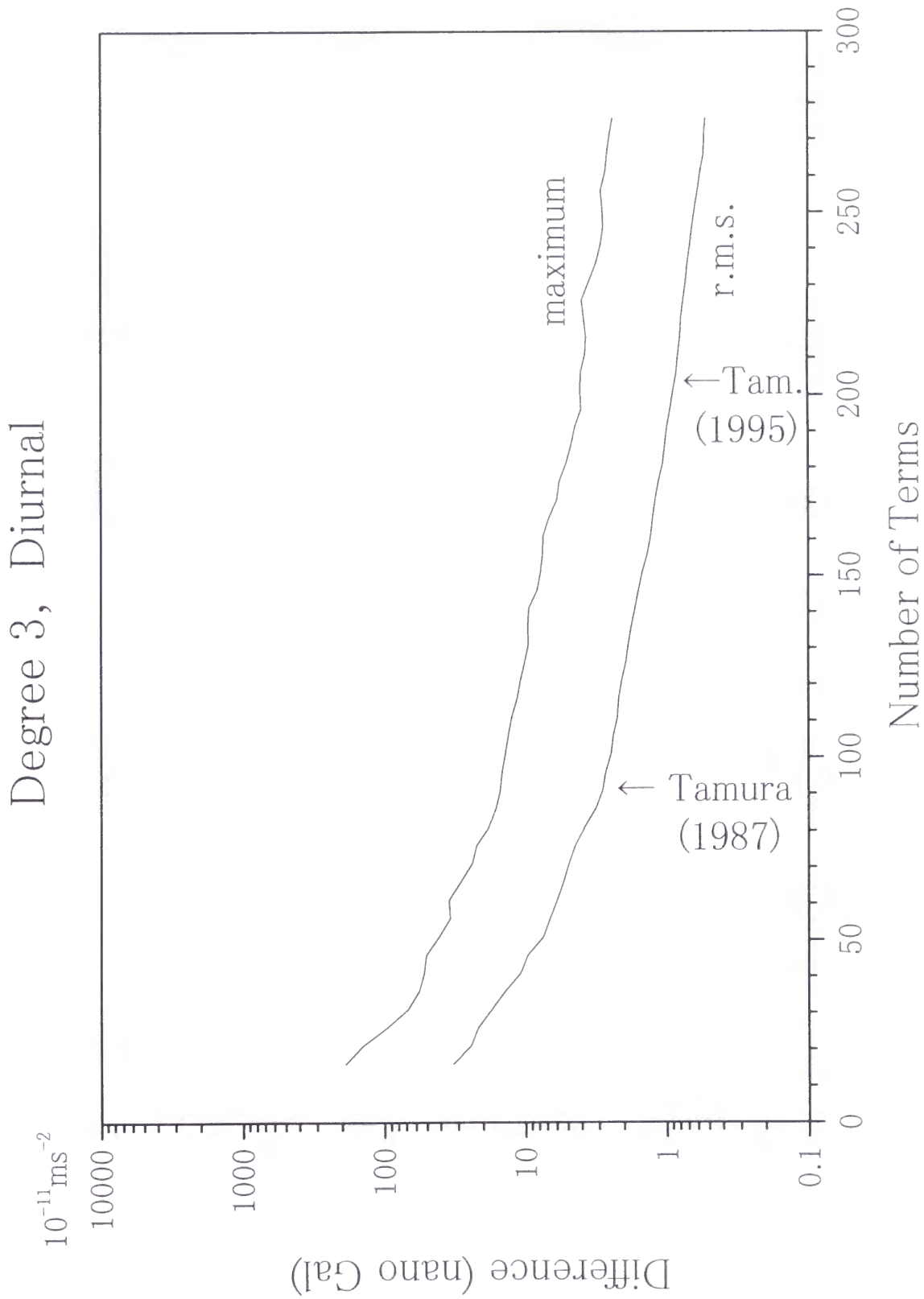
Degree 3, Diurnal
Difference (nano Gal)
$10^{-11}ms^{-2}$
10000
1000
100
10
1
0.1
0
50
100
150
200
250
300
Number of Terms
maximum
r.m.s.
←Tam.
(1995)
← Tamura
(1987)

Fig. 3-32

Degree 3, Semidiurnal
Difference (nano Gal)
$10^{-11}ms^{-2}$
10000
1000
100
10
1
0.1
0
50
100
150
200
250
300
Number of Terms
maximum
r.m.s.
←Tam.
(1995)
← Tamura
(1987)

Fig. 3-33

Degree 3, Terdiurnal
Difference (nano Gal)
$10^{-11}ms^{-2}$
10000
1000
100
10
1
0.1
0
50
100
150
200
250
300
Number of Terms
maximum
r.m.s.
←Tam.
(1995)
← Tamura
(1987)

Fig. 3-40

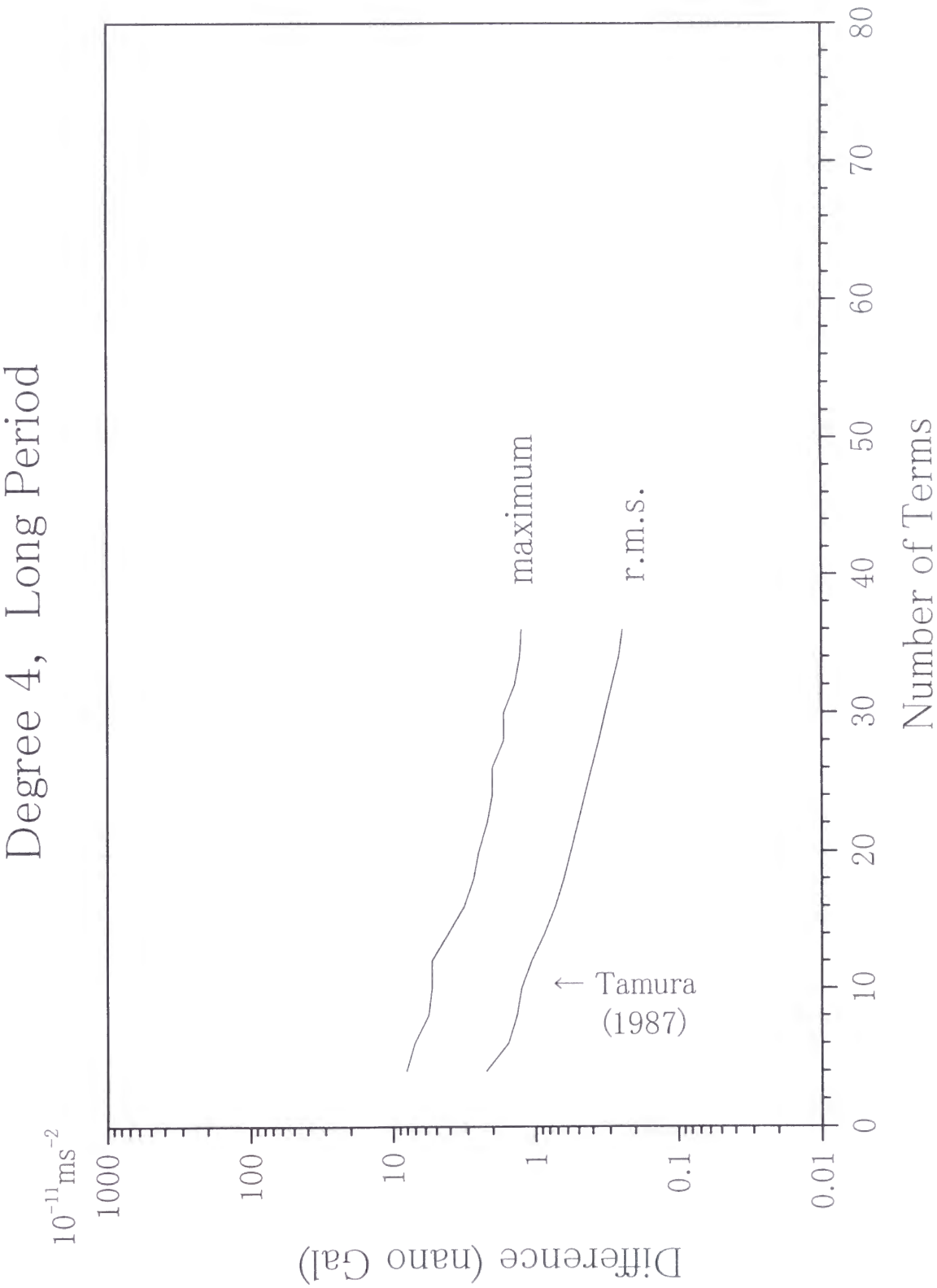
Degree 4, Long Period
Difference (nano Gal)
$10^{-11}ms^{-2}$
1000
100
10
1
0.1
0.01
0
10
20
30
40
50
60
70
80
Number of Terms
maximum
r.m.s.
← Tamura
(1987)

Fig. 3-41

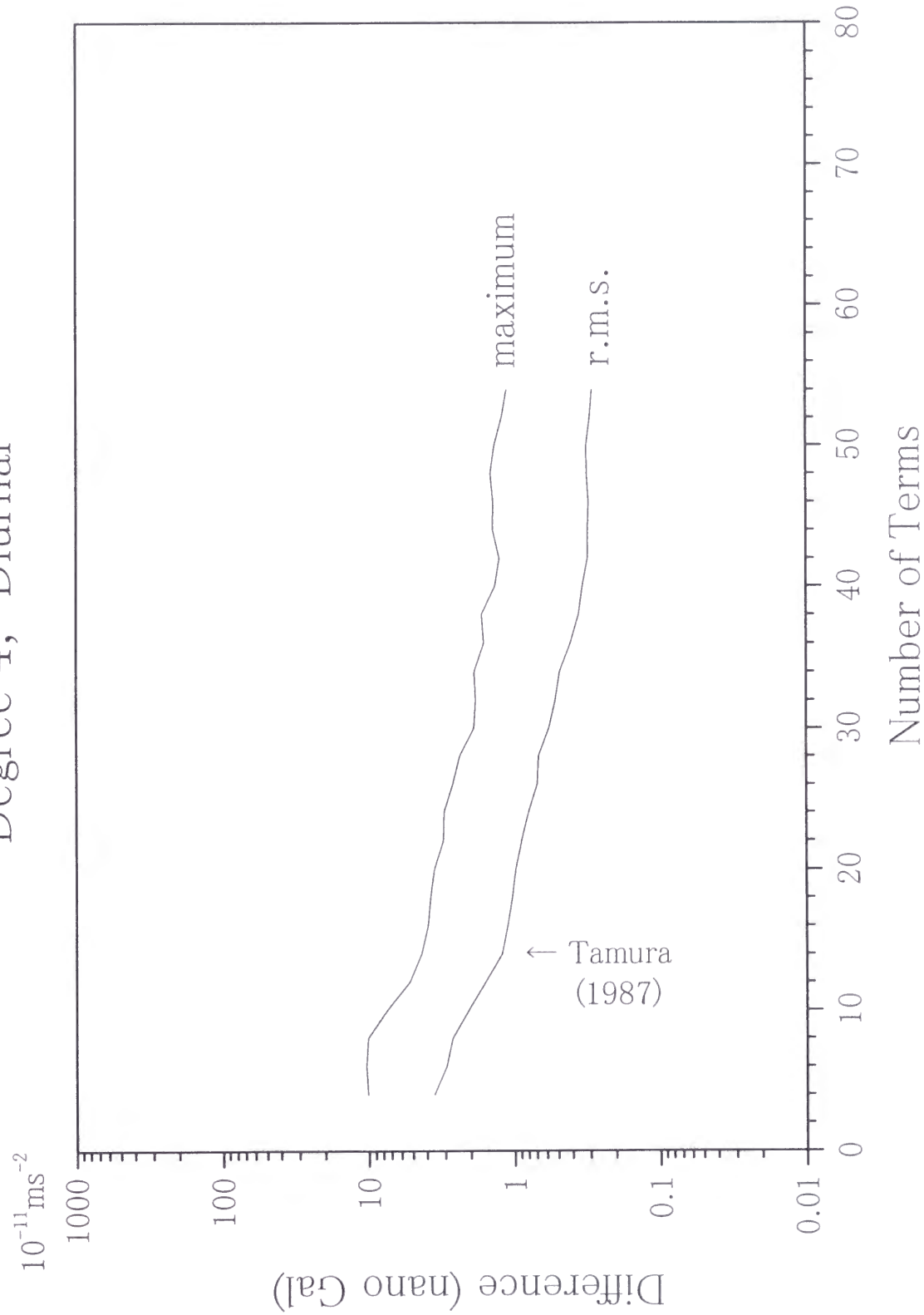
Degree 4, Diurnal
Difference (nano Gal)
$10^{-11}ms^{-2}$
1000
100
10
1
0.1
0.01
0
10
20
30
40
50
60
70
80
Number of Terms
maximum
r.m.s.
← Tamura
(1987)

Fig. 3-42

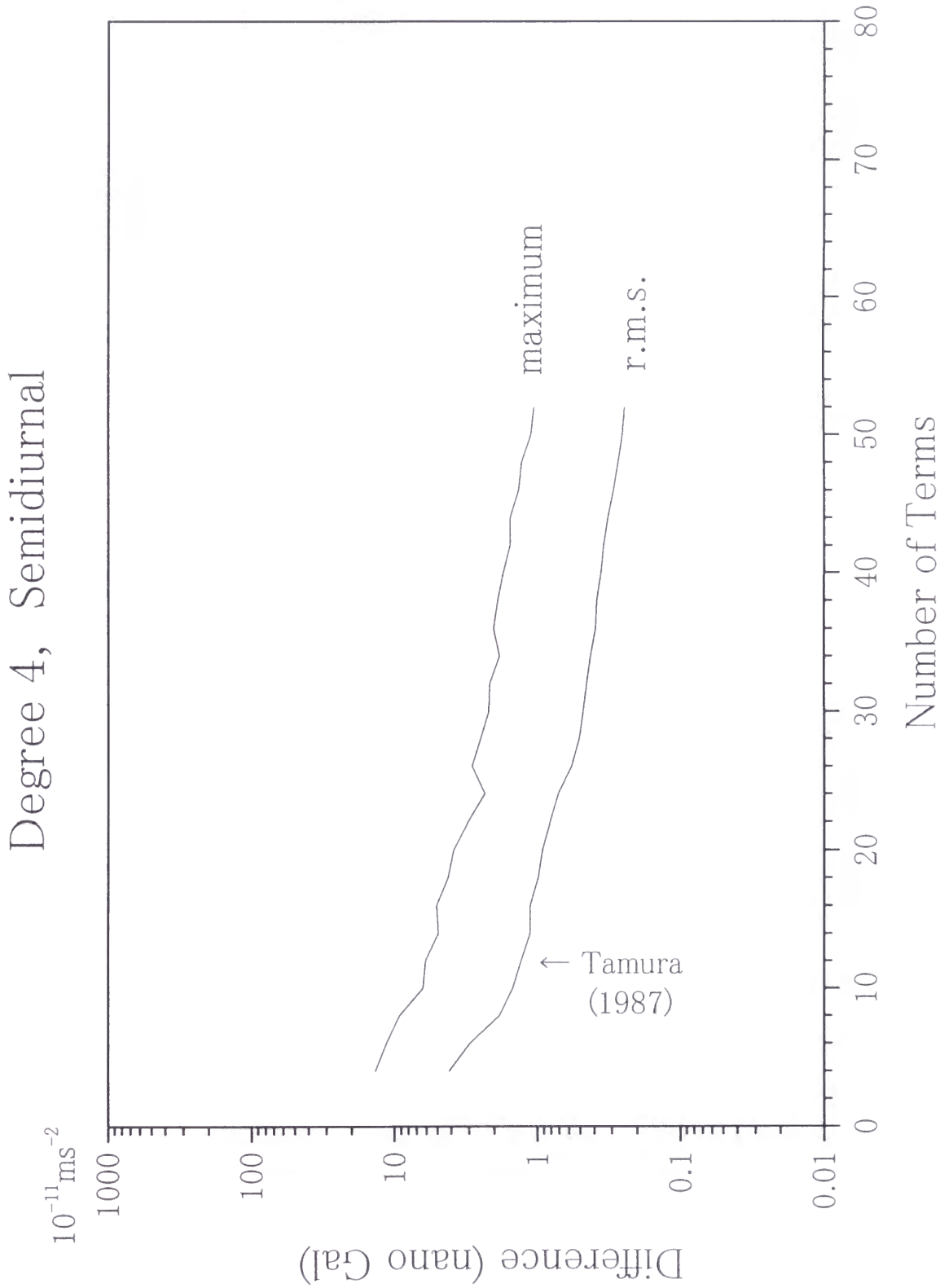
Degree 4, Semidiurnal
Difference (nano Gal)
$10^{-11}ms^{-2}$
1000
100
10
1
0.1
0.01
0
10
20
30
40
50
60
70
80
Number of Terms
maximum
r.m.s.
← Tamura
(1987)

Fig. 3-43

Degree 4, Terdiurnal
Difference (nano Gal)
$10^{-11}ms^{-2}$
1000
100
10
1
0.1
0.01
0
10
20
30
40
50
60
70
80
Number of Terms
maximum
r.m.s.
← Tamura
(1987)

Fig. 3-44

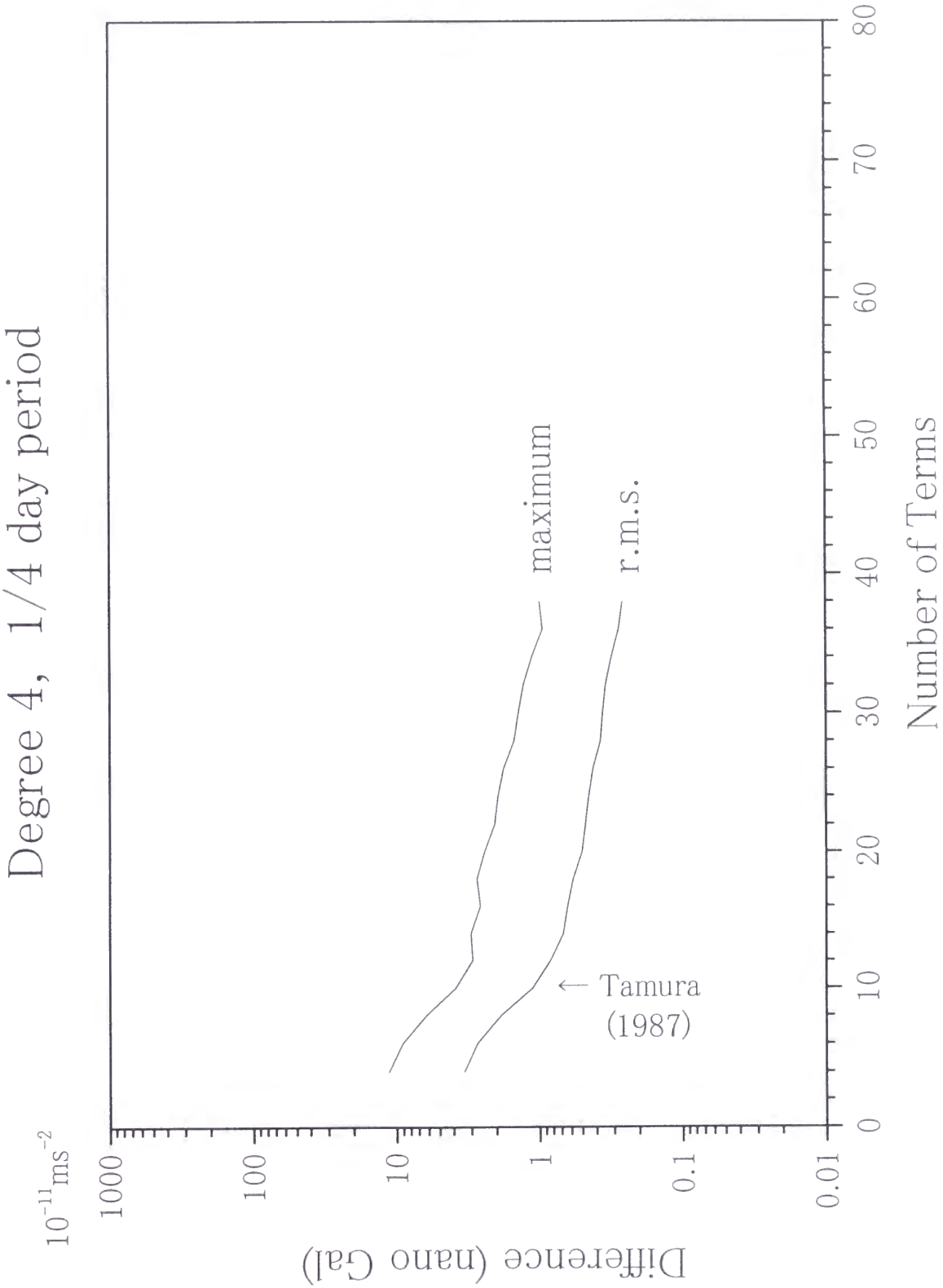
Degree 4, 1/4 day period
$10^{-11}ms^{-2}$
1000
100
10
1
0.1
0.01
Difference (nano Gal)
0
10
20
30
40
50
60
70
80
Number of Terms
maximum
r.m.s.
← Tamura
(1987)

Figure 4a.

Long period gravity tide generated by Venus. The amplitude becomes large at the Venus' inferior conjunctions. The distance of Venus from Earth is 1.7 a.u. at the superior conjunction, while it is 0.3 a.u. at the inferior conjunction. The ratio of tide generating potential by Venus at the superior and inferior conjunction is about 1/180 (= $(0.3/1.7)^3$), thus the amplitude at superior conjunctions become negligible small. The maximum amplitude at the inferior conjunction depends on the declination of Venus at that time.

Figure 4b.

Diurnal gravity tide generated by Venus. The amplitude becomes large at the Venus' inferior conjunctions and negligible small at the superior conjunctions. This situation is same as for long period tide. The maximum amplitude at the inferior conjunction depends on the declination of Venus at that time.

Figure 4c.

Semidiurnal gravity tide generated by Venus. The amplitude varies in large range, and this reason is same as for long period and semidiurnal tides.

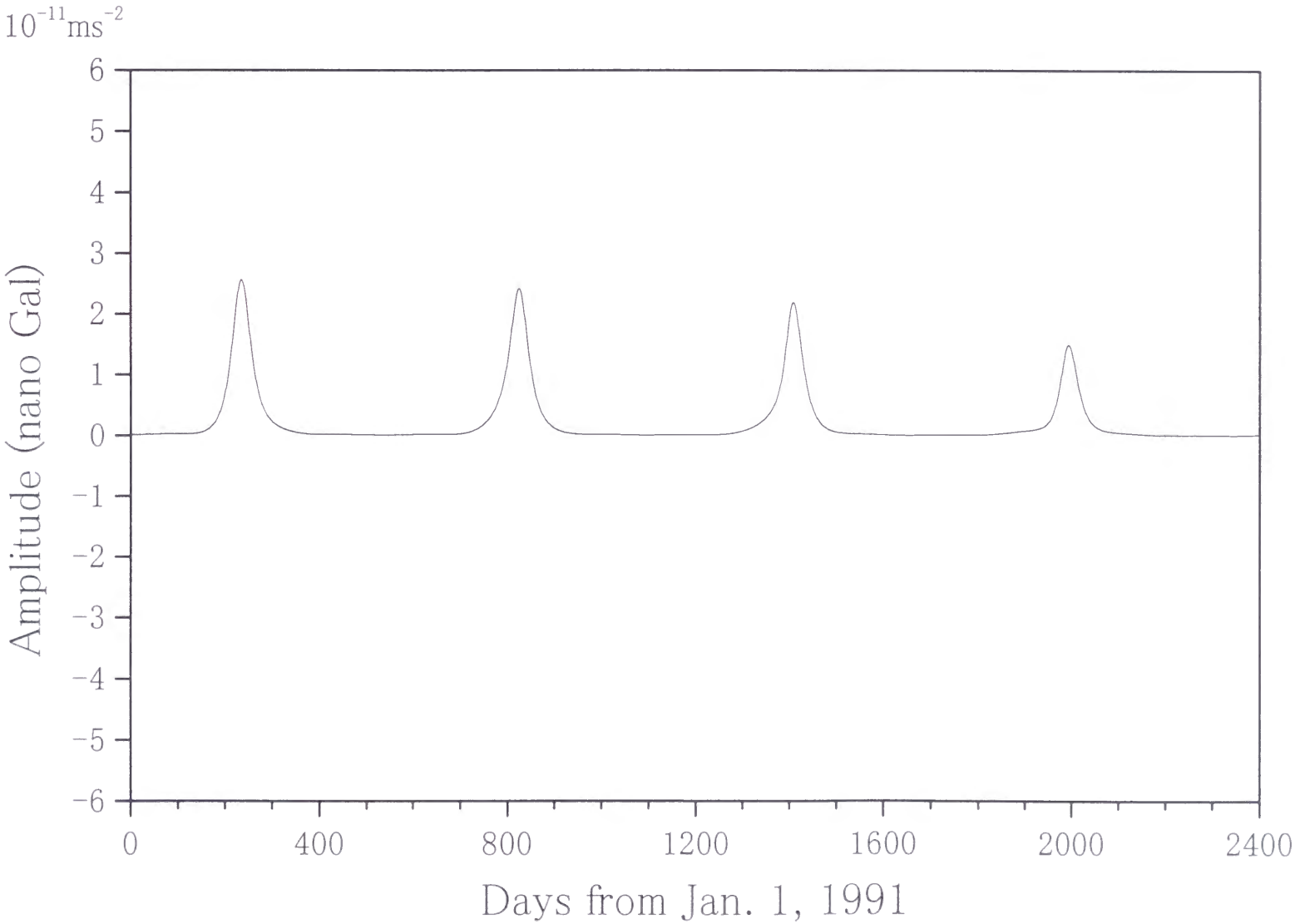
Venus direct term (long period)
$10^{-11}ms^{-2}$
Amplitude (nano Gal)
6
5
4
3
2
1
0
−1
−2
−3
−4
−5
−6
0
400
800
1200
1600
2000
2400
Days from Jan. 1, 1991

Fig. 4a

Fig. 4b

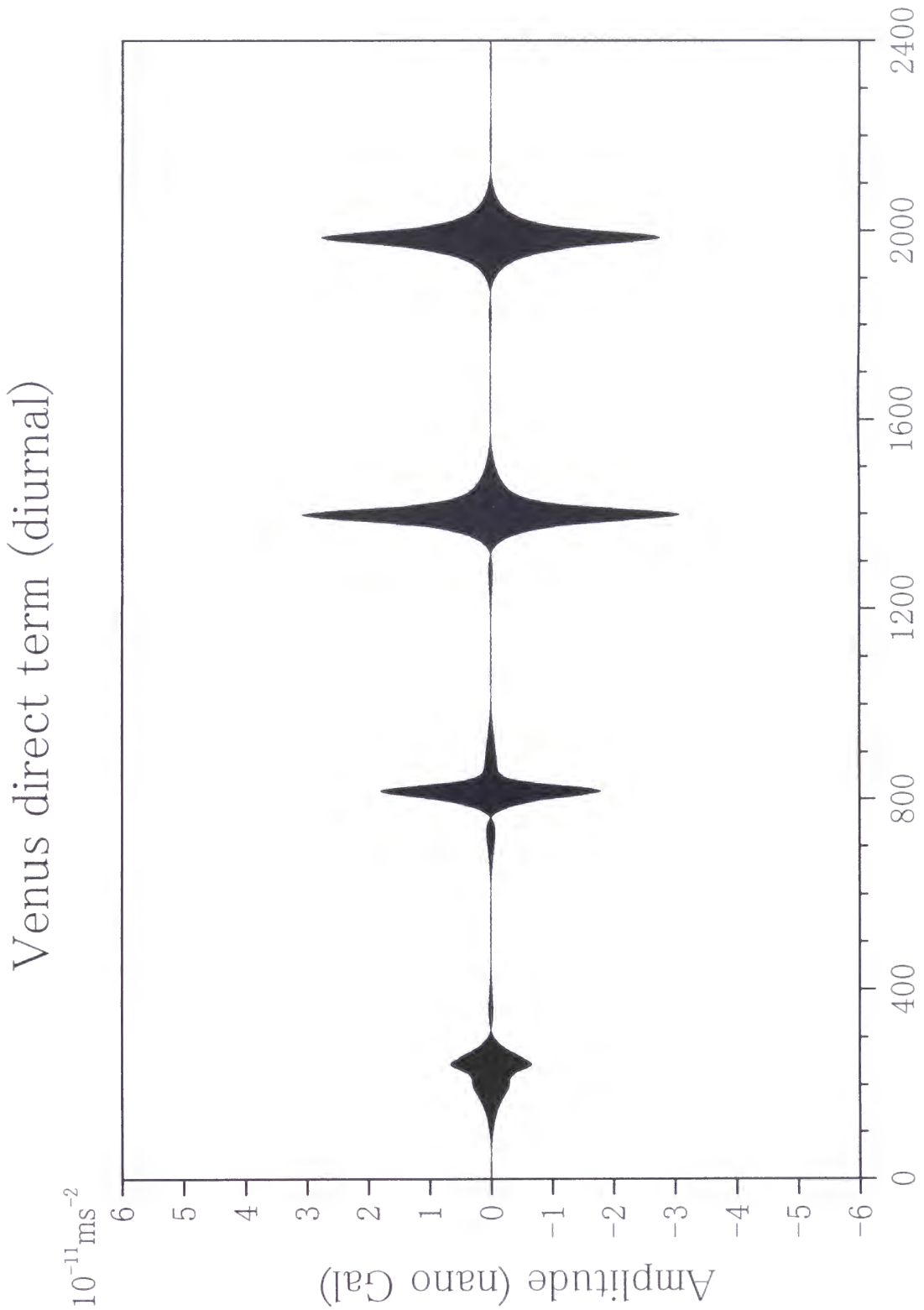
Venus direct term (diurnal)
10^{-11}ms^{-2}
6
5
4
3
2
1
0
−1
−2
−3
−4
−5
−6
Amplitude (nano Gal)
0
400
800
1200
1600
2000
2400
Days from Jan. 1, 1991

Fig. 4c

Venus direct term (semidiurnal)
10^{-11}ms^{-2}
6
5
4
3
2
1
0
−1
−2
−3
−4
−5
−6
Amplitude (nano Gal)
0
400
800
1200
1600
2000
2400
Days from Jan. 1, 1991

Figure 5a.

Long period gravity tide generated by Jupiter.

Figure 5b.

Diurnal gravity tide generated by Jupiter.

Figure 5c.

Semidiurnal gravity tide generated by Jupiter. The maximum amplitude is about 0.5 nano Gal at the Jupiter's opposition. The distance of Jupiter from Earth is 4.2 a.u. at the opposition, while it is 6.2 a.u. at the superior conjunction. The ratio of tide generating potential by Jupiter at the superior conjunction and opposition is about 0.3 ($= (4.2/6.2)^3$).

Fig. 5a

Jupiter direct term (long period)
10^{-11}ms^{-2}
6
5
4
3
2
1
0
−1
−2
−3
−4
−5
−6
Amplitude (nano Gal)
0
400
800
1200
1600
2000
2400
Days from Jan. 1, 1991

Jupiter direct term (diurnal)
$10^{-11}ms^{-2}$
Amplitude (nano Gal)
6
5
4
3
2
1
0
-1
-2
-3
-4
-5
-6
0
400
800
1200
1600
2000
2400
Days from Jan. 1, 1991

Fig.5b

Jupiter direct term (semidiurnal)
$10^{-11}ms^{-2}$
Amplitude (nano Gal)
6
5
4
3
2
1
0
-1
-2
-3
-4
-5
-6
0
400
800
1200
1600
2000
2400
Days from Jan. 1, 1991

Fig.5c

Figures 6a, 6b.

Comparison of harmonic tables between Tamura (1987) and CTE (Cartwright and Tayler, 1971; Cartwright and Edden, 1973) in the analysis of actual gravity tide records. Figure 6a is a spectrum of residual time series around terdiurnal band which residuals are obtained by applying Tamura (1987) tables. Figure 6b is that obtained by applying CTE tables. The gravity tide data used hear is obtained by using a superconducting gravimeter at Esashi Earth Tides Station. In Figure 6b, several tidal components whose periods are 8.1772, 8.3863 and 8.4940 hours remain in the spectrum. Those tidal components derived from degree 4 potential which is not taken into account in CTE tables. While those residual spectrum peaks disappear in Figure 6a. This comparison result shows that the CTE harmonic table has not enough precision for the precise tidal analysis at present and a superconducting gravimeter has a potential sensitivity to detect a few nano Gal gravity changes if the signals are coherent and continues for a few months.

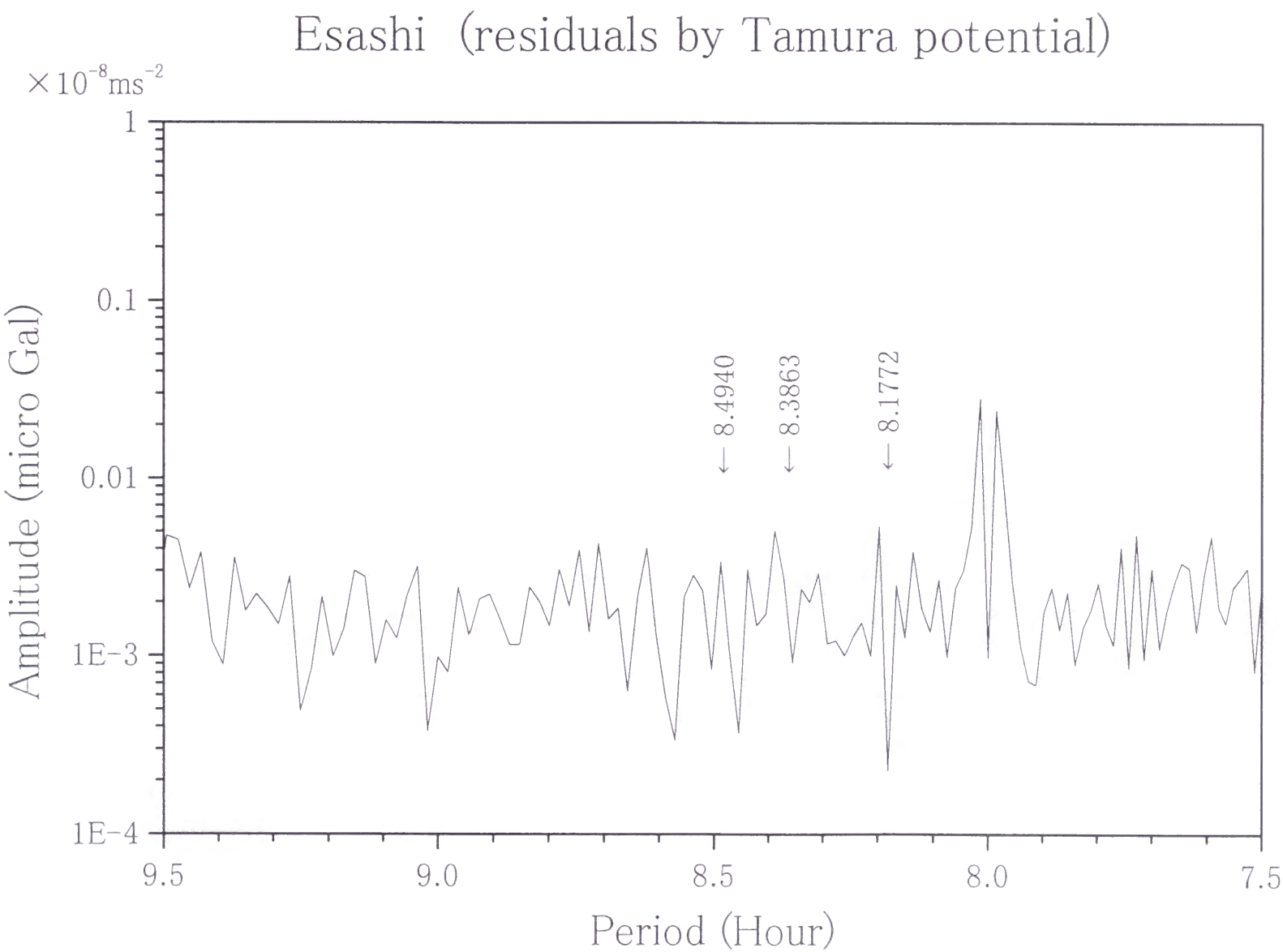
Esashi (residuals by Tamura potential)
×10⁻⁸ms⁻²
1
0.1
0.01
1E-3
1E-4
Amplitude (micro Gal)
← 8.4940
← 8.3863
← 8.1772
9.5
9.0
8.5
8.0
7.5
Period (Hour)

Fig. 6a

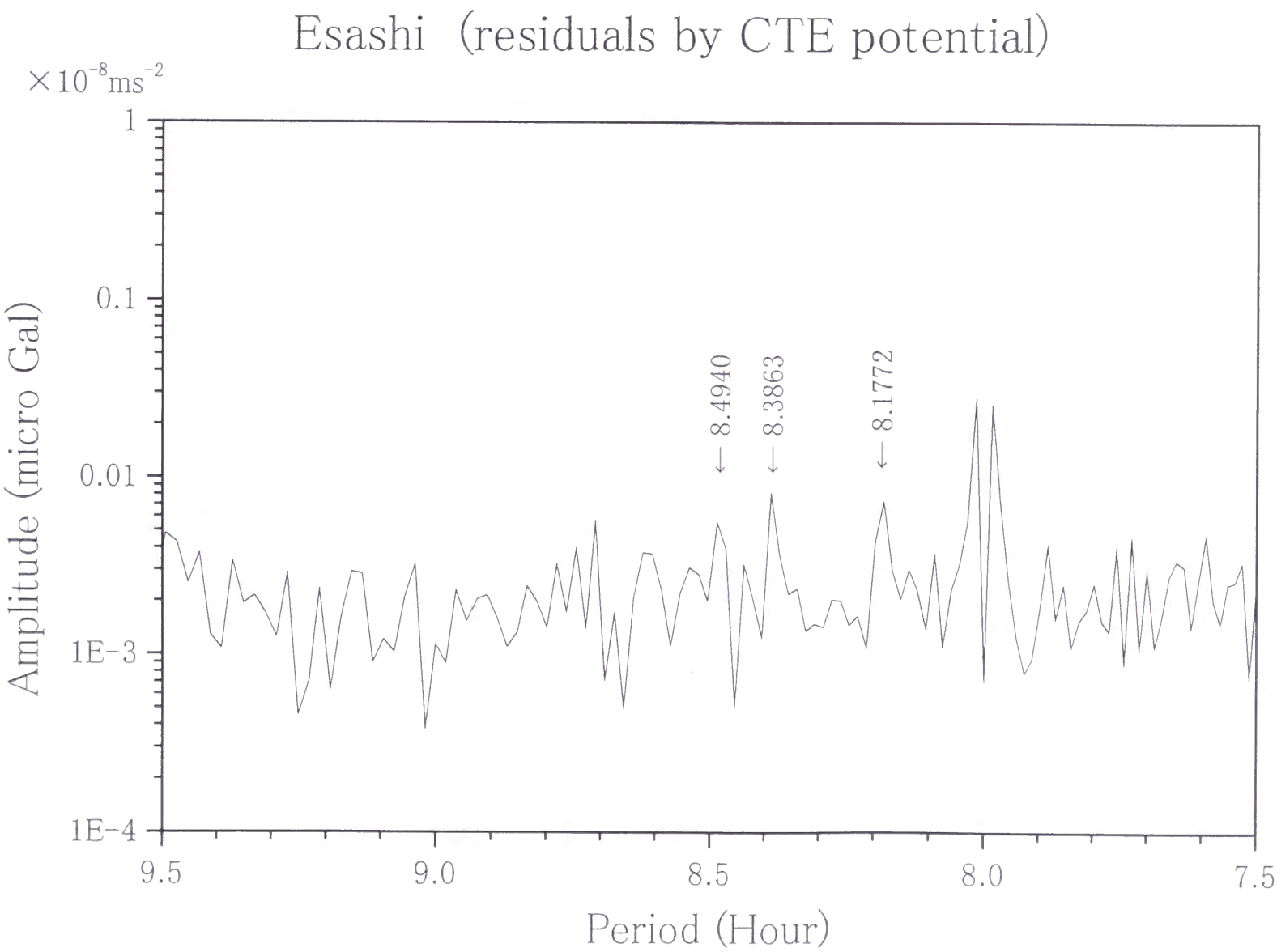
Esashi (residuals by CTE potential)
×10⁻⁸ms⁻²
1
0.1
0.01
1E-3
1E-4
Amplitude (micro Gal)
← 8.4940
← 8.3863
← 8.1772
9.5
9.0
8.5
8.0
7.5
Period (Hour)

Fig. 6b

Figure 7a.

Spectrum of gravity tide record of one year which is obtained with a super-conducting gravimeter at Esashi Earth Tides Station. The effect of atmospheric pressure change in gravity change is corrected in the analysis.

Figure 7b.

Spectrum of residual time series data of one year. The original gravity data is same as used in Figure 7a. The tidal components and atmospheric pressure change effect are subtracted from original data in the analysis. This residual spectrum is a rather good sample experimentally though several peaks remain in tidal bands.

Figure 7c.

Spectrum of gravity tide residuals around semidiurnal band. In this case, 15 tidal components are assumed in the analysis for one year records.

Figure 7d.

Spectrum of gravity tide residuals around semidiurnal band. In this case, 31 tidal components are assumed in the analysis for one year records. Several peaks ($2N_2$, μ_2, T_2) which are seen in Figure 7c diminish in Figure 7d. The amplitudes and phases of minor tidal components (ex. $2N_2$, μ_2, ν_2, T_2) are usually assumed that they are same as those of major components whose angular velocities are close to them. This assumption works well when the frequency response structure of tidal signal is rather flat and usually this assumption is acceptable. The sample shown here suggests that it may be better to assume fine tidal admittance structure for precise tidal data processing.

Fig. 7a

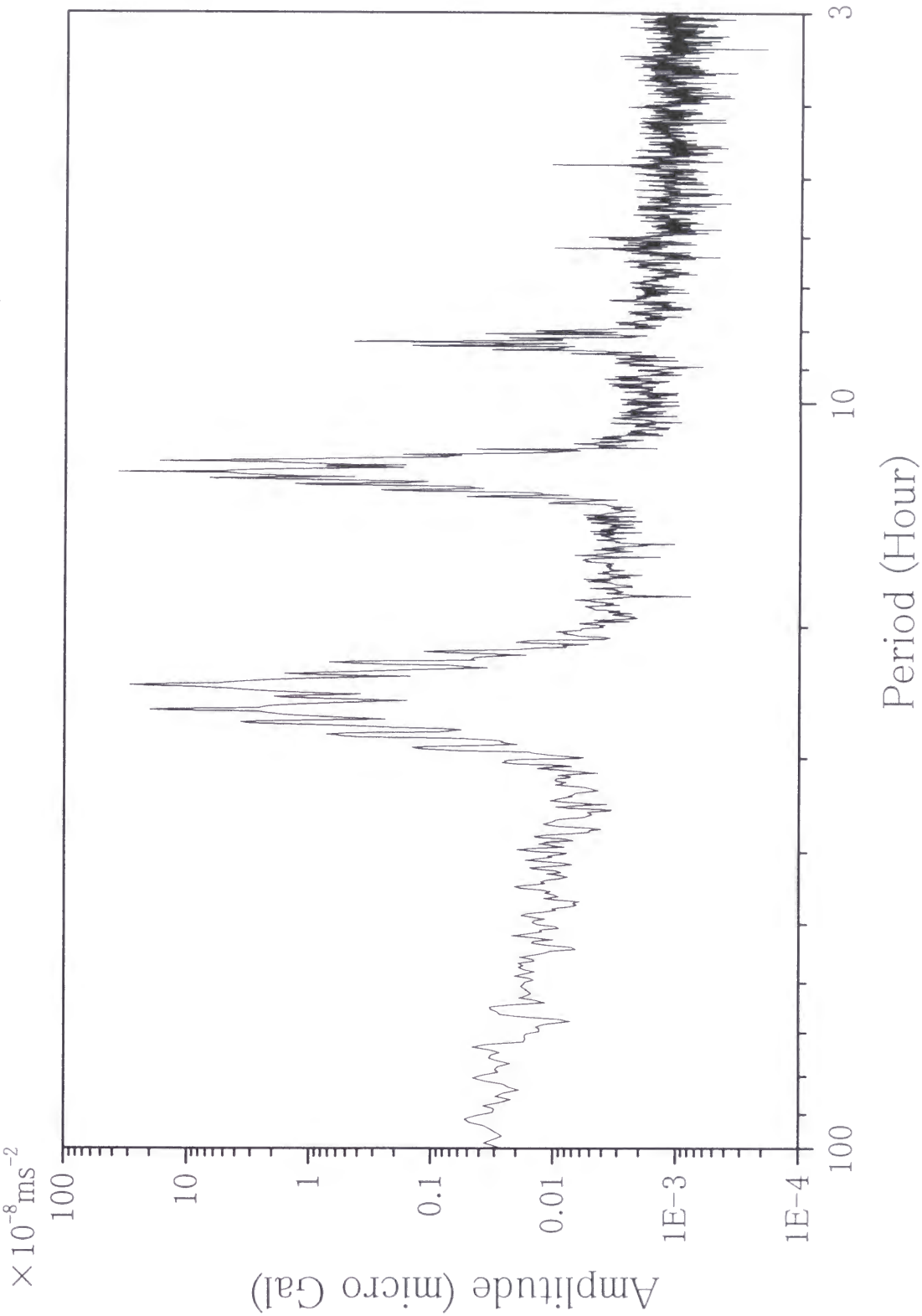
Esashi ('98.01.01 – '99.01.04)
Amplitude (micro Gal)
$\times 10^{-8}$ms^{-2}
100
10
1
0.1
0.01
1E-3
1E-4
100
10
3
Period (Hour)

Fig. 7b

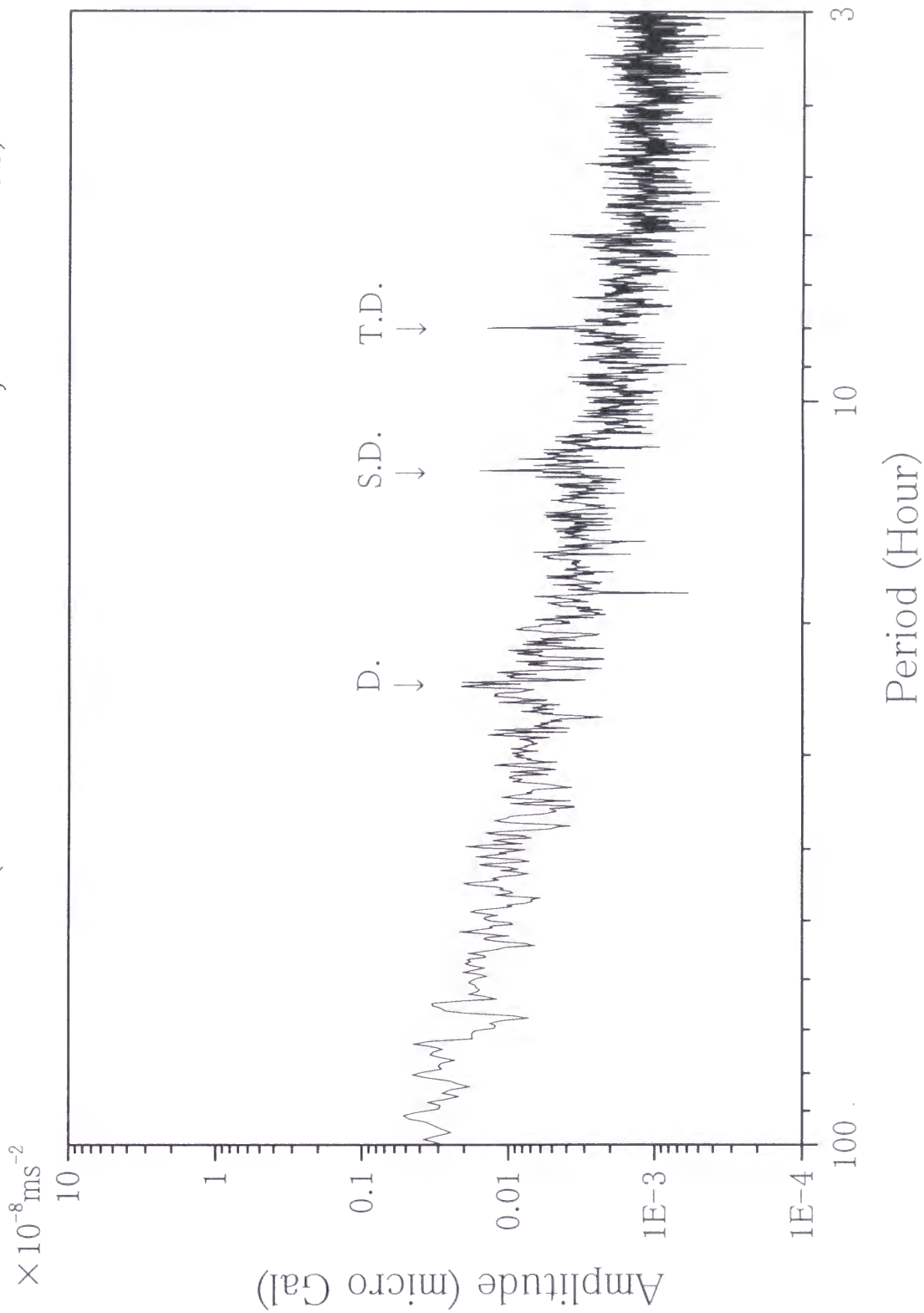
Esashi ('98.01.01 – '99.01.04, 31 waves)
Amplitude (micro Gal)
$\times 10^{-8}$ms^{-2}
10
1
0.1
0.01
1E-3
1E-4
D.
S.D.
T.D.
100
10
3
Period (Hour)

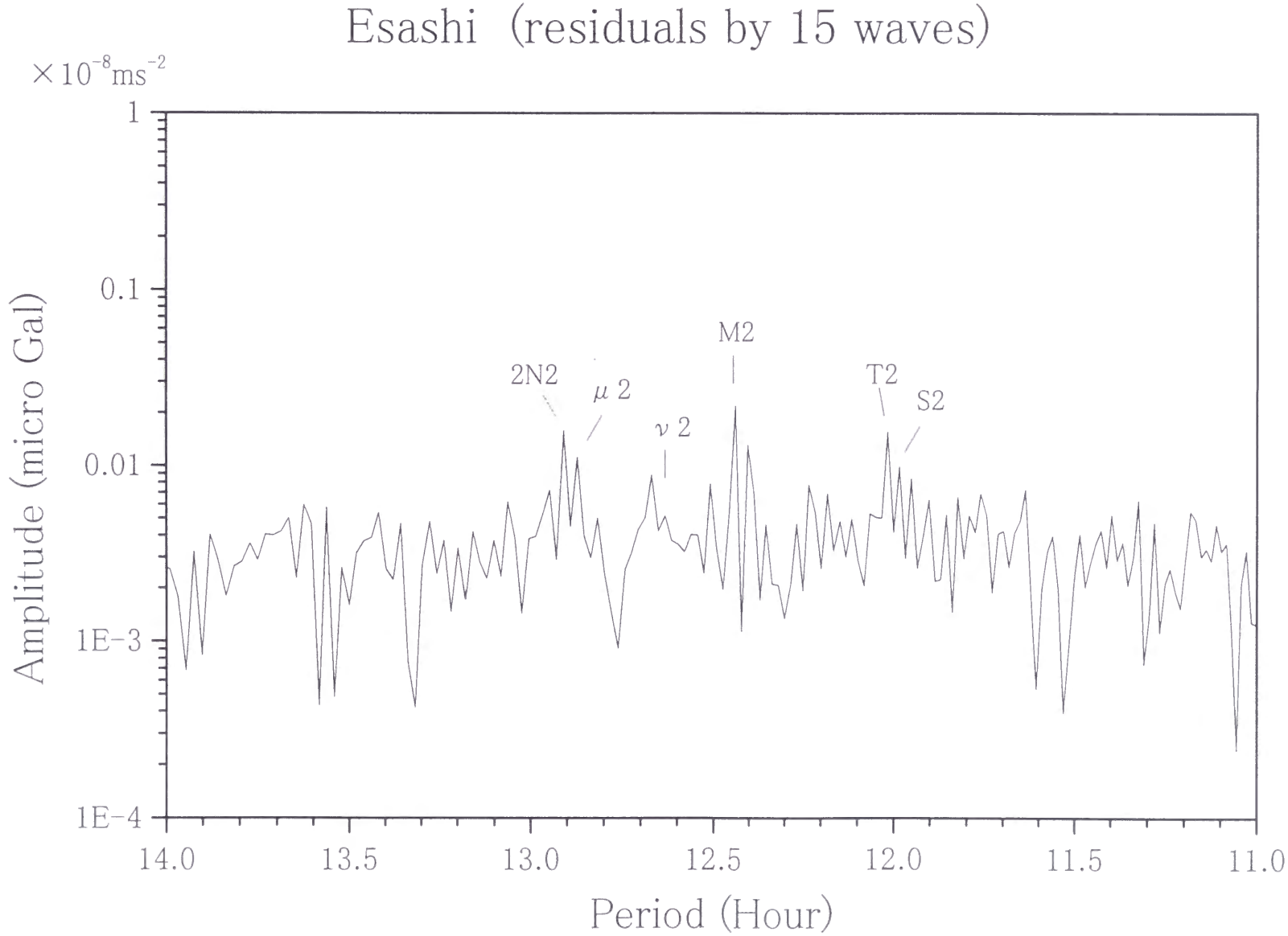
Esashi (residuals by 15 waves)
×10⁻⁸ms⁻²
1
0.1
0.01
1E-3
1E-4
Amplitude (micro Gal)
2N2
μ 2
ν 2
M2
T2
S2
14.0
13.5
13.0
12.5
12.0
11.5
11.0
Period (Hour)

Fig. 7c

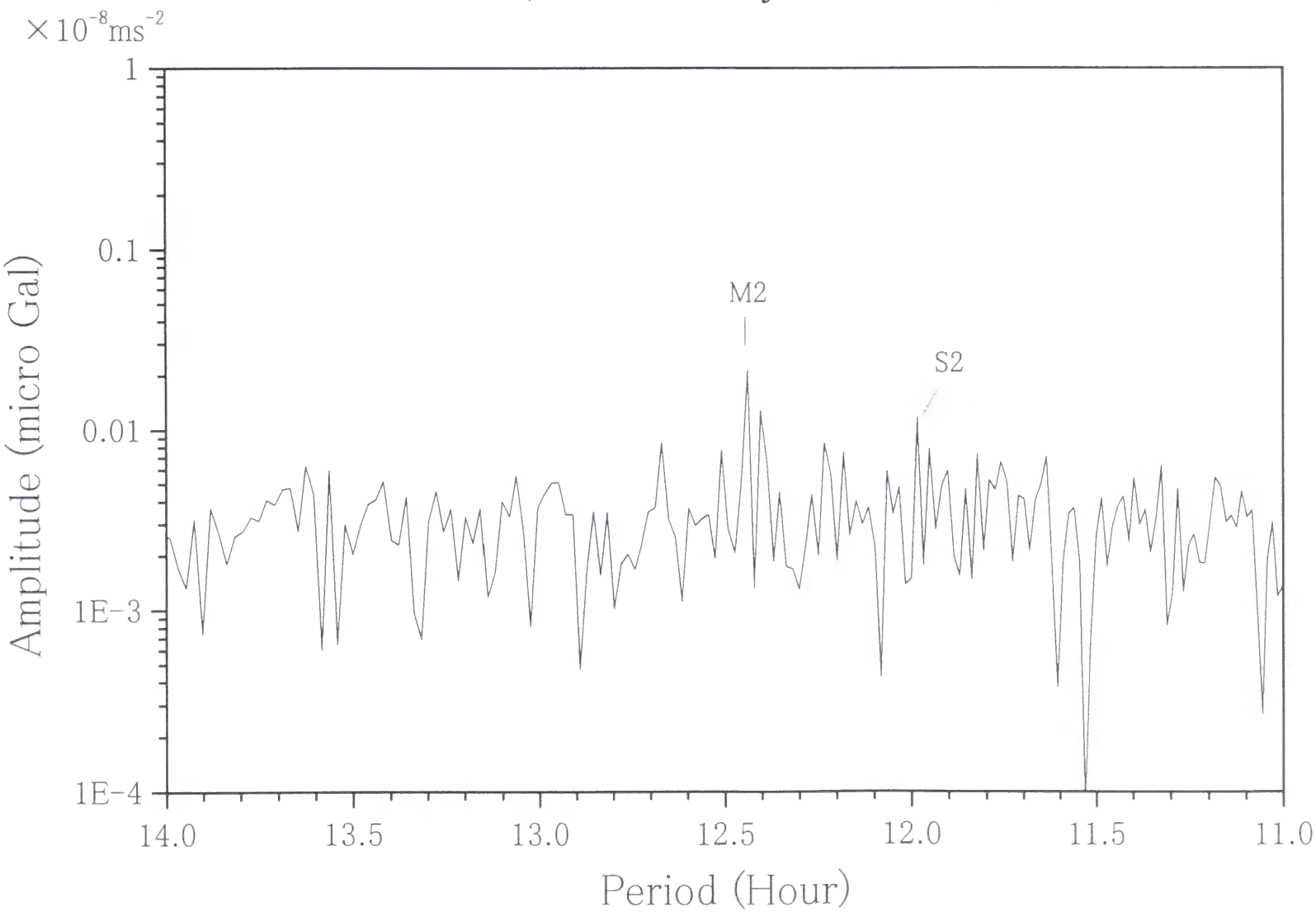
Esashi (residuals by 31 waves)
×10⁻⁸ms⁻²
1
0.1
0.01
1E-3
1E-4
Amplitude (micro Gal)
M2
S2
14.0
13.5
13.0
12.5
12.0
11.5
11.0
Period (Hour)

Fig. 7d

Figure 8a.

A sample of gravity tide residual spectrum in which rather large spectrum peaks remain in tidal bands. In this analysis, 31 tidal components are assumed for one year records and the tidal factors and phases are assumed in constant for the whole period.

Figure 8b.

Spectrum of gravity tide residuals. The tidal factors and phases are determined at every one month assuming 12 components successively for the same data used in Figure 8a. The spectrum peaks in semidiurnal band become lower and those of diurnal and terdiurnal disappear compared with Figure 8a. This result suggests that there may be a sensitivity change in gravity records or the existence of poor data period in one year records.

Figure 8c.

Spectrum of gravity tide residuals. The tidal factors and phases are determined at every 24 days assuming 12 components successively. Each analysis period of 24 days is shorter than the recommended period of one month which is necessary to resolve major tidal components. As a result of "over resolution" of tidal components, the power density around tidal bands shrinks abnormally.

Fig. 8a

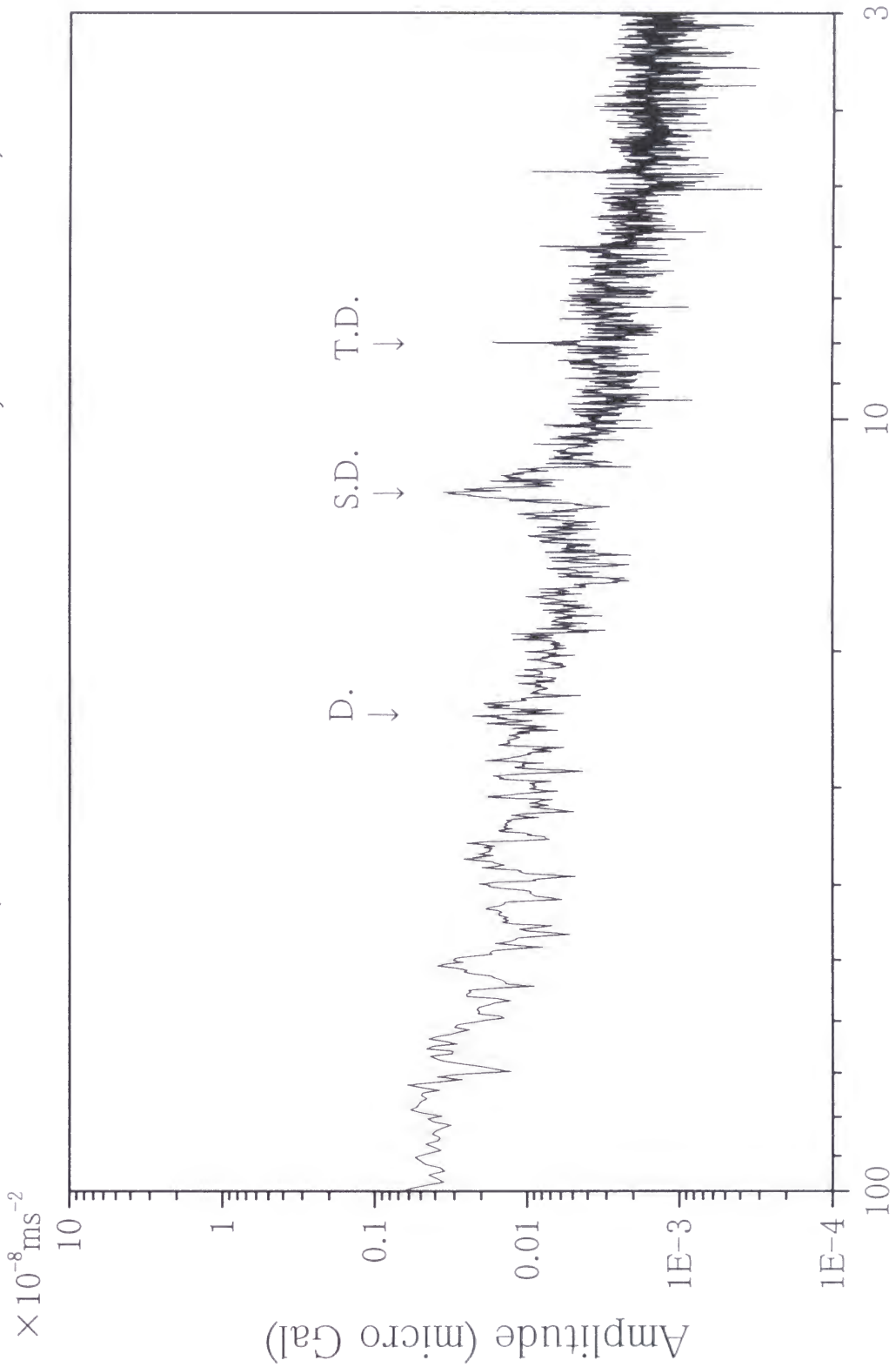
Esashi ('96.04.26 – '97.04.29, 31 waves)
D.
S.D.
T.D.
Amplitude (micro Gal)
×10⁻⁸ms⁻²
10
1
0.1
0.01
1E-3
1E-4
100
10
3
Period (Hour)

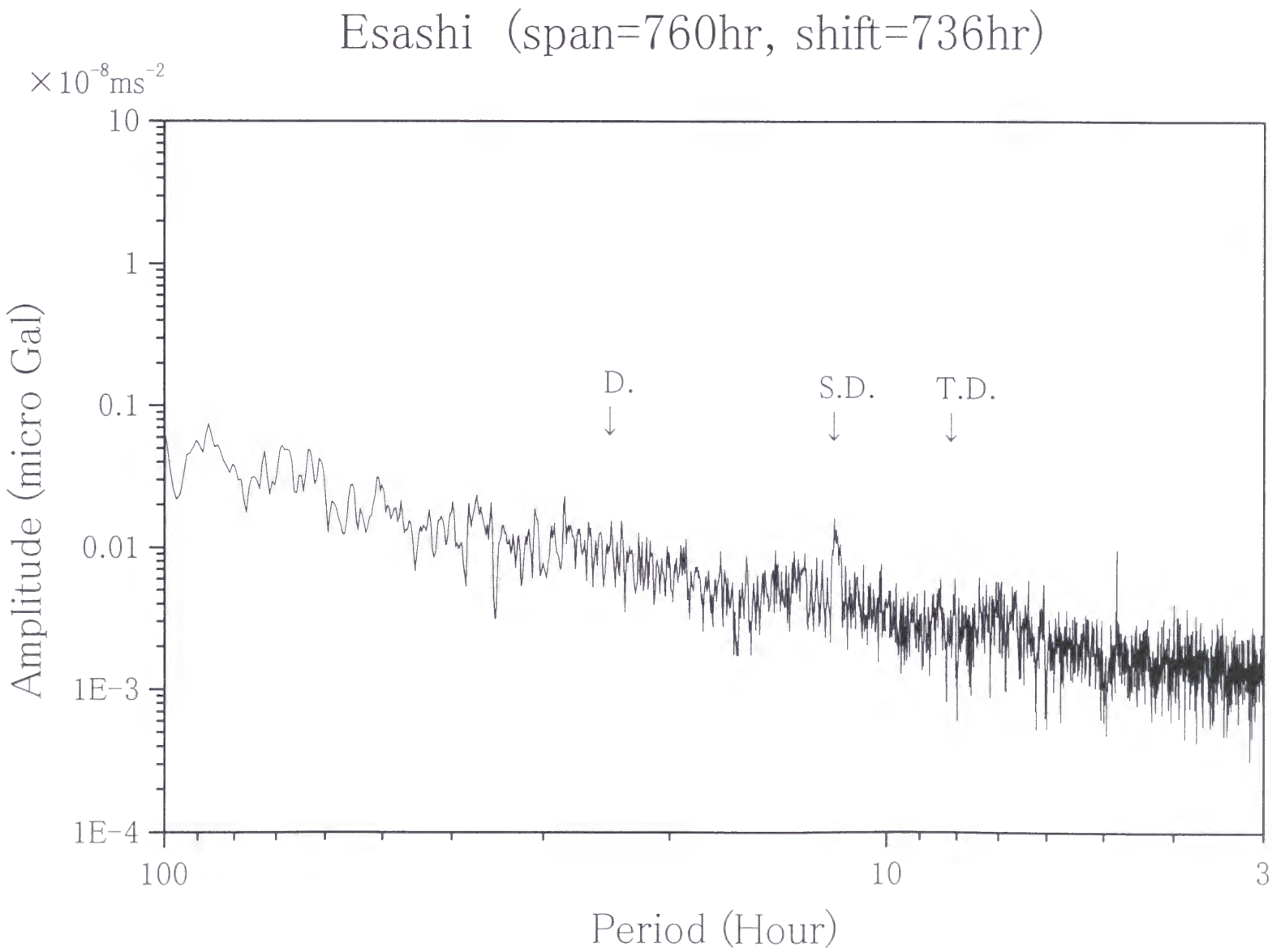
Esashi (span=760hr, shift=736hr)
×10⁻⁸ms⁻²
10
1
0.1
0.01
1E-3
1E-4
Amplitude (micro Gal)
D.
S.D.
T.D.
100
10
3
Period (Hour)

Fig. 8b

Fig. 8c

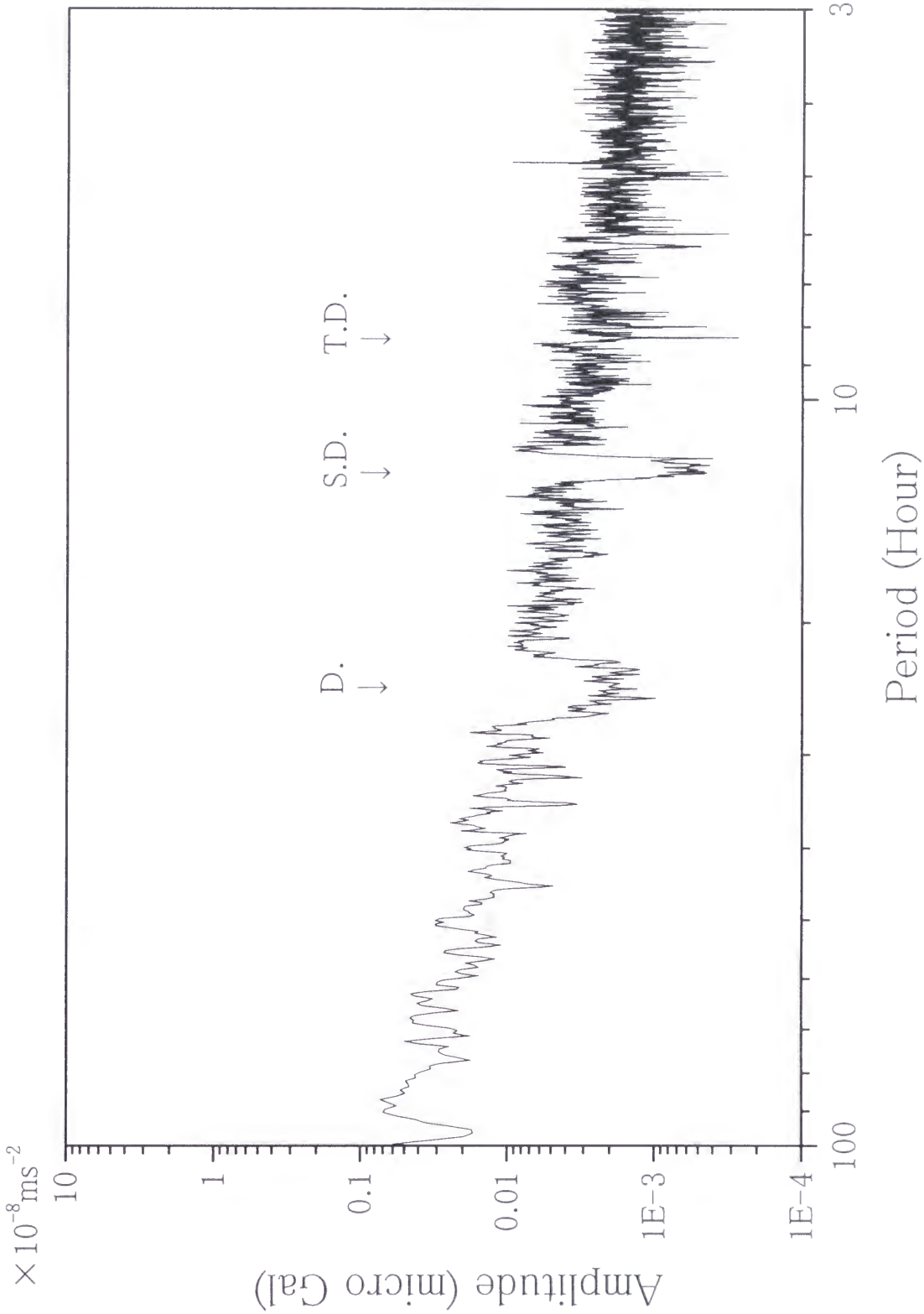
Esashi (span=576hr, shift=552hr)
×10⁻⁸ms⁻²
10
1
0.1
0.01
1E-3
1E-4
Amplitude (micro Gal)
D.
S.D.
T.D.
100
10
3
Period (Hour)

Figure 9.

Relative sensitivity change of a superconducting gravimeter at Esashi Earth Tides Station. There is unusual low sensitivity period in March 1997 (around 50580 modified Julian date) . The quality of tidal data around this period is considered not good. (The reason of bad observation condition is not certain.) In Figure 8a, one year gravity data which contains this poor observation period is used to demonstrate large residual peaks in tidal bands.

Fig. 9

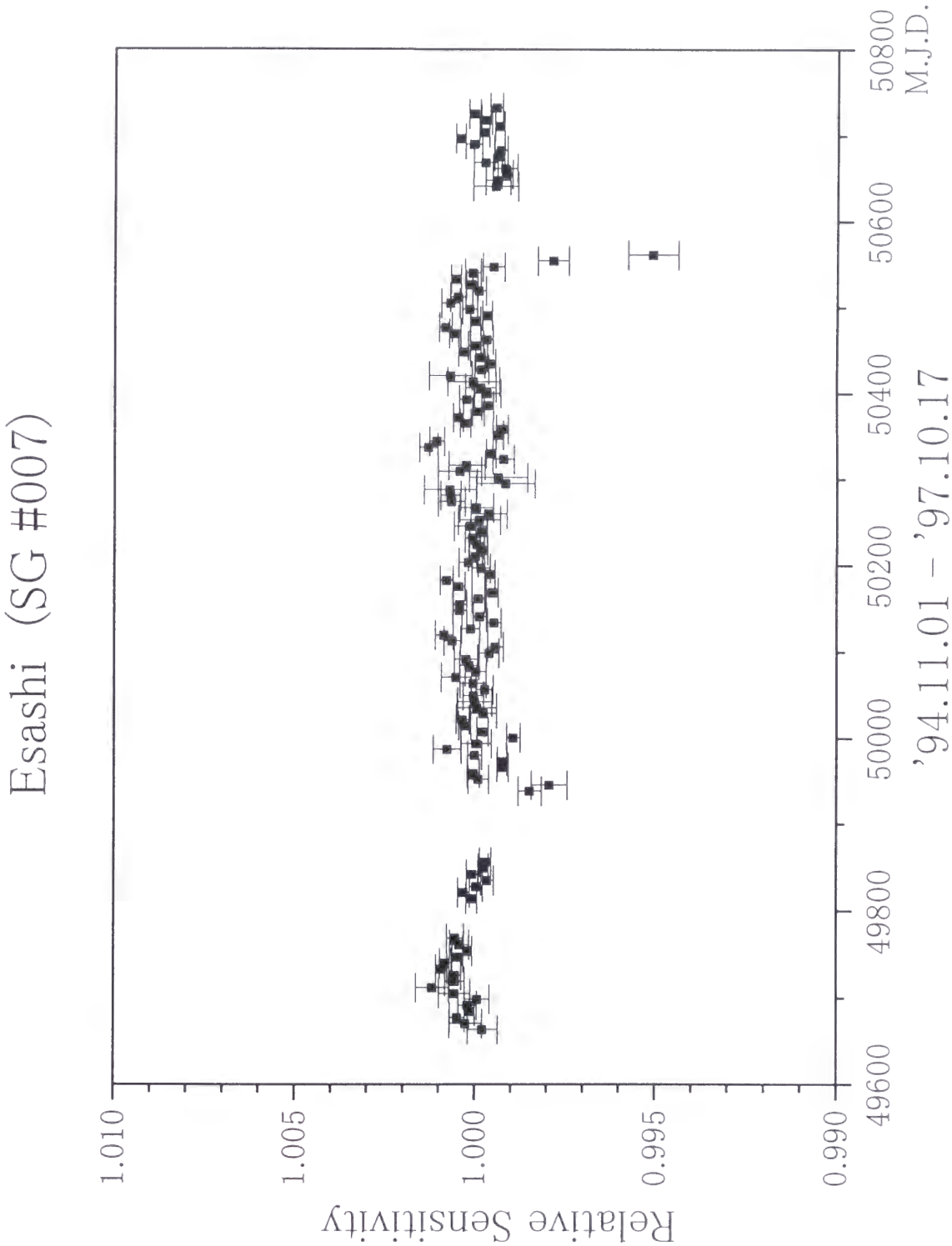
Esashi (SG #007)
Relative Sensitivity
1.010
1.005
1.000
0.995
0.990
49600
49800
50000
50200
50400
50600
50800
M.J.D.
'94.11.01 – '97.10.17

Figure 10.

The test of minimum ABIC search for the synthesized drift data. The minimum ABIC is obtained at D=4.0 in this case. The estimated drift becomes more straight and the residuals become larger if a larger hyperparameter D is given. In opposite, the estimated drift becomes winding and the residuals becomes smaller if a smaller hyperparameter D is given.

Minimum ABIC Search by Hyperparameter D

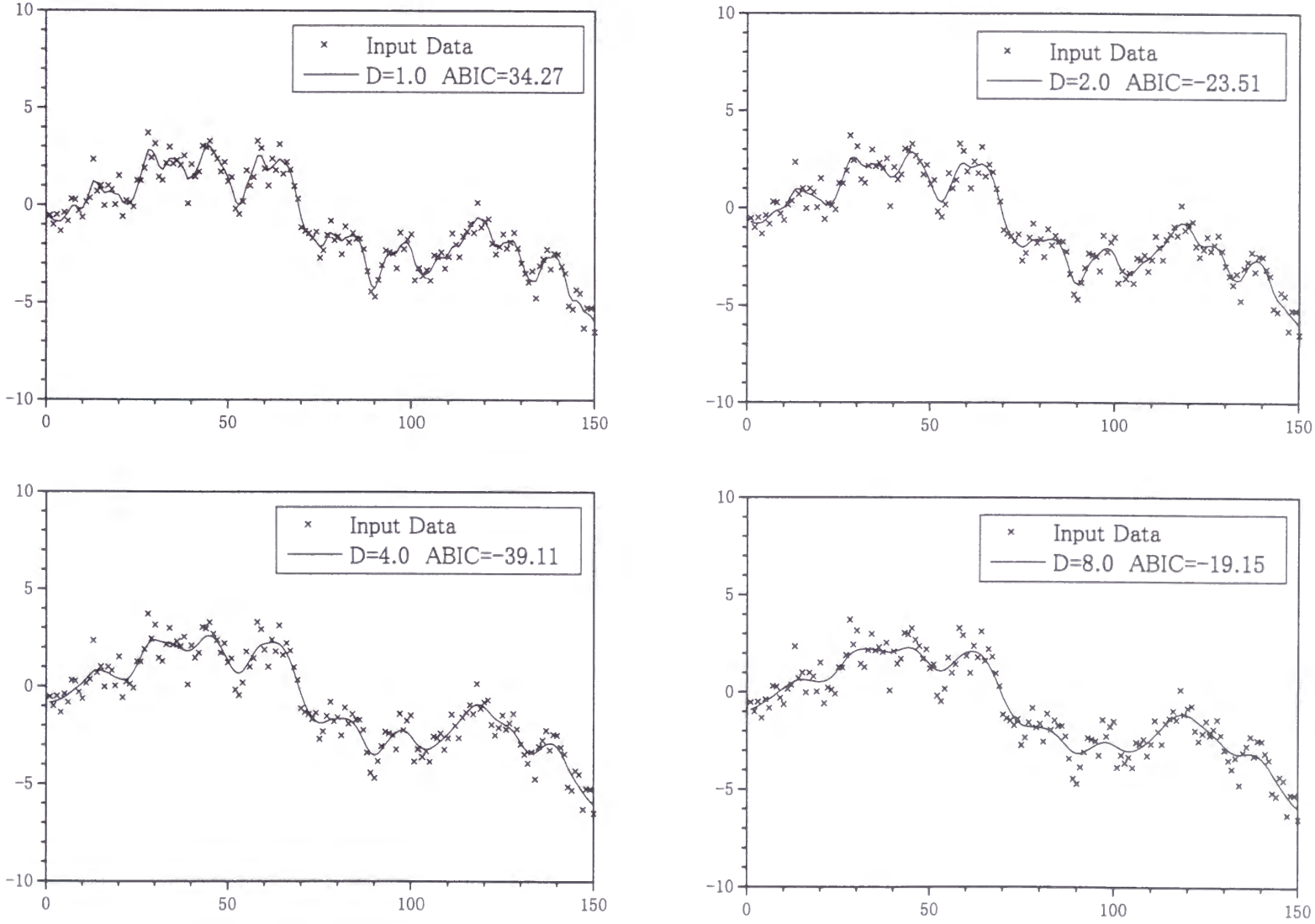

Fig. 1

Figure 11.

Minimum ABIC search for varying maximum lag number for associated data set. The gravity tide record is used as a tidal data set and the atmospheric pressure records is used as a associated data set in the analysis. Upper Figure shows the variation of ABIC against the maximum lag number of response model in atmospheric pressure data. Lower Figure shows the decrease of mean residual against maximum lag number. Minimum ABIC is obtained at the 0 lags. This means that the assuming simple minded a linear coefficient without time delay (i.e. proportional) model is the best model for atmospheric pressure effect. There is a local minimum ABIC at the 4 lags. This means that there is a very weak frequency response structure in atmospheric response, but the decrease of mean residual is not so clear even considering the frequency response structure.

Figure 12.

Minimum ABIC search for varying hyperparameter D which characterizes the drift component. Synthesized tidal data set is used in this test. The global minimum ABIC is obtained at D=16.0 and a local minimum ABIC is obtained at D=1.0. Usually, local minimums never come if the analysis model is suitable and there is no outlying data in the input data set. The sample used here is generated by giving a systematic sinusoid residuals in the synthesized tidal data.

Figure 13.

Determined drift models of two cases for the synthesized tidal data set. The synthesized input data has systematic error of sinusoid wave of about 7 hour period. The mark × shows the given drift data of one hour interval. The black line is a drift model determined with a hyperparameter D=1.0 (in the case of local minimum ABIC). The red line is a drift model determined with D=16.0 (in the case of global minimum ABIC). More smooth drift model is obtained in the latter case.

Fig. 11

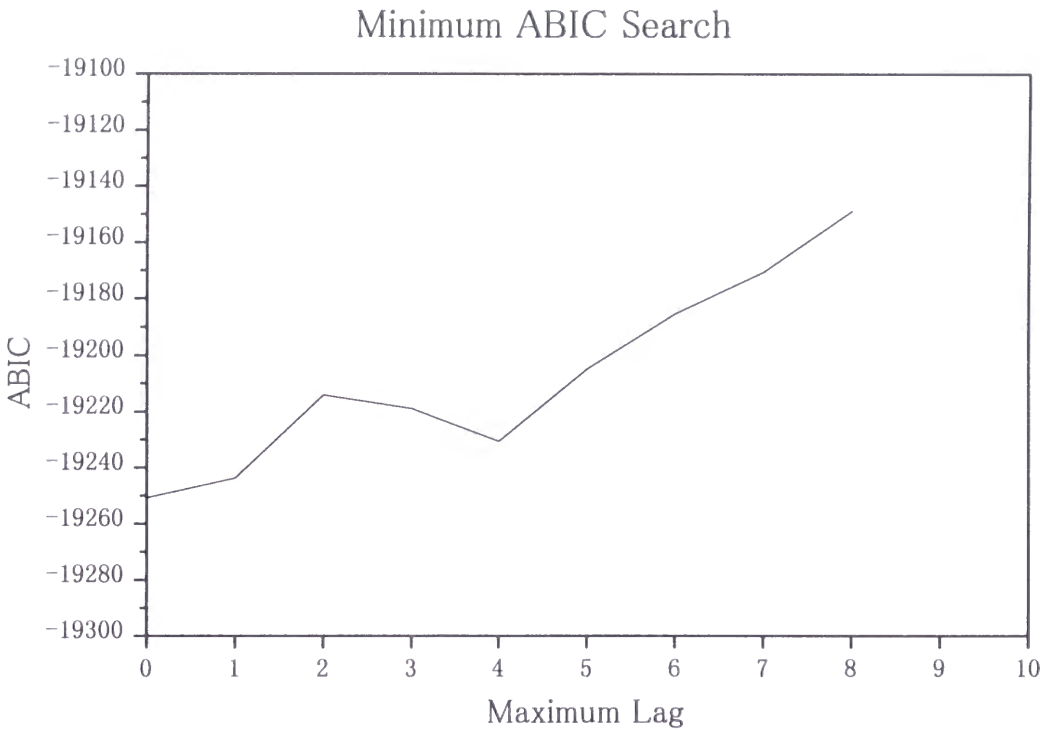
Minimum ABIC Search
ABIC
-19100
-19120
-19140
-19160
-19180
-19200
-19220
-19240
-19260
-19280
-19300
0
1
2
3
4
5
6
7
8
9
10
Maximum Lag

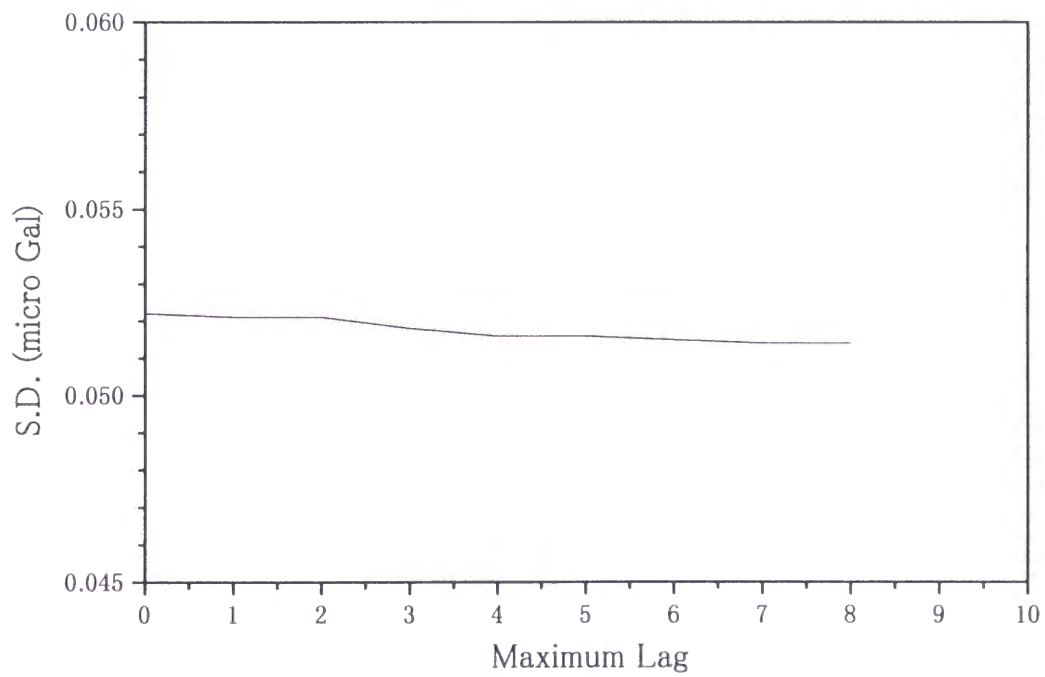
S.D. (micro Gal)
0.060
0.055
0.050
0.045
0
1
2
3
4
5
6
7
8
9
10
Maximum Lag

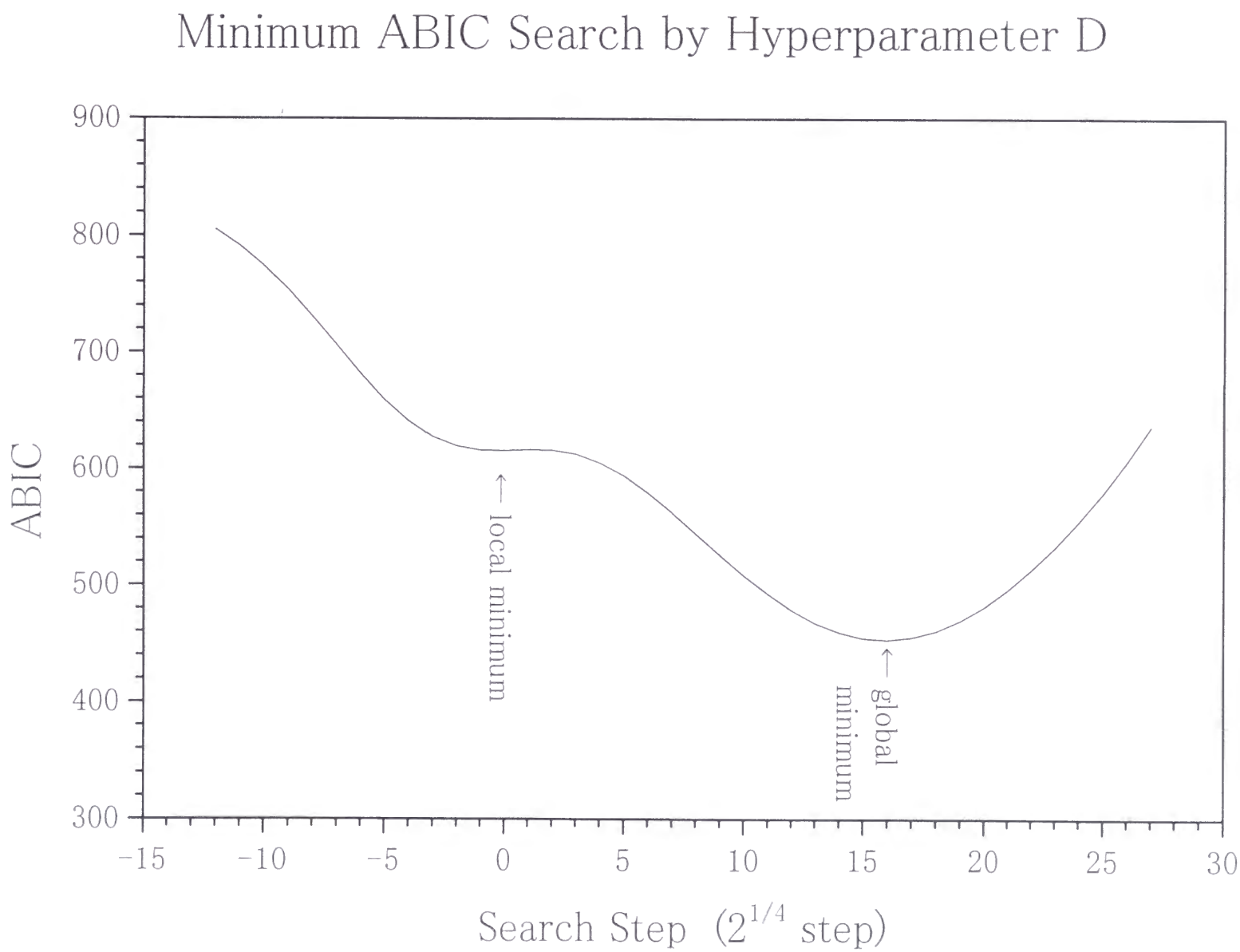
Minimum ABIC Search by Hyperparameter D
ABIC
900
800
700
600
500
400
300
−15
−10
−5
0
5
10
15
20
25
30
Search Step (2^1/4 step)
local minimum
global minimum

Fig. 12

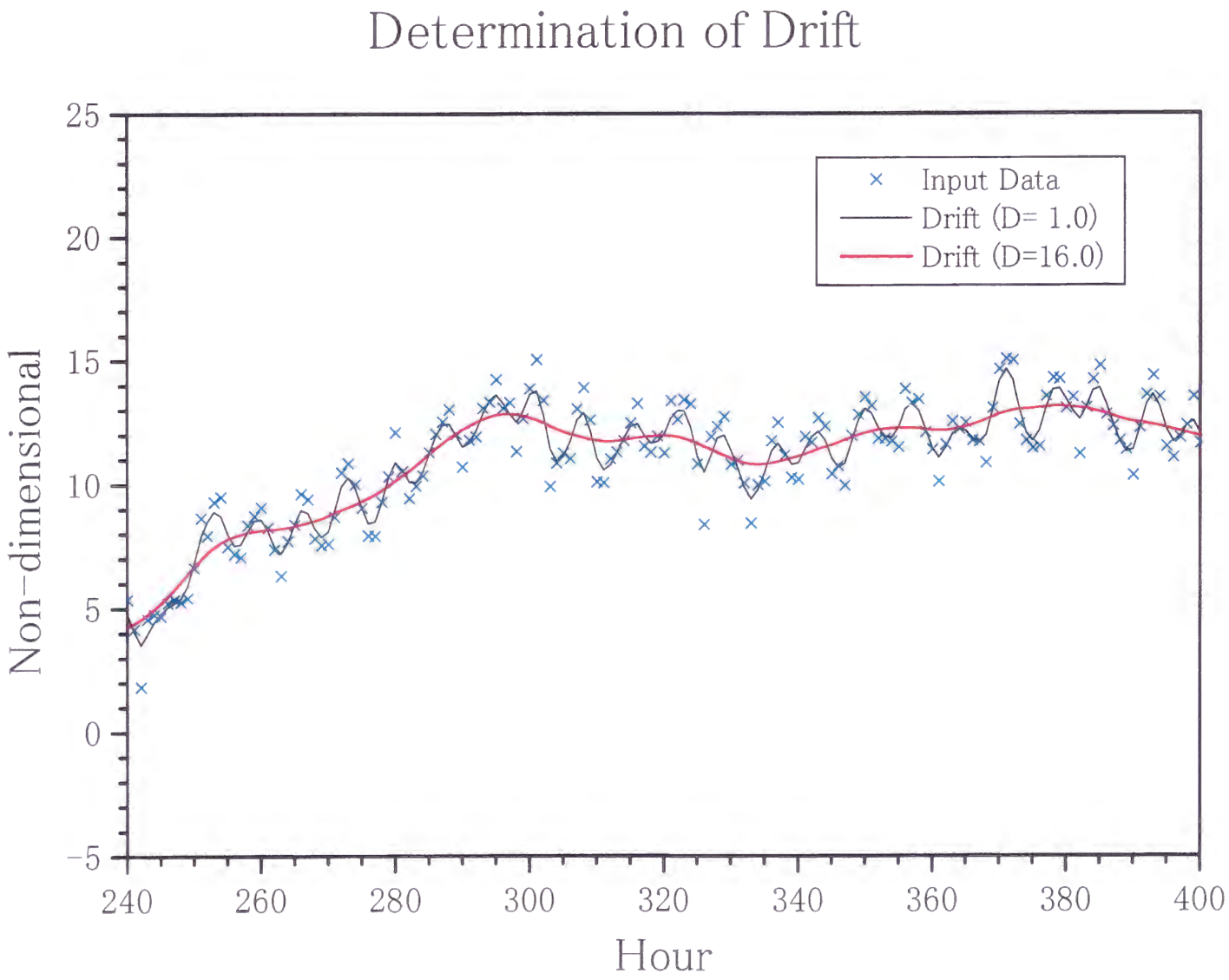
Determination of Drift
Input Data
Drift (D= 1.0)
Drift (D=16.0)
Non-dimensional
Hour
25
20
15
10
5
0
-5
240
260
280
300
320
340
360
380
400

Fig. 13

Figure 14.

Example of the tidal analysis of the crustal strain data using BAYTAP-G. The sample strain data is NS component of strain data observed at the Esashi Earth Tides Station. BAYTAP-G resolves input data into four parts of tidal part, response part, drift part and irregular part.

Left side in the upper part: Observed values including missing data periods,

Left side in the middle: Tidal part,

Left side in the bottom: Response part of atmospheric pressure,

Right side in the upper part: Drift part,

Right side in the middle: Irregular part (residuals),

Right side in the bottom: Drift part not in consideration of the response of the atmospheric pressure. The large fluctuation in the drift is strongly caused by the changes of atmospheric pressure.

Fig. 14

Tidal Analysis of Strain Data

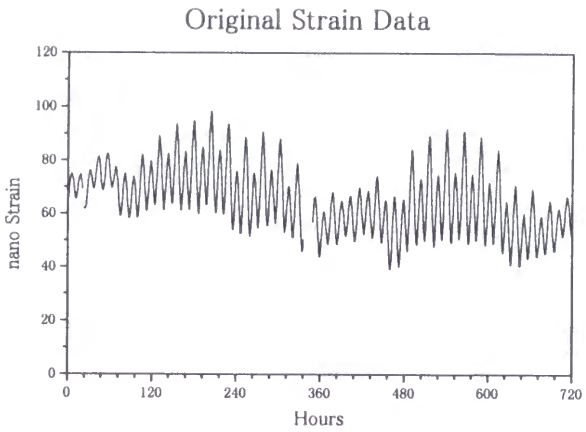

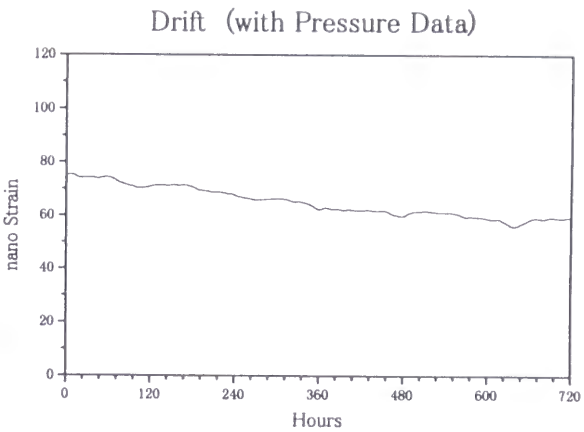

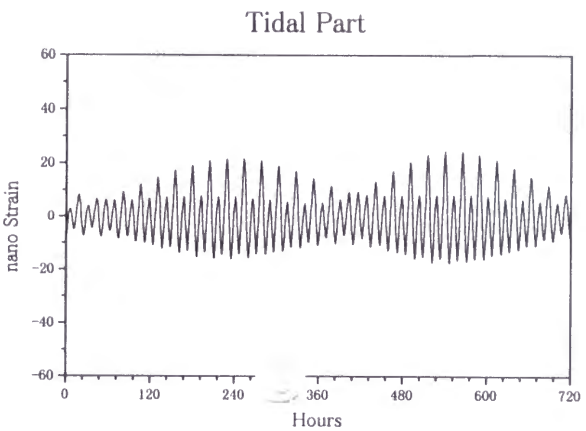

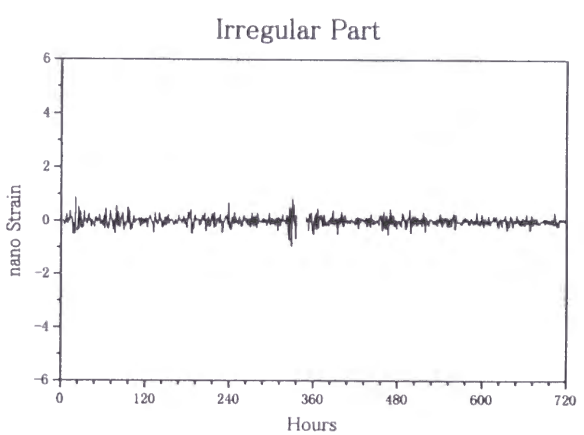

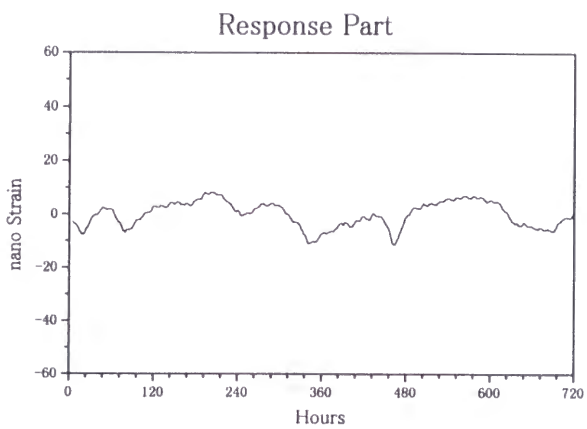

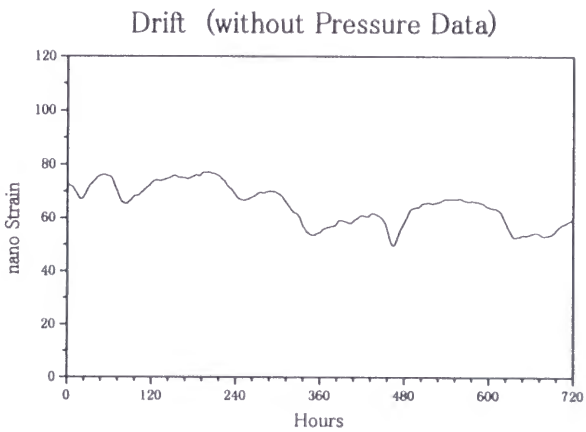

Figure 15.

Result of gravity tide analysis at the Syowa Station, Antarctica. The marks ■ show tidal admittances on diurnal band of raw analysis result. The marks ◆ show the result of after correcting ocean tide effects. The solid line gives theoretical admittance curve considering the fluid core resonance effect.

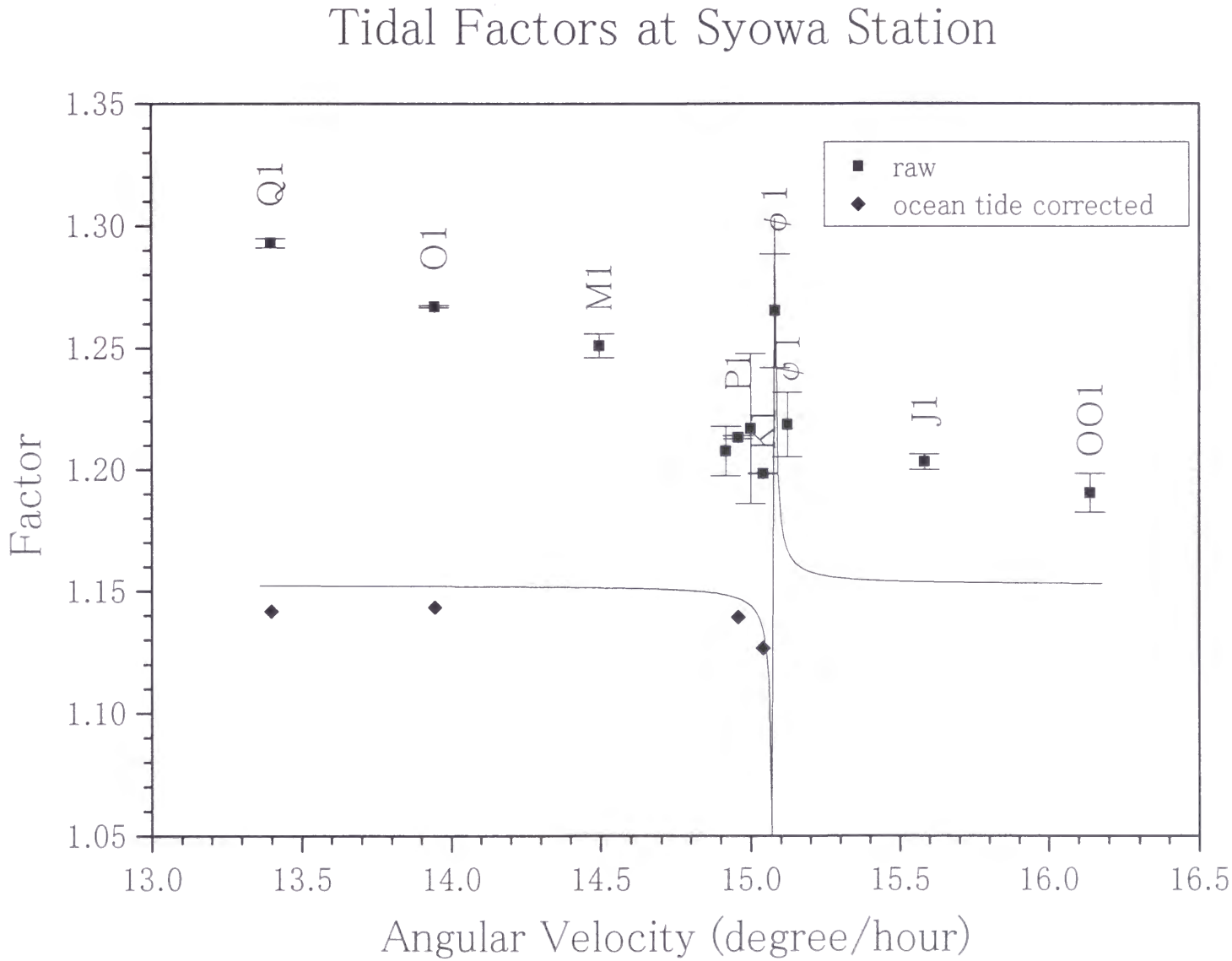
Tidal Factors at Syowa Station
raw
ocean tide corrected
Q1
O1
M1
P1
K1
φ1
φ1
J1
OO1
Factor
1.35
1.30
1.25
1.20
1.15
1.10
1.05
13.0
13.5
14.0
14.5
15.0
15.5
16.0
16.5
Angular Velocity (degree/hour)

Fig. 15

Appendix

List of the Additional Harmonic Terms

Additional Terms Pnm = 20

11.187 cos(0.46712915 Td + 358.239)
9.354 cos(2.07724348 Td + 37.872)
8.855 cos(1.09584225 Td + 199.067)
8.604 cos(2.58986261 Td + 162.589)
8.583 cos(2.70157967 Td + 139.522)
8.484 cos(2.07758153 Td + 302.711)
8.414 cos(2.77222067 Td + 300.153)
8.409 cos(1.53288460 Td + 284.973)
8.339 cos(1.64930639 Td + 260.285)
7.850 cos(1.51700545 Td + 139.148)
7.788 cos(0.51041874 Td + 238.033)
7.749 cos(1.47814133 Td + 14.625)
7.592 cos(3.20709695 Td + 333.428)
7.428 cos(1.21415876 Td + 163.338)
7.423 cos(1.59913552 Td + 314.656)
7.391 cos(0.41896697 Td + 240.599)
7.265 cos(3.05696642 Td + 155.026)
7.084 cos(1.67417903 Td + 216.982)
7.032 cos(2.69472775 Td + 107.806)
7.014 cos(1.67883113 Td + 49.344)
7.000 cos(2.50331655 Td + 204.498)
6.989 cos(1.68788737 Td + 141.532)
6.961 cos(0.53288512 Td + 273.212)
6.814 cos(0.03854404 Td + 55.857)
6.786 cos(1.13666236 Td + 149.815)
6.583 cos(0.04548130 Td + 318.990)
6.496 cos(1.60572570 Td + 309.896)
6.423 cos(3.16382109 Td + 99.402)
6.387 cos(3.09096412 Td + 65.594)
6.355 cos(0.38496301 Td + 327.150)
6.296 cos(1.00220053 Td + 139.492)
6.190 cos(3.60134121 Td + 289.692)
6.150 cos(1.14351415 Td + 9.692)
6.145 cos(1.08434133 Td + 160.471)
6.062 cos(4.21857061 Td + 98.948)
5.931 cos(2.19146956 Td + 161.265)
5.916 cos(2.53510013 Td + 246.958)
5.912 cos(0.20533785 Td + 191.085)
5.904 cos(3.12054359 Td + 16.327)
5.705 cos(1.04548068 Td + 216.284)
5.677 cos(2.12762004 Td + 50.460)
5.636 cos(2.26184051 Td + 75.751)
5.530 cos(1.11172940 Td + 354.202)
5.487 cos(0.42581579 Td + 280.303)
5.426 cos(1.18016571 Td + 253.241)
5.393 cos(2.00221681 Td + 155.995)
5.344 cos(2.04548836 Td + 28.044)
5.141 cos(1.09801070 Td + 155.083)
5.115 cos(1.61034533 Td + 289.679)
5.001 cos(2.67199524 Td + 184.929)
4.985 cos(2.27332649 Td + 118.981)
4.949 cos(0.46223616 Td + 247.171)
4.896 cos(1.16160125 Td + 123.874)
4.893 cos(2.07970621 Td + 169.184)
4.834 cos(1.13202689 Td + 145.996)
4.813 cos(1.06166466 Td + 69.281)
4.742 cos(1.52385046 Td + 354.661)
4.665 cos(2.62190513 Td + 86.967)
4.641 cos(3.24374301 Td + 40.392)
4.627 cos(3.13423820 Td + 298.151)

Additional Terms Pnm = 20 (cnt)

4.583 cos(2.62651783 Td + 230.193)
4.577 cos(0.43510345 Td + 86.309)
4.567 cos(2.57838212 Td + 311.766)
4.559 cos(0.58078773 Td + 328.232)
4.536 cos(0.07526878 Td + 157.100)
4.534 cos(1.98852004 Td + 238.160)
4.504 cos(3.63312966 Td + 326.184)
4.450 cos(3.81990245 Td + 32.321)
4.435 cos(1.66051447 Td + 57.737)
4.259 cos(1.57617558 Td + 342.568)
4.251 cos(0.67199002 Td + 263.276)
4.216 cos(2.64681159 Td + 44.772)
4.209 cos(1.64895136 Td + 2.059)
4.194 cos(1.41456517 Td + 302.351)
4.190 cos(1.48742341 Td + 244.049)
4.168 cos(0.11976455 Td + 88.147)
4.114 cos(1.47592943 Td + 115.223)
4.085 cos(0.15725528 Td + 308.958)
4.058 cos(1.04985390 Td + 309.771)
4.024 cos(0.55367392 Td + 204.920)
4.004 cos(0.51005846 Td + 341.386)
3.925 cos(0.64020051 Td + 252.976)
3.875 cos(0.63313572 Td + 320.117)
3.857 cos(1.71967637 Td + 177.077)
3.823 cos(1.05448580 Td + 289.884)
3.783 cos(2.12053444 Td + 114.201)
3.771 cos(2.74485014 Td + 219.000)
3.721 cos(1.05917409 Td + 40.610)
3.679 cos(1.12761498 Td + 35.623)
3.630 cos(2.69230372 Td + 359.082)
3.618 cos(0.02568122 Td + 80.939)
3.607 cos(0.13350942 Td + 184.621)
3.546 cos(1.56488505 Td + 170.091)
3.493 cos(1.10019931 Td + 329.527)
3.452 cos(1.09309444 Td + 8.762)
3.353 cos(1.75632578 Td + 64.375)
3.343 cos(2.72187421 Td + 314.815)
3.310 cos(1.65171700 Td + 358.996)
3.266 cos(2.51259296 Td + 19.973)
3.254 cos(1.52847997 Td + 88.410)
3.207 cos(1.60608133 Td + 206.280)
3.204 cos(2.77442879 Td + 174.465)
3.199 cos(0.59446248 Td + 230.980)
3.183 cos(4.29142399 Td + 133.177)
3.122 cos(1.40528495 Td + 340.838)
3.075 cos(1.44855660 Td + 37.227)
3.036 cos(0.03416968 Td + 153.929)
3.007 cos(0.41675667 Td + 6.212)
2.983 cos(3.05917669 Td + 29.674)
2.982 cos(3.17089317 Td + 5.574)
2.954 cos(2.19112679 Td + 265.216)
2.933 cos(2.69693253 Td + 339.873)
2.933 cos(0.07493002 Td + 253.685)
2.895 cos(1.44414602 Td + 104.131)
2.807 cos(0.53066877 Td + 37.936)
2.804 cos(0.11613842 Td + 73.704)
2.804 cos(2.19336372 Td + 127.684)
2.752 cos(2.17970324 Td + 234.016)
2.738 cos(4.14571651 Td + 64.709)
2.728 cos(1.22564491 Td + 206.070)

Additional Terms Pnm = 20 (cnt)

2.709 cos(0.45562123 Td + 309.259)
2.706 cos(0.00468568 Td + 173.657)
2.705 cos(2.03399311 Td + 258.849)
2.663 cos(0.55118610 Td + 328.754)
2.633 cos(3.19339785 Td + 54.707)
2.627 cos(0.89048764 Td + 343.101)
2.614 cos(0.12324463 Td + 294.362)
2.600 cos(0.00927442 Td + 160.472)
2.598 cos(1.05021046 Td + 205.536)
2.589 cos(1.01591075 Td + 140.338)
2.559 cos(0.93596675 Td + 295.357)
2.538 cos(3.60355151 Td + 164.073)
2.523 cos(0.07710207 Td + 90.797)
2.513 cos(0.54854670 Td + 165.995)
2.483 cos(4.22077983 Td + 333.229)
2.482 cos(1.61070011 Td + 188.638)
2.479 cos(3.04768995 Td + 332.672)
2.470 cos(0.03599151 Td + 215.091)
2.454 cos(0.51477600 Td + 263.008)
2.437 cos(0.34611415 Td + 207.078)
2.433 cos(2.07710147 Td + 129.621)
2.427 cos(0.16647388 Td + 252.085)
2.424 cos(2.08212704 Td + 92.936)
2.401 cos(2.14572051 Td + 260.867)
2.389 cos(2.62406162 Td + 304.882)
2.373 cos(2.62155269 Td + 192.738)
2.361 cos(3.70598507 Td + 0.237)
2.325 cos(2.60795471 Td + 282.176)
2.320 cos(1.64022375 Td + 335.288)
2.311 cos(2.12983068 Td + 283.978)
2.297 cos(0.51260738 Td + 24.960)
2.272 cos(0.10782900 Td + 283.697)
2.265 cos(1.68104848 Td + 284.763)
2.250 cos(1.06620628 Td + 32.076)
2.207 cos(0.62650655 Td + 229.177)
2.188 cos(1.72454066 Td + 28.117)
2.185 cos(2.50110724 Td + 335.925)
2.180 cos(0.59913034 Td + 225.249)
2.177 cos(0.70863851 Td + 152.753)
2.169 cos(1.55584142 Td + 76.958)
2.161 cos(1.63773963 Td + 208.176)
2.152 cos(1.52167882 Td + 135.902)
2.148 cos(2.15940604 Td + 238.943)
2.114 cos(1.02059205 Td + 51.085)
2.110 cos(2.19370793 Td + 27.524)
2.104 cos(1.94966194 Td + 115.530)
2.103 cos(0.03662725 Td + 58.129)
2.098 cos(0.48302408 Td + 322.237)
2.089 cos(0.01590828 Td + 151.370)
2.086 cos(2.07283396 Td + 212.586)
2.084 cos(1.05485354 Td + 191.274)
2.072 cos(1.56028897 Td + 285.200)
2.072 cos(1.10050676 Td + 236.485)
2.063 cos(1.18898982 Td + 316.950)
2.039 cos(1.99294502 Td + 175.031)
2.033 cos(0.59481891 Td + 129.795)
2.029 cos(2.67420430 Td + 58.529)
2.004 cos(2.57617179 Td + 146.756)
2.002 cos(2.27553795 Td + 352.905)
1.951 cos(2.80400728 Td + 336.315)

Additional Terms Pnm = 20 (cnt)

1.946 cos(3.11833545 Td + 145.993)
1.945 cos(0.64241800 Td + 128.142)
1.941 cos(0.08230555 Td + 130.396)
1.939 cos(0.04793725 Td + 239.622)
1.900 cos(1.11393980 Td + 229.481)
1.849 cos(3.27995425 Td + 9.166)
1.847 cos(0.51700719 Td + 53.325)
1.828 cos(0.08195871 Td + 230.743)
1.825 cos(0.98634301 Td + 97.332)
1.824 cos(3.63533913 Td + 200.549)
1.823 cos(3.82211276 Td + 266.839)
1.812 cos(2.65122594 Td + 336.449)
1.810 cos(0.08439967 Td + 57.016)
1.803 cos(0.54331128 Td + 207.189)
1.796 cos(3.24595181 Td + 274.888)
1.795 cos(2.62872299 Td + 105.410)
1.769 cos(0.42360745 Td + 220.918)
1.769 cos(0.50109005 Td + 336.073)
1.758 cos(2.06584654 Td + 221.533)
1.743 cos(0.58763806 Td + 286.022)
1.731 cos(0.12067424 Td + 246.751)
1.699 cos(2.23226158 Td + 275.253)
1.692 cos(1.12982100 Td + 337.407)
1.682 cos(0.98412679 Td + 275.628)
1.669 cos(1.06131498 Td + 160.558)
1.642 cos(1.48962300 Td + 112.135)
1.638 cos(0.09244535 Td + 351.740)
1.630 cos(0.89976691 Td + 149.574)
1.592 cos(1.65387261 Td + 223.165)
1.589 cos(1.09348148 Td + 249.602)
1.577 cos(2.07065224 Td + 52.354)
1.571 cos(0.46674385 Td + 99.944)
1.567 cos(1.64455038 Td + 140.493)
1.560 cos(2.15009631 Td + 82.608)
1.550 cos(1.18237493 Td + 127.866)
1.544 cos(0.61942952 Td + 219.219)
1.543 cos(2.06138512 Td + 275.235)
1.537 cos(1.64235356 Td + 289.132)
1.533 cos(1.52132260 Td + 235.398)
1.515 cos(0.89269890 Td + 244.448)
1.514 cos(0.11171330 Td + 336.206)
1.511 cos(2.74705859 Td + 93.279)
1.509 cos(1.10242158 Td + 182.348)
1.502 cos(1.61503054 Td + 104.588)
1.483 cos(1.91787263 Td + 78.870)
1.479 cos(0.39643955 Td + 6.030)
1.466 cos(2.15471735 Td + 68.708)
1.463 cos(0.97040026 Td + 123.473)
1.416 cos(0.90417611 Td + 259.891)
1.411 cos(2.46224935 Td + 211.907)
1.402 cos(1.52629614 Td + 282.202)
1.402 cos(0.00428839 Td + 279.249)
1.381 cos(0.39158084 Td + 159.588)
1.371 cos(3.16627651 Td + 216.105)
1.363 cos(0.54911237 Td + 2.394)
1.349 cos(0.48080370 Td + 88.180)
1.347 cos(2.51480514 Td + 253.976)
1.340 cos(0.50577302 Td + 264.800)
1.330 cos(2.22321564 Td + 183.969)
1.328 cos(2.10022953 Td + 213.407)

Additional Terms Pnm = 20 (cnt)

1.312 cos(3.23447072 Td + 258.086)
1.310 cos(0.93840569 Td + 216.935)
1.306 cos(4.29363343 Td + 7.519)
1.305 cos(1.75853268 Td + 298.234)
1.301 cos(1.48300897 Td + 229.723)
1.288 cos(0.58548530 Td + 58.614)
1.275 cos(2.06823731 Td + 131.868)
1.272 cos(0.98170304 Td + 281.536)
1.272 cos(2.53289882 Td + 13.379)
1.258 cos(0.69936515 Td + 9.634)
1.248 cos(3.21637130 Td + 319.533)
1.244 cos(3.67861449 Td + 74.383)
1.233 cos(2.11859164 Td + 118.605)
1.231 cos(3.04548225 Td + 111.548)
1.222 cos(0.86090888 Td + 205.825)
1.215 cos(2.14351161 Td + 87.617)
1.210 cos(2.50552122 Td + 282.246)
1.191 cos(2.66296989 Td + 250.610)
1.177 cos(1.95673124 Td + 201.455)
1.171 cos(3.17310211 Td + 240.369)
1.171 cos(1.69253186 Td + 325.187)
1.162 cos(1.54877851 Td + 147.955)
1.154 cos(3.01589988 Td + 157.129)
1.126 cos(1.64705049 Td + 229.069)
1.120 cos(0.00212255 Td + 327.976)
1.115 cos(3.56027674 Td + 292.173)
1.111 cos(4.14792607 Td + 298.821)
1.107 cos(0.07865609 Td + 209.470)
1.100 cos(0.07752716 Td + 187.598)
1.100 cos(0.07175201 Td + 133.112)
1.066 cos(0.35760575 Td + 69.191)
1.063 cos(0.05645166 Td + 305.024)
1.047 cos(1.22785367 Td + 80.725)
1.043 cos(2.13644525 Td + 181.816)
1.043 cos(3.75147277 Td + 109.425)
1.035 cos(2.02738051 Td + 3.537)
1.028 cos(0.50542694 Td + 8.249)
1.026 cos(1.64955394 Td + 135.454)
1.011 cos(1.12518162 Td + 107.163)
0.992 cos(0.07959956 Td + 72.932)
0.977 cos(0.03888996 Td + 107.465)
0.959 cos(0.08559617 Td + 34.946)

Additional Terms Pnm = 21

13.459 cos(12.84959881 Td + 208.222)
12.943 cos(13.39183950 Td + 133.425)
9.805 cos(17.08434848 Td + 344.378)
9.160 cos(16.13419416 Td + 21.113)
8.953 cos(14.53065404 Td + 138.608)
8.299 cos(13.38939466 Td + 19.008)
8.298 cos(16.02051482 Td + 45.212)
8.129 cos(13.82690914 Td + 207.540)
8.126 cos(15.46003280 Td + 251.909)
8.092 cos(16.09570586 Td + 344.126)
8.092 cos(17.18679084 Td + 174.333)
8.088 cos(14.65167709 Td + 86.646)
8.054 cos(13.28474026 Td + 306.655)
8.011 cos(14.13909035 Td + 347.062)
8.009 cos(15.94304219 Td + 35.185)
7.917 cos(12.52847040 Td + 351.033)
7.894 cos(18.17309755 Td + 253.971)
7.820 cos(14.06159970 Td + 331.794)
7.792 cos(13.86577463 Td + 150.719)
7.775 cos(16.21637282 Td + 231.494)
7.657 cos(16.69937632 Td + 13.950)
7.639 cos(10.74964257 Td + 237.844)
7.634 cos(15.11171236 Td + 169.418)
7.527 cos(15.07749455 Td + 208.183)
7.513 cos(15.57395655 Td + 282.332)
7.469 cos(12.97748886 Td + 41.000)
7.438 cos(17.10464566 Td + 338.725)
7.407 cos(13.90439521 Td + 221.004)
7.395 cos(14.45341127 Td + 168.335)
7.393 cos(15.46931295 Td + 242.027)
7.391 cos(12.84994993 Td + 106.641)
7.267 cos(17.19605878 Td + 319.412)
7.152 cos(11.87017331 Td + 4.678)
7.137 cos(16.22564579 Td + 39.540)
7.136 cos(12.53775562 Td + 322.177)
7.136 cos(17.07065423 Td + 66.938)
7.095 cos(11.87724501 Td + 272.113)
7.007 cos(11.95010083 Td + 305.557)
6.988 cos(14.88376880 Td + 51.546)
6.943 cos(14.60840060 Td + 29.927)
6.921 cos(15.58103226 Td + 217.264)
6.826 cos(15.55586686 Td + 348.082)
6.708 cos(16.65164395 Td + 176.891)
6.668 cos(13.94302902 Td + 199.636)
6.649 cos(15.08654732 Td + 129.276)
6.609 cos(16.52627655 Td + 291.711)
6.571 cos(13.81542001 Td + 165.097)
6.567 cos(14.65388877 Td + 339.052)
6.566 cos(10.89534997 Td + 306.303)
6.474 cos(14.52626891 Td + 195.544)
6.416 cos(14.91345155 Td + 62.009)
6.399 cos(15.16868191 Td + 318.996)
6.327 cos(15.00468505 Td + 189.134)
6.268 cos(17.77663984 Td + 62.823)
6.237 cos(13.36687670 Td + 314.543)
6.192 cos(14.49198899 Td + 81.006)
6.148 cos(12.77922761 Td + 294.905)
5.969 cos(13.99558461 Td + 152.546)
5.939 cos(16.06844946 Td + 289.339)
5.852 cos(16.75853510 Td + 131.591)

Additional Terms Pnm = 21 (cnt)

5.849 cos(13.03885333 Td + 214.654)
5.795 cos(15.70864184 Td + 345.799)
5.794 cos(17.66051168 Td + 154.950)
5.719 cos(13.50804061 Td + 231.257)
5.593 cos(17.26891053 Td + 356.245)
5.592 cos(11.33508043 Td + 10.210)
5.582 cos(13.40574429 Td + 90.668)
5.548 cos(16.09096684 Td + 340.281)
5.506 cos(12.95892981 Td + 274.848)
5.466 cos(14.93324117 Td + 87.569)
5.385 cos(12.30553673 Td + 329.099)
5.370 cos(17.14350741 Td + 101.357)
5.345 cos(15.62430499 Td + 86.479)
5.239 cos(13.08213018 Td + 104.065)
5.232 cos(14.33242857 Td + 218.897)
5.187 cos(13.31652714 Td + 343.444)
5.133 cos(13.48521286 Td + 290.023)
5.096 cos(13.48079102 Td + 94.974)
5.024 cos(13.39391379 Td + 345.544)
5.002 cos(13.05255129 Td + 131.784)
5.001 cos(15.59229510 Td + 2.544)
4.977 cos(14.99778324 Td + 197.474)
4.972 cos(12.96136346 Td + 199.600)
4.929 cos(13.00706644 Td + 168.708)
4.925 cos(14.64239702 Td + 124.760)
4.908 cos(15.03178258 Td + 202.565)
4.888 cos(15.43973577 Td + 257.247)
4.842 cos(12.46490277 Td + 208.178)
4.813 cos(18.31659434 Td + 88.506)
4.754 cos(14.01147465 Td + 218.063)
4.712 cos(16.07066063 Td + 162.519)
4.666 cos(12.23705988 Td + 34.640)
4.660 cos(16.61724189 Td + 351.763)
4.626 cos(13.39429237 Td + 240.318)
4.574 cos(14.49423606 Td + 125.878)
4.570 cos(12.39425792 Td + 324.779)
4.569 cos(13.97482014 Td + 328.907)
4.562 cos(15.07867440 Td + 79.246)
4.503 cos(13.40084917 Td + 36.412)
4.458 cos(16.01368682 Td + 188.749)
4.368 cos(15.00340424 Td + 300.927)
4.328 cos(17.16161992 Td + 127.730)
4.315 cos(11.92052708 Td + 155.830)
4.293 cos(15.67419835 Td + 331.300)
4.286 cos(16.51699516 Td + 123.140)
4.250 cos(15.54684771 Td + 267.252)
4.195 cos(17.19143368 Td + 165.534)
4.187 cos(16.10025285 Td + 50.518)
4.165 cos(11.99338055 Td + 183.792)
4.149 cos(17.19827475 Td + 194.852)
4.143 cos(15.71085083 Td + 219.935)
4.087 cos(16.17307694 Td + 152.626)
4.069 cos(17.18900403 Td + 50.228)
4.057 cos(16.22785684 Td + 273.533)
4.054 cos(12.34876415 Td + 11.171)
4.031 cos(13.91344899 Td + 335.870)
4.005 cos(14.10951642 Td + 210.701)
3.989 cos(13.99097544 Td + 179.032)
3.989 cos(14.98967287 Td + 205.847)
3.948 cos(15.09244239 Td + 172.759)

Additional Terms Pnm = 21 (cnt)

3.905 cos(17.11831972 Td + 248.539)
3.901 cos(13.91124836 Td + 6.142)
3.780 cos(14.48078836 Td + 263.431)
3.773 cos(11.87482519 Td + 166.431)
3.755 cos(17.23448299 Td + 165.832)
3.686 cos(12.96384402 Td + 137.283)
3.675 cos(14.49238756 Td + 331.594)
3.644 cos(13.44900160 Td + 143.616)
3.644 cos(14.53557903 Td + 8.880)
3.613 cos(16.63313732 Td + 238.255)
3.574 cos(15.54217366 Td + 305.003)
3.514 cos(12.26663900 Td + 196.343)
3.506 cos(14.92043508 Td + 129.032)
3.497 cos(17.00000696 Td + 267.327)
3.454 cos(16.51920449 Td + 201.257)
3.434 cos(12.84746171 Td + 353.478)
3.395 cos(14.56026970 Td + 281.656)
3.316 cos(18.71526159 Td + 155.080)
3.290 cos(14.07064747 Td + 241.110)
3.289 cos(14.48979872 Td + 175.195)
3.286 cos(11.98188888 Td + 341.843)
3.248 cos(16.65390459 Td + 61.382)
3.245 cos(12.94083330 Td + 154.878)
3.242 cos(13.59692383 Td + 266.469)
3.219 cos(17.27112297 Td + 230.502)
3.212 cos(13.55806414 Td + 142.961)
3.210 cos(12.34413124 Td + 31.374)
3.195 cos(16.48962466 Td + 43.951)
3.182 cos(12.81786446 Td + 186.507)
3.159 cos(16.57396179 Td + 118.763)
3.159 cos(16.67199192 Td + 181.208)
3.102 cos(16.63775844 Td + 219.618)
3.098 cos(16.04768595 Td + 84.062)
3.066 cos(13.44437098 Td + 163.064)
3.059 cos(15.07968528 Td + 72.243)
3.057 cos(16.60572978 Td + 125.156)
3.043 cos(17.63092716 Td + 353.981)
3.035 cos(18.31880500 Td + 322.519)
3.033 cos(17.22077269 Td + 245.826)
3.019 cos(14.53099601 Td + 33.811)
3.012 cos(14.58545386 Td + 61.164)
2.992 cos(16.05256756 Td + 319.232)
2.979 cos(16.13454026 Td + 280.259)
2.966 cos(11.82470008 Td + 51.563)
2.957 cos(14.34170189 Td + 0.267)
2.947 cos(12.45121193 Td + 28.705)
2.942 cos(11.80659375 Td + 110.879)
2.932 cos(15.98189504 Td + 334.525)
2.913 cos(15.93155654 Td + 351.524)
2.909 cos(17.54438155 Td + 40.897)
2.895 cos(15.63114463 Td + 330.817)
2.889 cos(14.45562974 Td + 332.517)
2.847 cos(16.71525566 Td + 51.629)
2.832 cos(15.97702962 Td + 304.466)
2.814 cos(13.56292667 Td + 173.745)
2.801 cos(17.19362577 Td + 35.368)
2.797 cos(11.43751625 Td + 206.759)
2.785 cos(15.00431712 Td + 286.944)
2.750 cos(12.02516488 Td + 213.744)
2.743 cos(13.34854251 Td + 44.830)

Additional Terms Pnm = 21 (cnt)

2.741 cos(18.78811582 Td + 189.278)
2.739 cos(17.61943921 Td + 307.572)
2.736 cos(14.09581606 Td + 292.969)
2.728 cos(17.58544288 Td + 246.780)
2.722 cos(12.92246942 Td + 245.876)
2.714 cos(10.82028874 Td + 37.189)
2.711 cos(15.38718159 Td + 217.210)
2.677 cos(18.24815950 Td + 163.628)
2.670 cos(14.99557648 Td + 240.769)
2.655 cos(11.48079064 Td + 78.636)
2.654 cos(11.72447268 Td + 296.050)
2.651 cos(14.98462284 Td + 69.224)
2.634 cos(16.77001709 Td + 174.750)
2.634 cos(15.08434559 Td + 338.985)
2.626 cos(14.87459772 Td + 117.261)
2.580 cos(15.15719221 Td + 97.999)
2.580 cos(12.50596958 Td + 295.183)
2.565 cos(12.91123491 Td + 87.084)
2.547 cos(14.94862988 Td + 14.749)
2.526 cos(13.01369034 Td + 9.511)
2.519 cos(13.51938388 Td + 241.271)
2.514 cos(13.36002389 Td + 85.584)
2.493 cos(16.17552078 Td + 105.321)
2.476 cos(12.41699404 Td + 66.147)
2.476 cos(17.24154397 Td + 275.531)
2.458 cos(16.72895446 Td + 330.223)
2.429 cos(13.47615011 Td + 164.943)
2.428 cos(14.99313234 Td + 135.613)
2.423 cos(14.95549591 Td + 326.492)
2.401 cos(12.53996217 Td + 33.850)
2.392 cos(11.83400614 Td + 225.830)
2.345 cos(14.03665569 Td + 176.548)
2.343 cos(14.46018363 Td + 201.138)
2.332 cos(12.37807658 Td + 104.970)
2.332 cos(13.39219506 Td + 202.190)
2.325 cos(17.74043133 Td + 95.263)
2.318 cos(18.16160944 Td + 210.579)
2.294 cos(11.80196855 Td + 130.611)
2.276 cos(10.27812113 Td + 137.120)
2.269 cos(11.32580144 Td + 229.401)
2.268 cos(15.05697060 Td + 161.454)
2.263 cos(14.03887271 Td + 51.840)
2.252 cos(16.04326583 Td + 329.481)
2.248 cos(14.92480178 Td + 21.024)
2.246 cos(14.55805657 Td + 48.395)
2.241 cos(14.95666807 Td + 292.831)
2.236 cos(13.43536182 Td + 234.230)
2.234 cos(16.64678153 Td + 139.376)
2.234 cos(12.84502360 Td + 246.033)
2.223 cos(13.39867282 Td + 65.045)
2.220 cos(12.36686141 Td + 311.339)
2.214 cos(12.76553097 Td + 18.220)
2.192 cos(14.65609717 Td + 222.103)
2.178 cos(14.92283854 Td + 310.161)
2.176 cos(12.93423515 Td + 355.122)
2.167 cos(14.39864776 Td + 243.621)
2.164 cos(15.47608869 Td + 259.386)
2.155 cos(10.86356103 Td + 269.607)
2.152 cos(15.54649417 Td + 10.465)
2.150 cos(17.57616726 Td + 78.882)

Additional Terms Pnm = 21 (cnt)

2.134 cos(15.08001808 Td + 328.591)
2.122 cos(11.92273507 Td + 223.879)
2.095 cos(13.27104305 Td + 29.592)
2.092 cos(18.71747207 Td + 29.030)
2.078 cos(13.92713605 Td + 140.878)
2.074 cos(16.68815557 Td + 218.739)
2.034 cos(13.39652222 Td + 182.657)
2.026 cos(14.57881497 Td + 36.391)
2.026 cos(13.94770913 Td + 190.669)
2.017 cos(12.30519052 Td + 70.844)
1.996 cos(11.40572910 Td + 170.256)
1.996 cos(11.21895716 Td + 103.499)
1.994 cos(11.79511193 Td + 96.516)
1.992 cos(16.25301677 Td + 120.354)
1.973 cos(14.96237782 Td + 199.968)
1.950 cos(15.97482402 Td + 347.435)
1.922 cos(15.46467714 Td + 230.185)
1.918 cos(12.41234786 Td + 265.919)
1.917 cos(17.08655532 Td + 218.637)
1.896 cos(12.99557918 Td + 163.138)
1.894 cos(15.43045786 Td + 211.102)
1.891 cos(16.18457523 Td + 196.930)
1.888 cos(14.95231735 Td + 8.276)
1.884 cos(13.55145036 Td + 228.375)
1.883 cos(12.84941291 Td + 313.848)
1.882 cos(13.89754312 Td + 315.014)
1.881 cos(13.35320280 Td + 61.834)
1.875 cos(17.69229268 Td + 345.276)
1.848 cos(15.42608035 Td + 171.693)
1.842 cos(16.56489653 Td + 181.169)
1.835 cos(11.25295007 Td + 195.344)
1.825 cos(15.11834614 Td + 165.228)
1.824 cos(15.66050250 Td + 236.041)
1.821 cos(10.35097510 Td + 171.358)
1.816 cos(17.61502714 Td + 202.088)
1.812 cos(17.03400254 Td + 177.348)
1.811 cos(13.43071135 Td + 255.192)
1.808 cos(12.97041093 Td + 314.544)
1.799 cos(12.22336424 Td + 117.630)
1.799 cos(15.63336676 Td + 203.213)
1.798 cos(14.96925111 Td + 126.084)
1.794 cos(13.87946619 Td + 66.682)
1.793 cos(14.54217016 Td + 348.419)
1.781 cos(14.99657968 Td + 239.195)
1.769 cos(15.59014405 Td + 154.590)
1.757 cos(16.20267240 Td + 314.598)
1.755 cos(13.38716550 Td + 137.957)
1.745 cos(14.14129740 Td + 221.830)
1.738 cos(13.00465114 Td + 73.821)
1.735 cos(12.97968133 Td + 96.139)
1.733 cos(18.79032606 Td + 63.266)
1.728 cos(14.92934777 Td + 33.318)
1.725 cos(18.20267709 Td + 55.419)
1.717 cos(14.96138245 Td + 274.149)
1.703 cos(15.46224556 Td + 309.148)
1.702 cos(14.60597115 Td + 106.045)
1.700 cos(13.51479867 Td + 89.762)
1.699 cos(14.96598540 Td + 335.147)
1.670 cos(17.58765592 Td + 121.163)
1.670 cos(12.29400735 Td + 277.340)

Additional Terms Pnm = 21 (cnt)

1.668 cos(15.62186607 Td + 160.697)
1.667 cos(18.12981986 Td + 22.114)
1.667 cos(14.05475035 Td + 272.008)
1.662 cos(13.85869996 Td + 245.650)
1.651 cos(15.11632514 Td + 343.426)
1.643 cos(13.98847506 Td + 51.218)
1.643 cos(15.57615506 Td + 337.904)
1.635 cos(18.17530481 Td + 128.493)
1.622 cos(16.09541911 Td + 265.687)
1.602 cos(12.46268877 Td + 36.515)
1.600 cos(13.78805757 Td + 83.811)
1.588 cos(16.77223060 Td + 48.911)
1.588 cos(16.70157768 Td + 249.161)
1.585 cos(13.38055582 Td + 130.122)
1.575 cos(15.59474638 Td + 32.810)
1.573 cos(15.94525261 Td + 269.185)
1.573 cos(17.24375270 Td + 148.874)
1.566 cos(12.96346990 Td + 236.887)
1.566 cos(12.37843007 Td + 3.516)
1.565 cos(11.90684044 Td + 255.618)
1.563 cos(15.58976336 Td + 267.665)
1.560 cos(13.39618152 Td + 283.653)
1.555 cos(16.64014814 Td + 130.866)
1.553 cos(17.30069883 Td + 32.514)
1.551 cos(15.43266151 Td + 171.683)
1.546 cos(13.39462105 Td + 140.828)
1.544 cos(16.14793972 Td + 309.130)
1.538 cos(14.36907992 Td + 287.156)
1.526 cos(15.71305834 Td + 94.374)
1.524 cos(15.63582275 Td + 333.023)
1.520 cos(13.91733886 Td + 26.582)
1.516 cos(14.49461002 Td + 45.449)
1.515 cos(13.51721754 Td + 199.592)
1.515 cos(16.45563315 Td + 133.568)
1.513 cos(13.39974006 Td + 87.576)
1.506 cos(13.62650051 Td + 248.885)
1.506 cos(16.02275742 Td + 284.852)
1.504 cos(15.04102113 Td + 103.222)
1.493 cos(14.95866819 Td + 354.342)
1.484 cos(12.52626687 Td + 117.203)
1.450 cos(15.50331205 Td + 15.043)
1.445 cos(17.04107389 Td + 111.389)
1.437 cos(13.28253409 Td + 72.246)
1.432 cos(13.96872661 Td + 13.736)
1.431 cos(12.93178542 Td + 36.017)
1.430 cos(10.74743400 Td + 3.108)
1.426 cos(13.94083299 Td + 120.117)
1.425 cos(16.68780192 Td + 321.010)
1.420 cos(16.55807176 Td + 325.941)
1.411 cos(16.69033794 Td + 88.891)
1.407 cos(14.91790413 Td + 264.415)
1.400 cos(12.50817393 Td + 356.389)
1.398 cos(13.79732649 Td + 225.054)
1.393 cos(15.63799469 Td + 191.003)
1.379 cos(16.76074270 Td + 6.832)
1.374 cos(14.53523027 Td + 116.902)
1.373 cos(14.48739641 Td + 344.814)
1.368 cos(17.10684247 Td + 210.105)
1.365 cos(12.89755255 Td + 281.687)
1.352 cos(17.74264721 Td + 330.815)

Additional Terms Pnm = 21 (cnt)

1.348 cos(11.99558603 Td + 258.737)
1.333 cos(15.01537465 Td + 101.129)
1.332 cos(14.64460318 Td + 356.900)
1.330 cos(14.61502320 Td + 3.342)
1.327 cos(13.32140336 Td + 18.658)
1.321 cos(15.06675072 Td + 268.707)
1.308 cos(12.93642009 Td + 304.724)
1.294 cos(16.64711162 Td + 40.178)
1.283 cos(12.49208086 Td + 341.102)
1.280 cos(10.93641587 Td + 303.723)
1.279 cos(13.40330648 Td + 128.563)
1.279 cos(15.16436615 Td + 125.502)
1.278 cos(11.86796564 Td + 130.544)
1.278 cos(11.75184477 Td + 17.387)
1.278 cos(13.08433638 Td + 168.260)
1.273 cos(14.97265124 Td + 84.658)
1.269 cos(16.58984827 Td + 159.384)
1.256 cos(13.51247108 Td + 94.933)
1.255 cos(15.00253356 Td + 151.966)
1.248 cos(16.09808077 Td + 251.164)
1.238 cos(14.88185642 Td + 92.333)
1.233 cos(14.62209202 Td + 310.168)
1.230 cos(10.89314068 Td + 71.811)
1.227 cos(16.13690634 Td + 51.304)
1.214 cos(17.76294005 Td + 145.873)
1.213 cos(12.31919555 Td + 235.684)
1.199 cos(16.25522567 Td + 354.202)
1.188 cos(13.90543795 Td + 226.711)
1.184 cos(12.85022191 Td + 350.947)
1.178 cos(14.02068605 Td + 203.290)
1.177 cos(13.41235834 Td + 76.130)
1.172 cos(11.44900303 Td + 47.636)
1.158 cos(13.81321246 Td + 290.373)
1.145 cos(15.55146640 Td + 83.235)
1.145 cos(14.44661819 Td + 321.827)
1.141 cos(15.93376470 Td + 61.697)
1.140 cos(18.08875862 Td + 174.201)
1.132 cos(12.85230587 Td + 46.144)
1.111 cos(14.88604938 Td + 132.973)
1.097 cos(15.03895140 Td + 211.974)
1.076 cos(11.94770576 Td + 205.522)
1.068 cos(15.58546058 Td + 23.848)
1.064 cos(15.50823643 Td + 196.933)
1.057 cos(14.96569406 Td + 57.403)
1.053 cos(12.56953724 Td + 348.495)
1.050 cos(18.20488705 Td + 289.856)
1.050 cos(12.82250249 Td + 174.917)
1.047 cos(11.33286953 Td + 137.176)
1.031 cos(18.13203162 Td + 256.320)
0.995 cos(17.66268018 Td + 18.102)
0.979 cos(15.03641206 Td + 6.974)
0.972 cos(12.41948673 Td + 3.873)

Additional Terms Pnm = 22

10.274 cos(27.89098289 Td + 124.549)
9.644 cos(27.57881905 Td + 141.486)
9.018 cos(27.92957224 Td + 176.244)
8.557 cos(27.41925140 Td + 327.099)
8.277 cos(28.93861898 Td + 172.402)
8.082 cos(29.60133089 Td + 114.204)
8.067 cos(29.45121257 Td + 296.103)
8.064 cos(30.71305961 Td + 107.381)
8.046 cos(31.16868099 Td + 55.668)
7.925 cos(29.11171896 Td + 72.900)
7.889 cos(28.59913403 Td + 334.329)
7.887 cos(28.44194244 Td + 231.632)
7.831 cos(31.01589345 Td + 224.611)
7.816 cos(31.64682774 Td + 321.695)
7.770 cos(28.40793951 Td + 130.567)
7.754 cos(27.98190524 Td + 345.720)
7.633 cos(27.85893257 Td + 17.928)
7.460 cos(28.51722109 Td + 4.199)
7.284 cos(27.34635966 Td + 284.658)
7.210 cos(31.08653419 Td + 36.895)
7.198 cos(26.84766389 Td + 301.921)
7.187 cos(29.38277143 Td + 190.839)
7.132 cos(26.86576056 Td + 242.217)
6.910 cos(27.03444314 Td + 7.155)
6.875 cos(30.07772232 Td + 90.678)
6.871 cos(29.96156433 Td + 328.675)
6.842 cos(32.11613701 Td + 186.467)
6.795 cos(26.40573236 Td + 182.910)
6.787 cos(31.14131412 Td + 138.496)
6.709 cos(28.38959850 Td + 235.884)
6.660 cos(30.00229201 Td + 59.636)
6.580 cos(27.06623174 Td + 44.680)
6.571 cos(29.98968287 Td + 206.013)
6.522 cos(31.12982760 Td + 112.909)
6.512 cos(27.96351249 Td + 75.462)
6.460 cos(30.02568754 Td + 262.972)
6.364 cos(26.52185734 Td + 269.675)
6.362 cos(26.76553871 Td + 126.822)
6.186 cos(30.17089199 Td + 206.450)
6.108 cos(29.03446806 Td + 293.721)
6.063 cos(31.08874808 Td + 269.686)
6.020 cos(28.05476086 Td + 198.598)
5.840 cos(31.22122997 Td + 96.977)
5.823 cos(27.50817316 Td + 9.476)
5.765 cos(31.13445191 Td + 98.205)
5.763 cos(29.48983409 Td + 7.430)
5.738 cos(29.99652158 Td + 150.698)
5.629 cos(26.33287854 Td + 148.844)
5.604 cos(31.68347824 Td + 43.637)
5.458 cos(26.84303011 Td + 321.761)
5.457 cos(25.31918748 Td + 327.972)
5.437 cos(26.36686764 Td + 60.436)
5.391 cos(27.53554782 Td + 89.675)
5.354 cos(28.43290693 Td + 136.086)
5.272 cos(31.21195757 Td + 288.728)
5.266 cos(29.96389852 Td + 141.256)
5.205 cos(28.35097234 Td + 163.740)
5.194 cos(25.90462819 Td + 100.486)
5.155 cos(31.60354857 Td + 88.647)
5.129 cos(27.88606604 Td + 74.242)

Additional Terms Pnm = 22 (cnt)

5.095 cos(31.25301511 Td + 134.180)
5.085 cos(30.15940303 Td + 344.473)
5.042 cos(29.96586690 Td + 202.882)
5.031 cos(28.31211232 Td + 220.977)
4.995 cos(31.64020135 Td + 336.767)
4.964 cos(27.89062613 Td + 221.605)
4.945 cos(27.87944238 Td + 62.802)
4.773 cos(29.57175259 Td + 155.776)
4.761 cos(32.81329304 Td + 322.748)
4.689 cos(28.43556037 Td + 328.373)
4.677 cos(29.48520737 Td + 26.668)
4.663 cos(30.00346357 Td + 19.632)
4.627 cos(26.96159068 Td + 331.693)
4.508 cos(28.43740997 Td + 29.547)
4.452 cos(29.62431032 Td + 197.069)
4.445 cos(27.38055720 Td + 241.615)
4.393 cos(26.29401690 Td + 26.160)
4.365 cos(25.39204129 Td + 2.230)
4.355 cos(30.53996290 Td + 205.062)
4.351 cos(27.26442960 Td + 308.668)
4.303 cos(32.81550773 Td + 195.757)
4.280 cos(30.03761675 Td + 65.313)
4.259 cos(28.44437844 Td + 327.770)
4.196 cos(30.63118874 Td + 152.275)
4.166 cos(28.56513948 Td + 242.694)
4.055 cos(28.04569490 Td + 263.515)
4.046 cos(31.25522663 Td + 8.011)
4.019 cos(29.02953302 Td + 243.294)
4.006 cos(30.50331471 Td + 134.352)
3.944 cos(30.61723953 Td + 167.568)
3.931 cos(28.48300017 Td + 67.526)
3.906 cos(28.86797686 Td + 217.356)
3.884 cos(29.62209681 Td + 322.106)
3.858 cos(30.50110448 Td + 262.578)
3.850 cos(27.97284686 Td + 229.377)
3.845 cos(28.94552048 Td + 238.623)
3.839 cos(28.82912072 Td + 274.586)
3.815 cos(28.95841936 Td + 221.448)
3.752 cos(32.15499696 Td + 153.592)
3.742 cos(28.44078712 Td + 273.029)
3.727 cos(30.01030689 Td + 333.370)
3.712 cos(28.12319395 Td + 273.197)
3.660 cos(31.52848567 Td + 180.675)
3.653 cos(29.56955532 Td + 351.753)
3.647 cos(30.00017045 Td + 326.061)
3.602 cos(31.18899475 Td + 137.598)
3.577 cos(30.61501702 Td + 293.641)
3.499 cos(32.74485151 Td + 39.332)
3.473 cos(29.00979461 Td + 206.889)
3.392 cos(32.25963282 Td + 21.762)
3.388 cos(26.91831535 Td + 281.537)
3.387 cos(31.61062035 Td + 18.575)
3.374 cos(27.90464430 Td + 21.675)
3.371 cos(32.65830474 Td + 87.400)
3.356 cos(28.83839614 Td + 56.282)
3.309 cos(26.99117442 Td + 313.996)
3.305 cos(29.14837133 Td + 320.447)
3.296 cos(29.58323484 Td + 171.883)
3.260 cos(29.99971237 Td + 187.195)
3.251 cos(29.99740479 Td + 70.236)

Additional Terms Pnm = 22 (cnt)

3.242 cos(29.65609652 Td + 207.815)
3.240 cos(27.96387826 Td + 334.368)
3.223 cos(31.68569349 Td + 280.581)
3.189 cos(27.97749325 Td + 133.344)
3.173 cos(32.15721354 Td + 27.721)
3.141 cos(31.22343903 Td + 330.579)
3.125 cos(30.08211061 Td + 277.633)
3.072 cos(26.79290748 Td + 208.144)
3.069 cos(25.97748181 Td + 134.739)
3.019 cos(27.82029147 Td + 304.846)
3.016 cos(30.07994526 Td + 320.647)
3.005 cos(29.03664525 Td + 162.824)
2.998 cos(30.12321888 Td + 281.065)
2.997 cos(28.04813352 Td + 186.242)
2.946 cos(30.59693317 Td + 355.898)
2.894 cos(29.50109341 Td + 354.693)
2.889 cos(29.92292259 Td + 292.528)
2.885 cos(28.94650493 Td + 57.605)
2.881 cos(30.46689662 Td + 124.965)
2.876 cos(28.97748670 Td + 318.785)
2.875 cos(29.91345863 Td + 48.370)
2.828 cos(28.43772178 Td + 298.774)
2.827 cos(29.36907555 Td + 273.659)
2.822 cos(29.56734000 Td + 203.557)
2.814 cos(28.45341822 Td + 265.322)
2.793 cos(30.01370292 Td + 274.605)
2.782 cos(30.08431435 Td + 92.329)
2.766 cos(30.09583677 Td + 297.359)
2.763 cos(28.07992226 Td + 224.399)
2.747 cos(31.76560220 Td + 232.239)
2.732 cos(30.00264185 Td + 140.145)
2.707 cos(29.53315489 Td + 325.625)
2.690 cos(30.06844230 Td + 103.243)
2.685 cos(27.53311266 Td + 164.286)
2.654 cos(31.06133891 Td + 175.655)
2.626 cos(31.13666917 Td + 336.327)
2.619 cos(29.02172985 Td + 11.237)
2.600 cos(31.61282992 Td + 254.291)
2.527 cos(27.61060540 Td + 179.652)
2.525 cos(31.13203049 Td + 348.770)
2.497 cos(27.78143312 Td + 2.544)
2.476 cos(28.98378545 Td + 150.137)
2.476 cos(29.02990486 Td + 144.413)
2.475 cos(28.98653842 Td + 72.724)
2.449 cos(32.66757736 Td + 256.808)
2.427 cos(29.92823783 Td + 255.922)
2.393 cos(28.95230813 Td + 182.788)
2.384 cos(29.49449062 Td + 172.839)
2.365 cos(28.51966108 Td + 143.263)
2.364 cos(25.71785576 Td + 34.586)
2.351 cos(28.43960763 Td + 312.269)
2.337 cos(26.98874173 Td + 29.784)
2.334 cos(30.63084414 Td + 252.947)
2.310 cos(26.87485022 Td + 186.743)
2.309 cos(29.44634118 Td + 83.211)
2.307 cos(28.09361758 Td + 139.192)
2.301 cos(28.98439495 Td + 258.490)
2.299 cos(30.63335131 Td + 12.895)
2.298 cos(28.51489334 Td + 286.782)
2.202 cos(30.51699156 Td + 50.373)

Additional Terms Pnm = 22 (cnt)

2.197 cos(28.39417955 Td + 36.385)
2.192 cos(31.65831087 Td + 3.603)
2.184 cos(27.43530581 Td + 337.043)
2.158 cos(32.73115282 Td + 122.469)
2.156 cos(29.57856440 Td + 179.597)
2.142 cos(29.53528500 Td + 130.872)
2.139 cos(31.13911144 Td + 333.104)
2.135 cos(32.07285981 Td + 315.537)
2.110 cos(28.09139830 Td + 214.225)
2.109 cos(26.49006768 Td + 232.452)
2.107 cos(31.55806179 Td + 136.527)
2.087 cos(28.63580042 Td + 242.904)
2.080 cos(32.66978682 Td + 129.995)
2.078 cos(28.90680015 Td + 148.668)
2.068 cos(29.92132908 Td + 107.541)
2.060 cos(32.20268275 Td + 138.483)
2.048 cos(25.24633432 Td + 293.724)
2.039 cos(33.28481452 Td + 63.545)
2.038 cos(30.71526721 Td + 341.947)
2.032 cos(28.58543342 Td + 237.783)
2.027 cos(31.71968065 Td + 356.434)
2.012 cos(31.21415391 Td + 163.522)
1.987 cos(27.81322402 Td + 39.875)
1.985 cos(31.76781440 Td + 106.276)
1.979 cos(28.00243873 Td + 206.951)
1.963 cos(28.95453870 Td + 347.897)
1.958 cos(27.50131879 Td + 129.366)
1.942 cos(30.19604895 Td + 235.017)
1.940 cos(30.00706331 Td + 97.471)
1.939 cos(28.00584219 Td + 136.083)
1.938 cos(27.38983724 Td + 22.946)
1.931 cos(30.09362792 Td + 64.423)
1.929 cos(28.98166342 Td + 17.260)
1.924 cos(27.97045137 Td + 136.647)
1.911 cos(29.92715713 Td + 324.891)
1.856 cos(27.84523960 Td + 101.058)
1.851 cos(28.82469997 Td + 139.023)
1.844 cos(33.28702867 Td + 296.472)
1.817 cos(30.24640964 Td + 37.960)
1.805 cos(30.12102649 Td + 353.495)
1.796 cos(28.46541262 Td + 72.023)
1.783 cos(29.69274580 Td + 97.397)
1.782 cos(29.18015636 Td + 357.565)
1.781 cos(27.45119326 Td + 16.197)
1.780 cos(27.89299635 Td + 301.029)
1.779 cos(27.86356471 Td + 356.264)
1.775 cos(29.99498463 Td + 46.222)
1.753 cos(32.27554057 Td + 173.980)
1.753 cos(28.43719895 Td + 118.553)
1.752 cos(25.83177202 Td + 66.143)
1.747 cos(26.37150492 Td + 221.094)
1.735 cos(30.98410569 Td + 46.365)
1.730 cos(27.41957769 Td + 41.300)
1.722 cos(29.03202043 Td + 182.710)
1.718 cos(28.41403577 Td + 87.360)
1.712 cos(29.96820698 Td + 171.391)
1.707 cos(28.56269822 Td + 303.272)
1.707 cos(27.30769989 Td + 208.088)
1.695 cos(29.90755985 Td + 18.032)
1.689 cos(30.20753961 Td + 97.041)

Additional Terms Pnm = 22 (cnt)

1.683 cos(31.25743773 Td + 242.500)
1.661 cos(26.93861335 Td + 276.315)
1.654 cos(29.10266593 Td + 343.949)
1.645 cos(30.11854806 Td + 218.821)
1.632 cos(29.96341867 Td + 171.189)
1.624 cos(32.14571318 Td + 349.577)
1.609 cos(28.47735821 Td + 234.561)
1.605 cos(28.55020704 Td + 270.204)
1.601 cos(30.12070142 Td + 94.075)
1.589 cos(32.12320485 Td + 122.454)
1.577 cos(29.06161378 Td + 142.201)
1.570 cos(27.02295703 Td + 352.250)
1.569 cos(27.43753655 Td + 212.524)
1.564 cos(29.69495753 Td + 341.714)
1.561 cos(27.89757329 Td + 98.573)
1.545 cos(27.88849773 Td + 359.871)
1.540 cos(31.68814247 Td + 46.416)
1.536 cos(31.53069184 Td + 54.796)
1.515 cos(31.69032871 Td + 271.274)
1.514 cos(28.99442130 Td + 280.078)
1.501 cos(28.63799682 Td + 276.143)
1.488 cos(31.57397070 Td + 287.345)
1.480 cos(27.38519600 Td + 40.439)
1.476 cos(30.00506436 Td + 142.047)
1.476 cos(28.59250664 Td + 312.210)
1.468 cos(28.97378920 Td + 153.291)
1.465 cos(27.50595182 Td + 28.695)
1.446 cos(32.26183942 Td + 256.335)
1.445 cos(29.10506510 Td + 260.094)
1.437 cos(29.62651971 Td + 71.859)
1.425 cos(30.97261708 Td + 4.551)
1.420 cos(28.43997048 Td + 203.659)
1.417 cos(27.99554318 Td + 149.422)
1.415 cos(28.93272099 Td + 320.100)
1.396 cos(32.66050833 Td + 321.199)
1.396 cos(28.98205655 Td + 310.368)
1.392 cos(30.20975078 Td + 330.417)
1.379 cos(32.12541401 Td + 355.466)
1.363 cos(31.01810527 Td + 316.720)
1.362 cos(32.81770542 Td + 73.128)
1.359 cos(28.40119484 Td + 108.852)
1.350 cos(28.98618110 Td + 136.305)
1.344 cos(30.03858404 Td + 221.186)
1.337 cos(26.47858277 Td + 217.692)
1.329 cos(26.00926884 Td + 171.323)
1.328 cos(30.05135923 Td + 162.054)
1.326 cos(30.59443590 Td + 56.927)
1.321 cos(30.42824016 Td + 229.577)
1.321 cos(26.73375121 Td + 90.458)
1.316 cos(29.96033187 Td + 123.627)
1.314 cos(28.40212430 Td + 281.348)
1.312 cos(28.56047995 Td + 261.709)
1.304 cos(29.99884892 Td + 231.444)
1.300 cos(25.86135595 Td + 48.242)
1.297 cos(33.21195150 Td + 31.397)
1.291 cos(30.04575459 Td + 210.305)
1.288 cos(30.08653245 Td + 322.163)
1.276 cos(13.98410399 Td + 124.351)
1.268 cos(30.19826166 Td + 108.882)
1.261 cos(29.95453224 Td + 75.627)

Additional Terms Pnm = 22 (cnt)

1.260 cos(28.01953539 Td + 229.945)
1.255 cos(26.32138622 Td + 107.441)
1.253 cos(31.73823374 Td + 151.122)
1.253 cos(30.64462539 Td + 180.952)
1.248 cos(29.91563948 Td + 130.836)
1.247 cos(29.40085716 Td + 310.647)
1.240 cos(28.01858167 Td + 62.297)
1.231 cos(28.49887930 Td + 106.633)
1.230 cos(28.48089876 Td + 75.382)
1.230 cos(30.58322486 Td + 58.180)
1.230 cos(29.98336528 Td + 356.144)
1.221 cos(27.91806163 Td + 133.630)
1.213 cos(30.97483119 Td + 234.712)
1.211 cos(29.14349951 Td + 107.243)
1.206 cos(25.82249342 Td + 285.419)
1.187 cos(28.43490669 Td + 177.609)
1.178 cos(27.99390585 Td + 330.375)
1.158 cos(27.84059006 Td + 300.276)
1.142 cos(29.53772514 Td + 142.803)
1.138 cos(29.41919822 Td + 29.823)
1.133 cos(27.31456302 Td + 243.468)
1.128 cos(30.03654974 Td + 217.915)
1.123 cos(26.55364225 Td + 306.326)
1.123 cos(29.03548701 Td + 108.214)
1.117 cos(26.43971563 Td + 94.862)
1.117 cos(43.98410403 Td + 124.353)
1.116 cos(30.07284046 Td + 33.697)
1.102 cos(26.98410049 Td + 229.904)
1.102 cos(33.21416420 Td + 265.034)
1.091 cos(30.09802527 Td + 172.282)
1.087 cos(29.83573115 Td + 9.059)
1.084 cos(27.45805846 Td + 76.623)
1.081 cos(29.93324808 Td + 282.218)
1.079 cos(28.46120078 Td + 219.859)
1.078 cos(28.56392497 Td + 5.329)
1.068 cos(31.74044708 Td + 24.699)
1.064 cos(31.11174298 Td + 170.972)
1.055 cos(29.57891986 Td + 79.799)
1.052 cos(29.05253586 Td + 227.099)
1.052 cos(31.79738955 Td + 268.667)
1.045 cos(27.80659787 Td + 28.564)
1.033 cos(30.04114424 Td + 359.538)
1.028 cos(28.53827740 Td + 105.403)
1.021 cos(28.96818981 Td + 154.661)
1.015 cos(28.56735496 Td + 118.818)
1.014 cos(14.52847918 Td + 259.331)
1.013 cos(29.89725089 Td + 213.978)
1.012 cos(29.43972716 Td + 253.256)
1.012 cos(27.89637898 Td + 138.388)
0.962 cos(26.26002028 Td + 115.904)
0.959 cos(28.43865858 Td + 272.102)
0.953 cos(26.44679901 Td + 179.481)

Additional Terms Pnm = 30

3.394 cos(3.20952281 Td + 91.441)
3.373 cos(0.42581200 Td + 110.083)
3.274 cos(1.60598010 Td + 195.533)
2.949 cos(2.58080874 Td + 239.203)
2.689 cos(0.46908250 Td + 162.897)
2.551 cos(3.28016776 Td + 251.371)
2.429 cos(0.07529030 Td + 332.212)
2.352 cos(1.65367237 Td + 189.221)
2.337 cos(1.71989811 Td + 60.952)
2.335 cos(1.00904449 Td + 187.758)
2.306 cos(0.54460185 Td + 17.791)
2.273 cos(2.12298356 Td + 55.649)
2.222 cos(2.74021394 Td + 225.301)
2.209 cos(0.00905487 Td + 282.555)
2.203 cos(2.66735875 Td + 190.509)
2.109 cos(0.53752400 Td + 266.204)
2.094 cos(2.06822276 Td + 141.744)
2.006 cos(0.46246412 Td + 357.995)
1.965 cos(1.68810988 Td + 24.121)
1.878 cos(0.11856358 Td + 25.623)
1.788 cos(1.02494864 Td + 159.966)
1.620 cos(0.93839832 Td + 212.315)
1.594 cos(2.15035851 Td + 335.342)
1.574 cos(0.62186649 Td + 163.283)
1.563 cos(3.28237847 Td + 125.434)
1.547 cos(1.17994202 Td + 34.001)
1.523 cos(1.56932173 Td + 292.743)
1.519 cos(2.18434376 Td + 48.827)
1.489 cos(1.08410647 Td + 276.479)
1.459 cos(1.72210749 Td + 295.008)
1.312 cos(1.52605795 Td + 240.542)
1.304 cos(2.62187398 Td + 83.231)
1.244 cos(1.59670879 Td + 41.111)
1.191 cos(1.06161179 Td + 47.398)
1.142 cos(0.03643536 Td + 189.305)
1.138 cos(0.47837070 Td + 329.048)
1.137 cos(1.48277133 Td + 352.831)
1.118 cos(0.04570558 Td + 351.583)
1.116 cos(3.75168927 Td + 352.091)
1.065 cos(1.67883021 Td + 215.256)
1.065 cos(2.23248374 Td + 159.034)
1.064 cos(1.64216211 Td + 325.437)
1.059 cos(3.13445737 Td + 183.055)
1.033 cos(2.07749984 Td + 307.016)
1.019 cos(0.98167433 Td + 107.630)
1.006 cos(1.60133128 Td + 22.584)
0.977 cos(0.54193782 Td + 196.861)
0.960 cos(0.55563137 Td + 113.590)
0.952 cos(1.60818864 Td + 76.916)
0.945 cos(2.72651443 Td + 308.484)
0.920 cos(1.69032116 Td + 258.108)
0.875 cos(1.05457419 Td + 149.811)
0.863 cos(2.03864720 Td + 337.295)
0.833 cos(1.57419048 Td + 352.462)
0.832 cos(1.55562765 Td + 18.933)
0.779 cos(0.58787425 Td + 251.690)
0.755 cos(2.62408416 Td + 318.166)
0.744 cos(3.12518203 Td + 13.522)
0.742 cos(0.39402764 Td + 73.071)
0.697 cos(2.65587757 Td + 146.833)

Additional Terms Pnm = 30 (cnt)

0.685 cos(1.13666237 Td + 316.918)
0.684 cos(3.75389968 Td + 226.112)
0.679 cos(2.15257404 Td + 213.455)
0.672 cos(3.21173315 Td + 327.565)
0.670 cos(2.19805184 Td + 328.121)
0.656 cos(2.59008470 Td + 48.456)
0.652 cos(3.13667029 Td + 57.001)
0.624 cos(3.67883451 Td + 317.898)
0.618 cos(1.99536365 Td + 107.451)
0.613 cos(1.05916162 Td + 116.817)
0.595 cos(1.16624726 Td + 117.485)
0.580 cos(3.19803392 Td + 49.164)
0.576 cos(1.10929824 Td + 234.658)
0.576 cos(1.49427313 Td + 203.427)
0.572 cos(2.07970796 Td + 182.727)
0.572 cos(2.23469586 Td + 33.406)
0.562 cos(1.00684130 Td + 133.959)
0.561 cos(2.26427214 Td + 195.666)
0.536 cos(1.49205570 Td + 330.332)
0.536 cos(2.15500389 Td + 328.990)
0.533 cos(1.09806023 Td + 77.901)
0.533 cos(2.10929205 Td + 137.140)
0.531 cos(3.20732446 Td + 35.400)
0.528 cos(0.59228895 Td + 186.915)
0.527 cos(2.03643557 Td + 102.713)
0.515 cos(0.97019078 Td + 245.393)
0.514 cos(1.57639933 Td + 226.751)
0.493 cos(1.63555027 Td + 343.372)
0.483 cos(0.59008904 Td + 122.956)
0.474 cos(0.00685188 Td + 47.237)
0.468 cos(2.11856499 Td + 304.913)
0.467 cos(1.48056643 Td + 288.270)
0.466 cos(1.08896903 Td + 155.897)
0.464 cos(0.93619137 Td + 154.082)
0.459 cos(0.12319419 Td + 31.258)
0.453 cos(1.63996515 Td + 273.173)
0.446 cos(1.01125636 Td + 246.670)
0.444 cos(0.62407866 Td + 38.654)
0.443 cos(2.11151422 Td + 7.250)
0.443 cos(0.55123710 Td + 359.307)
0.442 cos(2.10707585 Td + 265.984)
0.442 cos(3.16624842 Td + 218.312)
0.439 cos(2.17992657 Td + 120.319)
0.437 cos(2.65366730 Td + 272.414)
0.431 cos(1.02274860 Td + 103.244)
0.430 cos(0.47395187 Td + 38.866)
0.423 cos(2.58301935 Td + 111.767)
0.418 cos(1.10267577 Td + 257.575)
0.407 cos(1.10708057 Td + 183.654)
0.406 cos(0.08897698 Td + 249.892)
0.403 cos(2.59229569 Td + 282.164)
0.402 cos(1.52385259 Td + 7.720)
0.401 cos(2.20511433 Td + 78.484)
0.392 cos(1.72431804 Td + 169.687)
0.384 cos(2.53974041 Td + 242.127)
0.381 cos(3.68104543 Td + 192.041)
0.380 cos(0.97725476 Td + 179.570)
0.378 cos(0.63777289 Td + 134.384)
0.374 cos(1.64705262 Td + 206.562)
0.364 cos(1.02052687 Td + 230.785)

Additional Terms Pnm = 30 (cnt)

0.363 cos(0.50574515 Td + 100.065)
0.361 cos(1.09118491 Td + 28.869)
0.359 cos(0.97946775 Td + 50.442)
0.356 cos(0.42360457 Td + 55.371)
0.346 cos(2.15719329 Td + 199.535)
0.344 cos(0.08186176 Td + 302.383)
0.340 cos(0.06820754 Td + 39.838)
0.332 cos(2.11369056 Td + 67.138)
0.329 cos(0.51260574 Td + 116.634)
0.320 cos(2.07042585 Td + 14.485)
0.316 cos(1.55342481 Td + 323.785)
0.311 cos(1.13225240 Td + 23.470)

Additional Terms Pnm = 31

6.280 cos(12.38740526 Td + 277.254)
6.186 cos(11.28937723 Td + 198.993)
6.132 cos(15.00000229 Td + 0.102)
5.978 cos(12.92957465 Td + 355.671)
5.931 cos(12.80858191 Td + 32.041)
5.882 cos(11.90660671 Td + 8.186)
5.875 cos(17.15256664 Td + 24.268)
5.792 cos(13.98410472 Td + 304.900)
5.637 cos(14.40550212 Td + 291.640)
5.546 cos(11.75868899 Td + 65.423)
5.297 cos(12.96356913 Td + 242.164)
5.242 cos(13.94324142 Td + 172.123)
5.162 cos(13.31895929 Td + 256.147)
5.159 cos(16.14373543 Td + 263.163)
5.070 cos(17.22320565 Td + 184.545)
4.996 cos(13.54901042 Td + 220.664)
4.796 cos(15.46688500 Td + 299.748)
4.653 cos(13.46687679 Td + 199.278)
4.629 cos(17.15963867 Td + 316.635)
4.421 cos(15.63115010 Td + 316.649)
4.417 cos(16.56491186 Td + 17.780)
4.412 cos(17.70400257 Td + 93.551)
4.384 cos(16.14594696 Td + 137.422)
4.314 cos(15.04351436 Td + 308.878)
4.291 cos(17.77686608 Td + 125.714)
4.105 cos(17.16185238 Td + 189.388)
4.062 cos(15.54902036 Td + 136.638)
3.922 cos(12.46025345 Td + 313.791)
3.796 cos(17.77908062 Td + 358.603)
3.704 cos(15.51722914 Td + 105.463)
3.658 cos(17.70621522 Td + 327.286)
3.612 cos(12.45097939 Td + 142.984)
3.596 cos(14.02982230 Td + 127.393)
3.505 cos(16.02053528 Td + 242.852)
3.501 cos(15.58300589 Td + 25.780)
3.459 cos(15.59670359 Td + 304.316)
3.457 cos(11.36223141 Td + 233.191)
3.250 cos(13.35074773 Td + 292.591)
3.207 cos(12.91808735 Td + 135.335)
3.188 cos(12.30085076 Td + 324.217)
3.186 cos(16.05011308 Td + 197.786)
3.184 cos(16.09339984 Td + 275.647)
3.136 cos(12.88607762 Td + 224.342)
3.135 cos(12.37370879 Td + 359.878)
3.123 cos(13.38739941 Td + 180.268)
3.122 cos(14.03202050 Td + 183.632)
3.121 cos(12.77679371 Td + 355.424)
3.112 cos(15.05012038 Td + 113.959)
3.107 cos(16.69473860 Td + 200.684)
2.960 cos(12.97284725 Td + 49.611)
2.916 cos(16.14815420 Td + 10.886)
2.897 cos(17.07749800 Td + 115.986)
2.829 cos(14.57860238 Td + 193.368)
2.766 cos(14.50354149 Td + 104.053)
2.750 cos(15.57859513 Td + 277.016)
2.729 cos(14.53532736 Td + 118.460)
2.728 cos(14.45319339 Td + 299.709)
2.712 cos(16.05940699 Td + 185.194)
2.697 cos(16.17552452 Td + 92.239)
2.631 cos(12.41698313 Td + 232.149)

Additional Terms Pnm = 31 (cnt)

2.623 cos(14.92249534 Td + 165.480)
2.566 cos(13.95208992 Td + 35.900)
2.564 cos(16.06602011 Td + 348.991)
2.529 cos(14.91786021 Td + 159.029)
2.418 cos(11.28716779 Td + 324.585)
2.370 cos(11.87481748 Td + 331.780)
2.335 cos(13.43288809 Td + 105.414)
2.319 cos(17.69472644 Td + 285.083)
2.311 cos(15.67442246 Td + 37.009)
2.290 cos(11.90439670 Td + 133.525)
2.283 cos(12.83595088 Td + 113.294)
2.242 cos(15.08213969 Td + 201.131)
2.203 cos(14.41919865 Td + 28.322)
2.183 cos(16.61039313 Td + 125.083)
2.178 cos(13.86112725 Td + 156.348)
2.136 cos(16.09802789 Td + 259.346)
2.083 cos(15.67663327 Td + 269.991)
2.062 cos(16.12517968 Td + 106.995)
2.049 cos(12.88850330 Td + 331.729)
2.039 cos(12.85672056 Td + 324.034)
2.028 cos(12.80637390 Td + 157.659)
2.020 cos(17.22541563 Td + 58.820)
1.955 cos(12.96135596 Td + 7.147)
1.910 cos(15.97947269 Td + 35.882)
1.841 cos(16.53312078 Td + 341.415)
1.821 cos(12.34633071 Td + 74.492)
1.808 cos(13.46466421 Td + 324.811)
1.799 cos(13.44436444 Td + 149.785)
1.737 cos(14.61525758 Td + 259.801)
1.731 cos(11.21652422 Td + 164.775)
1.718 cos(16.56712185 Td + 251.987)
1.690 cos(13.97947048 Td + 143.817)
1.684 cos(13.51501745 Td + 129.887)
1.660 cos(16.68324912 Td + 160.447)
1.618 cos(12.33705872 Td + 292.618)
1.556 cos(14.99535825 Td + 200.347)
1.551 cos(17.62187440 Td + 250.586)
1.545 cos(12.26420713 Td + 257.089)
1.520 cos(12.93399082 Td + 285.684)
1.518 cos(12.86113549 Td + 71.522)
1.513 cos(14.56711006 Td + 149.247)
1.507 cos(15.51944106 Td + 339.829)
1.489 cos(14.56270212 Td + 41.500)
1.466 cos(16.67662630 Td + 353.973)
1.439 cos(13.36224202 Td + 336.307)
1.429 cos(12.44876866 Td + 268.663)
1.387 cos(13.43972444 Td + 168.571)
1.379 cos(14.95208427 Td + 300.986)
1.370 cos(16.21879811 Td + 171.511)
1.357 cos(14.06380055 Td + 13.590)
1.356 cos(13.99094198 Td + 341.308)
1.350 cos(11.36002182 Td + 358.805)
1.344 cos(16.02274391 Td + 117.663)
1.342 cos(13.30747499 Td + 213.872)
1.339 cos(13.82447801 Td + 267.672)
1.339 cos(14.05939236 Td + 263.612)
1.333 cos(18.24837944 Td + 228.433)
1.329 cos(12.31455254 Td + 242.216)
1.298 cos(16.05452837 Td + 128.653)
1.283 cos(12.88144086 Td + 68.534)

Additional Terms Pnm = 31 (cnt)

1.269 cos(16.21658484 Td + 298.614)
1.239 cos(16.64704765 Td + 200.751)
1.226 cos(13.00242518 Td + 29.361)
1.215 cos(12.88387464 Td + 350.713)
1.183 cos(15.07748952 Td + 12.391)
1.177 cos(17.16404682 Td + 66.413)
1.177 cos(12.77458465 Td + 121.343)
1.154 cos(16.59670183 Td + 206.712)
1.150 cos(15.03201541 Td + 87.279)
1.149 cos(17.78127808 Td + 236.084)
1.137 cos(17.07970748 Td + 350.406)
1.124 cos(17.70842382 Td + 201.853)
1.110 cos(18.25059148 Td + 102.064)
1.102 cos(17.10928780 Td + 152.622)
1.089 cos(13.90881310 Td + 164.733)
1.075 cos(12.34169947 Td + 89.437)
1.072 cos(10.81785684 Td + 98.281)
1.049 cos(13.43508729 Td + 90.849)
1.034 cos(15.50353152 Td + 8.836)
1.028 cos(15.43509576 Td + 263.289)
1.027 cos(16.09561237 Td + 153.591)
1.017 cos(14.36664310 Td + 168.456)
0.999 cos(10.74500286 Td + 64.048)
0.981 cos(11.91588571 Td + 179.843)
0.979 cos(15.15962843 Td + 36.553)
0.967 cos(11.82933262 Td + 223.038)
0.952 cos(13.98187217 Td + 242.575)
0.935 cos(14.01612012 Td + 211.588)
0.930 cos(12.38519772 Td + 220.602)
0.922 cos(16.52384973 Td + 166.082)
0.910 cos(14.48275697 Td + 257.962)
0.908 cos(17.69693439 Td + 159.977)
0.903 cos(11.87260755 Td + 97.342)
0.889 cos(17.23912068 Td + 334.282)
0.884 cos(16.17772977 Td + 326.783)
0.881 cos(12.83374236 Td + 239.103)
0.876 cos(13.47835425 Td + 62.753)
0.867 cos(13.04570087 Td + 83.596)
0.866 cos(14.57198791 Td + 206.806)
0.848 cos(14.48056487 Td + 199.191)
0.845 cos(13.87482099 Td + 72.909)
0.842 cos(15.04088647 Td + 315.949)
0.832 cos(16.10023135 Td + 132.213)
0.829 cos(15.66293026 Td + 174.613)
0.827 cos(12.84304976 Td + 49.627)
0.825 cos(13.47172177 Td + 76.525)
0.821 cos(13.98660237 Td + 245.790)
0.816 cos(13.93177914 Td + 135.169)
0.815 cos(11.84303348 Td + 142.342)
0.805 cos(13.48056679 Td + 295.266)
0.801 cos(13.90440516 Td + 56.150)
0.797 cos(16.22100738 Td + 45.680)
0.797 cos(15.11637045 Td + 340.809)
0.796 cos(14.03422990 Td + 57.883)
0.785 cos(16.15035807 Td + 244.582)
0.752 cos(13.95695619 Td + 94.350)
0.752 cos(13.90198122 Td + 282.730)
0.738 cos(16.53533360 Td + 216.660)
0.733 cos(12.45805102 Td + 249.642)
0.733 cos(16.01125627 Td + 74.447)

Additional Terms Pnm = 31 (cnt)

0.727 cos(13.54680327 Td + 166.946)
0.716 cos(13.55121936 Td + 275.901)
0.688 cos(13.39883318 Td + 29.039)
0.679 cos(14.40990618 Td + 37.248)
0.678 cos(11.21431459 Td + 290.272)
0.678 cos(12.29157808 Td + 338.265)
0.677 cos(16.63777395 Td + 50.947)
0.675 cos(11.94767189 Td + 5.841)
0.622 cos(15.58788021 Td + 86.624)

Additional Terms Pnm = 32

6.403 cos(26.79975694 Td + 76.068)
6.315 cos(28.97504757 Td + 21.297)
6.253 cos(26.91588367 Td + 342.389)
6.153 cos(31.72210910 Td + 114.390)
6.071 cos(28.44216645 Td + 287.856)
6.051 cos(27.87701759 Td + 124.193)
5.986 cos(29.52870552 Td + 142.073)
5.925 cos(28.36002650 Td + 267.110)
5.757 cos(28.94767418 Td + 301.067)
5.458 cos(29.61746341 Td + 149.432)
5.372 cos(30.54681130 Td + 253.209)
5.371 cos(29.61526620 Td + 91.424)
5.065 cos(27.42847606 Td + 106.731)
4.988 cos(30.15962705 Td + 229.866)
4.862 cos(30.04107302 Td + 190.276)
4.751 cos(31.73359590 Td + 156.527)
4.634 cos(26.25759027 Td + 175.770)
4.616 cos(29.02517447 Td + 135.222)
4.516 cos(29.44657187 Td + 121.162)
4.453 cos(27.38739851 Td + 82.554)
4.312 cos(27.37812423 Td + 302.604)
4.174 cos(27.50132898 Td + 135.292)
4.144 cos(27.30527402 Td + 268.255)
4.059 cos(30.62407593 Td + 38.042)
4.025 cos(30.63777420 Td + 314.337)
3.990 cos(28.59007530 Td + 51.892)
3.837 cos(30.50794961 Td + 131.033)
3.765 cos(28.39181509 Td + 303.658)
3.622 cos(28.34853861 Td + 224.705)
3.600 cos(28.86554379 Td + 278.703)
3.354 cos(27.92249520 Td + 77.555)
3.198 cos(32.27577038 Td + 55.069)
3.179 cos(28.47394548 Td + 119.018)
3.143 cos(29.49426017 Td + 310.150)
3.079 cos(27.45804777 Td + 243.732)
3.000 cos(32.19142021 Td + 341.304)
2.936 cos(30.16183794 Td + 103.933)
2.930 cos(30.00243733 Td + 298.599)
2.915 cos(27.38276946 Td + 102.628)
2.874 cos(25.85892338 Td + 109.254)
2.865 cos(32.27355849 Td + 181.689)
2.793 cos(26.32823634 Td + 335.140)
2.678 cos(25.78606918 Td + 75.024)
2.675 cos(26.94546403 Td + 144.693)
2.588 cos(27.95914987 Td + 325.756)
2.550 cos(27.92956324 Td + 344.052)
2.517 cos(29.57639332 Td + 123.216)
2.504 cos(30.09119445 Td + 304.232)
2.445 cos(27.41478256 Td + 190.387)
2.388 cos(29.52383413 Td + 266.662)
2.379 cos(28.01391424 Td + 239.512)
2.342 cos(27.84744106 Td + 168.254)
2.313 cos(27.34194039 Td + 160.306)
2.300 cos(28.00242438 Td + 18.161)
2.270 cos(29.61966939 Td + 23.382)
2.250 cos(28.52164564 Td + 306.162)
2.237 cos(29.45098985 Td + 52.558)
2.126 cos(29.96357235 Td + 356.085)
2.111 cos(28.50573179 Td + 336.058)
2.031 cos(29.54239970 Td + 60.139)

Additional Terms Pnm = 32 (cnt)

2.017 cos(31.10708365 Td + 180.302)
1.901 cos(28.94302952 Td + 292.915)
1.879 cos(31.17332667 Td + 48.477)
1.873 cos(32.19363114 Td + 215.194)
1.811 cos(27.33264420 Td + 349.573)
1.809 cos(27.97064840 Td + 188.915)
1.792 cos(30.08189403 Td + 313.946)
1.790 cos(29.60818197 Td + 162.076)
1.788 cos(26.98873827 Td + 16.626)
1.764 cos(29.46026291 Td + 219.066)
1.764 cos(27.90220423 Td + 82.723)
1.750 cos(31.65146401 Td + 314.434)
1.737 cos(28.90219622 Td + 346.181)
1.733 cos(27.97505410 Td + 297.554)
1.705 cos(26.83375059 Td + 167.530)
1.660 cos(31.16624435 Td + 298.058)
1.632 cos(27.48984026 Td + 279.119)
1.628 cos(27.80416480 Td + 89.344)
1.583 cos(31.02053762 Td + 228.772)
1.576 cos(29.99315019 Td + 311.793)
1.572 cos(26.40108764 Td + 10.104)
1.566 cos(28.39865757 Td + 158.459)
1.551 cos(29.10487039 Td + 25.473)
1.506 cos(31.09560078 Td + 136.726)
1.501 cos(27.27348702 Td + 231.653)
1.476 cos(28.40329352 Td + 160.868)
1.457 cos(28.48542956 Td + 340.550)
1.444 cos(29.03200771 Td + 350.045)
1.442 cos(29.02052925 Td + 334.107)
1.409 cos(27.92493352 Td + 4.114)
1.377 cos(26.37150716 Td + 207.296)
1.375 cos(27.81565071 Td + 132.504)
1.346 cos(28.32116942 Td + 143.789)
1.321 cos(32.27797066 Td + 291.877)
1.285 cos(28.94988869 Td + 175.205)
1.255 cos(31.72431567 Td + 348.122)
1.254 cos(29.06601845 Td + 82.678)
1.246 cos(28.98426521 Td + 358.294)
1.238 cos(30.59008776 Td + 319.496)
1.236 cos(30.03642897 Td + 30.601)
1.208 cos(26.44436295 Td + 241.644)
1.169 cos(29.40770600 Td + 180.013)
1.166 cos(27.88605384 Td + 54.445)
1.153 cos(26.95695240 Td + 358.683)
1.083 cos(28.48079539 Td + 2.209)
1.078 cos(27.35562189 Td + 73.217)
1.072 cos(29.02742514 Td + 20.665)
1.048 cos(26.91367398 Td + 108.982)
1.021 cos(32.26427250 Td + 15.794)
1.021 cos(27.87480978 Td + 249.393)
1.018 cos(30.11855544 Td + 204.981)
1.016 cos(29.07307817 Td + 15.307)
1.001 cos(31.09118117 Td + 28.840)
0.991 cos(28.42846562 Td + 12.161)
0.981 cos(31.73580909 Td + 30.395)
0.973 cos(29.52162960 Td + 211.518)
0.958 cos(28.51942961 Td + 71.664)
0.941 cos(28.44877937 Td + 274.429)
0.922 cos(31.63776645 Td + 38.196)
0.902 cos(31.60597637 Td + 208.441)

Additional Terms Pnm = 32 (cnt)

0.885 cos(30.67221807 Td + 147.223)
0.880 cos(27.53311007 Td + 151.709)
0.878 cos(29.54461060 Td + 294.155)
0.878 cos(30.61965889 Td + 108.138)
0.841 cos(26.84302214 Td + 307.879)
0.830 cos(31.56491540 Td + 2.380)
0.828 cos(28.59228440 Td + 287.121)
0.824 cos(30.47616238 Td + 94.747)
0.805 cos(28.47615797 Td + 278.595)
0.785 cos(27.45565029 Td + 143.409)
0.784 cos(26.25538196 Td + 300.997)
0.776 cos(27.41919536 Td + 118.634)
0.775 cos(26.76089884 Td + 133.205)
0.754 cos(30.55829346 Td + 295.870)
0.726 cos(31.13446410 Td + 103.347)
0.723 cos(31.06159763 Td + 73.192)
0.719 cos(26.87041337 Td + 58.049)
0.713 cos(27.38519207 Td + 208.746)
0.711 cos(28.93841039 Td + 313.515)
0.694 cos(31.18214472 Td + 93.951)
0.684 cos(28.91589383 Td + 263.197)
0.677 cos(27.37591064 Td + 67.779)
0.662 cos(29.07088450 Td + 321.608)
0.637 cos(27.30306517 Td + 33.172)
0.635 cos(25.31454806 Td + 334.267)

Additional Terms Pnm = 33

6.457 cos(45.66293507 Td + 174.044)
5.976 cos(42.42383146 Td + 293.888)
5.964 cos(40.89998978 Td + 300.167)
5.595 cos(42.92729408 Td + 285.247)
5.562 cos(40.82713583 Td + 265.908)
5.096 cos(44.56490754 Td + 95.659)
4.636 cos(43.56270188 Td + 137.803)
4.404 cos(41.84082523 Td + 86.954)
4.382 cos(44.49205111 Td + 241.686)
4.140 cos(43.40109388 Td + 277.613)
4.090 cos(45.12297707 Td + 148.314)
4.045 cos(43.98409596 Td + 124.419)
3.758 cos(42.37370906 Td + 180.024)
3.720 cos(42.02980477 Td + 207.644)
3.684 cos(45.12784146 Td + 207.947)
3.544 cos(41.87481737 Td + 358.342)
3.418 cos(42.84523136 Td + 280.820)
3.304 cos(43.43973100 Td + 349.055)
3.215 cos(45.13005131 Td + 80.261)
3.211 cos(42.94106143 Td + 219.526)
3.197 cos(45.11635799 Td + 343.420)
3.123 cos(42.31455288 Td + 62.481)
3.113 cos(46.22100676 Td + 225.507)
2.877 cos(41.41257437 Td + 38.359)
2.839 cos(44.53311614 Td + 87.996)
2.802 cos(45.66514555 Td + 48.974)
2.795 cos(43.36223507 Td + 334.790)
2.792 cos(43.59935974 Td + 25.667)
2.752 cos(45.67883851 Td + 325.071)
2.609 cos(44.10707716 Td + 272.066)
2.586 cos(43.43288563 Td + 313.767)
2.515 cos(41.48542964 Td + 72.653)
2.446 cos(46.13446196 Td + 274.152)
2.379 cos(44.64704025 Td + 298.839)
2.232 cos(44.14373026 Td + 161.031)
2.225 cos(44.61524865 Td + 262.889)
2.164 cos(44.53532868 Td + 321.024)
2.162 cos(46.14373382 Td + 83.154)
2.145 cos(43.51501621 Td + 129.548)
2.076 cos(42.49912365 Td + 251.606)
1.977 cos(43.48984725 Td + 102.964)
1.963 cos(44.07087161 Td + 128.565)
1.939 cos(41.36930174 Td + 346.550)
1.877 cos(44.01611455 Td + 32.478)
1.875 cos(43.98874068 Td + 309.482)
1.859 cos(46.14594441 Td + 316.429)
1.859 cos(46.68810954 Td + 217.706)
1.851 cos(44.10046404 Td + 106.654)
1.832 cos(41.98653263 Td + 155.197)
1.823 cos(42.57418035 Td + 342.641)
1.794 cos(41.88409135 Td + 139.267)
1.789 cos(44.61746021 Td + 135.649)
1.712 cos(42.97063515 Td + 352.652)
1.633 cos(42.88850528 Td + 179.225)
1.610 cos(41.80196500 Td + 323.940)
1.582 cos(46.69032174 Td + 91.296)
1.579 cos(43.04349274 Td + 28.654)
1.569 cos(43.55608493 Td + 333.495)
1.469 cos(42.49668865 Td + 327.513)
1.459 cos(43.54679851 Td + 345.978)

Additional Terms Pnm = 33 (cnt)

1.431 cos(45.08214024 Td + 200.294)
1.396 cos(43.97945963 Td + 143.848)
1.363 cos(44.06623927 Td + 145.401)
1.361 cos(42.38286102 Td + 137.710)
1.320 cos(40.35561444 Td + 165.157)
1.320 cos(46.76096773 Td + 251.434)
1.317 cos(44.48764102 Td + 131.742)
1.286 cos(42.46954682 Td + 121.093)
1.279 cos(41.51721728 Td + 109.337)
1.278 cos(45.67001698 Td + 284.625)
1.263 cos(46.77245847 Td + 291.177)
1.236 cos(44.64924571 Td + 172.798)
1.227 cos(41.87945725 Td + 158.755)
1.226 cos(43.63114395 Td + 61.992)
1.204 cos(42.94327190 Td + 94.561)
1.190 cos(44.95893164 Td + 2.532)
1.181 cos(42.92698070 Td + 212.964)
1.180 cos(43.01612746 Td + 305.247)
1.154 cos(40.97284344 Td + 334.481)
1.149 cos(46.76317764 Td + 124.857)
1.138 cos(43.48323768 Td + 298.522)
1.137 cos(45.54901554 Td + 142.231)
1.128 cos(43.59007731 Td + 38.338)
1.113 cos(42.53090827 Td + 289.650)
1.100 cos(42.89535418 Td + 214.984)
1.098 cos(45.03421744 Td + 322.763)
1.084 cos(40.75428256 Td + 231.687)
1.077 cos(44.14594125 Td + 35.220)
1.067 cos(41.44216067 Td + 19.515)
1.039 cos(42.54239321 Td + 282.167)
1.026 cos(44.65852211 Td + 161.454)
1.025 cos(46.13666417 Td + 148.398)
1.014 cos(44.07307791 Td + 0.854)
1.010 cos(43.08678091 Td + 313.795)
0.999 cos(45.58787587 Td + 262.387)
0.953 cos(41.95231535 Td + 194.196)
0.949 cos(43.46246036 Td + 270.009)
0.949 cos(42.96601145 Td + 13.117)
0.937 cos(42.85672239 Td + 141.356)
0.932 cos(46.77025489 Td + 58.094)
0.885 cos(41.33044248 Td + 223.301)
0.884 cos(43.99095351 Td + 185.716)
0.842 cos(40.94105546 Td + 297.713)
0.824 cos(42.30085619 Td + 145.892)
0.819 cos(44.56976716 Td + 152.332)
0.817 cos(42.45582037 Td + 195.698)
0.801 cos(45.59449314 Td + 250.324)
0.791 cos(42.44656453 Td + 214.509)
0.781 cos(40.28276105 Td + 130.893)
0.780 cos(44.44878588 Td + 187.917)
0.771 cos(41.90218685 Td + 79.716)
0.753 cos(41.82933378 Td + 45.079)
0.753 cos(45.05011902 Td + 114.794)
0.748 cos(44.65632866 Td + 103.555)
0.744 cos(43.00022665 Td + 336.739)
0.725 cos(41.94767280 Td + 32.827)
0.724 cos(45.13225973 Td + 315.422)
0.719 cos(43.93397711 Td + 11.138)
0.716 cos(44.02518194 Td + 316.914)
0.714 cos(41.95474444 Td + 117.910)

Additional Terms Pnm = 33 (cnt)

0.692 cos(45.20069297 Td + 240.974)
0.665 cos(44.45098339 Td + 244.485)
0.660 cos(44.06846177 Td + 23.497)
0.659 cos(43.56049540 Td + 80.846)
0.659 cos(46.77466260 Td + 167.055)
0.628 cos(45.00463347 Td + 7.316)

Additional Terms Pnm = 40

4.129 cos(1.56954980 Td + 178.293)
4.120 cos(1.09583037 Td + 21.538)
3.975 cos(2.19826665 Td + 29.403)
3.812 cos(2.11392540 Td + 313.172)
3.416 cos(2.18677914 Td + 347.339)
2.357 cos(0.55365645 Td + 302.553)
2.276 cos(0.47152159 Td + 100.691)
2.086 cos(1.01589981 Td + 234.728)
1.744 cos(1.10244863 Td + 186.004)
1.714 cos(2.74043870 Td + 288.596)
1.622 cos(0.00441188 Td + 109.096)
1.525 cos(1.57176033 Td + 52.924)
1.481 cos(2.74265375 Td + 161.433)
1.392 cos(2.11613453 Td + 187.537)
1.261 cos(2.18898780 Td + 222.040)
1.247 cos(1.08874935 Td + 269.893)
1.166 cos(2.20047794 Td + 264.271)
1.080 cos(2.65830174 Td + 87.983)
1.009 cos(1.64020677 Td + 156.215)
0.886 cos(0.55586571 Td + 176.663)
0.878 cos(0.47372645 Td + 155.752)
0.874 cos(0.46931411 Td + 47.505)
0.813 cos(0.08214210 Td + 199.219)
0.778 cos(1.01810154 Td + 291.108)
0.627 cos(0.08434199 Td + 256.015)
0.492 cos(0.00220547 Td + 235.353)

Additional Terms Pnm = 41

4.455 cos(12.30063386 Td + 80.767)
4.296 cos(12.92714143 Td + 57.903)
4.129 cos(16.68347045 Td + 43.649)
3.848 cos(12.85428739 Td + 23.716)
2.739 cos(13.39645534 Td + 283.004)
2.667 cos(14.48741298 Td + 68.428)
2.646 cos(12.29842317 Td + 206.672)
2.541 cos(15.51258811 Td + 291.640)
2.537 cos(14.56954571 Td + 90.187)
2.507 cos(16.68568101 Td + 277.659)
2.309 cos(16.05696323 Td + 66.256)
2.299 cos(14.02517270 Td + 314.975)
1.927 cos(16.14351329 Td + 17.609)
1.911 cos(13.93862468 Td + 3.585)
1.865 cos(13.40086825 Td + 214.067)
1.822 cos(15.04548112 Td + 120.251)
1.538 cos(14.49889917 Td + 291.847)
1.530 cos(15.58765125 Td + 201.866)
1.418 cos(15.58323368 Td + 271.244)
1.407 cos(14.49448307 Td + 0.827)
1.391 cos(16.12981369 Td + 100.847)
1.391 cos(13.95231691 Td + 280.683)
1.342 cos(12.84058653 Td + 107.947)
1.213 cos(12.38276258 Td + 283.117)
1.056 cos(13.38938084 Td + 169.897)
0.953 cos(11.75625832 Td + 305.813)
0.933 cos(14.95892917 Td + 169.671)
0.840 cos(11.82911349 Td + 339.990)
0.818 cos(12.37348732 Td + 114.875)
0.798 cos(16.61061375 Td + 9.481)
0.738 cos(17.15499209 Td + 144.247)
0.653 cos(17.22785061 Td + 178.110)
0.639 cos(13.38717574 Td + 296.261)
0.585 cos(16.13688837 Td + 212.530)
0.573 cos(17.23934148 Td + 217.683)
0.567 cos(11.75404799 Td + 71.720)
0.526 cos(13.46931220 Td + 316.359)
0.498 cos(11.82690245 Td + 105.804)
0.486 cos(12.37127831 Td + 240.955)
0.483 cos(16.61282606 Td + 243.885)

Additional Terms Pnm = 42

3.983 cos(28.43751934 Td + 294.656)
3.385 cos(28.44193485 Td + 42.972)
3.307 cos(31.18016114 Td + 279.914)
3.109 cos(28.43044880 Td + 1.813)
2.901 cos(28.51258362 Td + 23.565)
2.814 cos(30.07993286 Td + 145.836)
2.785 cos(26.79732455 Td + 136.883)
2.768 cos(31.18237332 Td + 153.507)
2.687 cos(27.96820776 Td + 249.020)
2.455 cos(26.87017882 Td + 171.102)
2.411 cos(27.89535527 Td + 214.497)
2.379 cos(27.41455471 Td + 306.121)
2.239 cos(29.53996711 Td + 301.872)
2.238 cos(30.62871689 Td + 211.556)
1.656 cos(29.52847743 Td + 259.332)
1.174 cos(30.08655429 Td + 310.241)
1.161 cos(28.42824016 Td + 127.413)
1.143 cos(29.61061219 Td + 101.180)
1.142 cos(30.55365407 Td + 302.675)
1.039 cos(26.79511533 Td + 262.472)
1.038 cos(31.09802966 Td + 77.379)
1.022 cos(29.06624138 Td + 325.294)
0.915 cos(26.86796930 Td + 296.665)
0.885 cos(27.41234338 Td + 71.296)
0.883 cos(26.32580425 Td + 36.145)
0.848 cos(31.18458022 Td + 28.483)
0.847 cos(28.97969499 Td + 13.298)
0.836 cos(27.88165948 Td + 297.237)
0.811 cos(31.72453654 Td + 54.870)
0.769 cos(28.51037640 Td + 330.218)
0.763 cos(27.42383271 Td + 114.180)
0.754 cos(28.35759707 Td + 327.288)
0.710 cos(28.51478863 Td + 78.675)
0.703 cos(27.96600109 Td + 194.160)
0.680 cos(31.72674841 Td + 288.425)
0.633 cos(27.89314338 Td + 160.926)
0.626 cos(28.99338728 Td + 292.371)
0.623 cos(31.17088062 Td + 112.036)
0.600 cos(30.00000728 Td + 358.471)
0.535 cos(27.89755988 Td + 270.015)
0.448 cos(29.61282267 Td + 335.690)

Additional Terms Pnm = 43

3.683 cos(43.55364928 Td + 214.616)
3.387 cos(43.00927553 Td + 79.306)
3.375 cos(43.48300449 Td + 55.761)
3.047 cos(42.93641983 Td + 45.460)
2.138 cos(41.36687074 Td + 47.130)
2.080 cos(44.56954923 Td + 90.073)
1.826 cos(43.39866189 Td + 338.544)
1.719 cos(43.47859472 Td + 124.987)
1.523 cos(44.57882430 Td + 258.156)
1.519 cos(45.66757459 Td + 168.038)
1.462 cos(45.12761644 Td + 141.455)
1.143 cos(43.46930265 Td + 139.285)
1.124 cos(41.29401684 Td + 12.901)
1.049 cos(42.92273015 Td + 128.372)
1.009 cos(41.83618499 Td + 272.802)
0.968 cos(44.58103394 Td + 131.952)
0.966 cos(42.46489978 Td + 304.176)
0.965 cos(45.66978547 Td + 42.009)
0.910 cos(42.85428659 Td + 203.522)
0.895 cos(41.90903716 Td + 307.602)
0.868 cos(42.45341339 Td + 82.539)
0.749 cos(45.04106881 Td + 190.420)
0.745 cos(44.02958795 Td + 244.720)
0.696 cos(43.55585893 Td + 89.876)
0.606 cos(42.88607401 Td + 240.306)
0.533 cos(45.12100163 Td + 335.925)
0.518 cos(42.93862977 Td + 281.108)
0.505 cos(40.82249563 Td + 272.152)
0.497 cos(46.22122594 Td + 111.352)

Additional Terms Pnm = 44

4.332 cos(57.42162770 Td + 58.637)
3.945 cos(56.40793747 Td + 238.045)
3.366 cos(58.43972893 Td + 169.504)
3.096 cos(58.52407178 Td + 65.814)
2.075 cos(56.33508367 Td + 203.799)
1.874 cos(60.16426590 Td + 44.316)
1.680 cos(57.89535319 Td + 34.502)
1.632 cos(60.16647783 Td + 277.764)
1.591 cos(59.06403799 Td + 270.302)
1.366 cos(59.07064381 Td + 75.722)
1.361 cos(58.59471583 Td + 225.720)
1.237 cos(58.05034603 Td + 90.434)
1.125 cos(57.97748749 Td + 56.514)
1.119 cos(57.92714268 Td + 71.209)
1.042 cos(58.51037523 Td + 148.816)
0.998 cos(58.00927615 Td + 246.711)
0.933 cos(55.86356230 Td + 103.052)
0.917 cos(56.87725659 Td + 282.737)
0.820 cos(56.95010626 Td + 317.943)
0.807 cos(57.49447708 Td + 94.002)
0.771 cos(59.61061372 Td + 101.166)
0.762 cos(58.04106106 Td + 103.091)
0.748 cos(56.48079134 Td + 272.299)
0.746 cos(56.99337757 Td + 10.539)
0.719 cos(57.46489484 Td + 111.317)
0.692 cos(57.38276750 Td + 296.163)
0.636 cos(58.59692626 Td + 100.014)
0.519 cos(57.53775160 Td + 145.494)
0.482 cos(55.93641626 Td + 137.322)